DEVELOPMENT OF MOLECULAR SYSTEMS FOR THE DETECTION OF ENVIRONMENTAL ARSENIC

Immacolata Antonucci

Dottorato in Scienze Biotecnologiche – 28° ciclo
Indirizzo Biotecnologie Industriali e Molecolari
Università di Napoli Federico II

Dottorato in Scienze Biotecnologiche – 28° ciclo
Indirizzo Biotecnologie Industriali e Molecolari
Università di Napoli Federico II

DEVELOPMENT OF MOLECULAR SYSTEMS FOR THE DETECTION OF ENVIRONMENTAL ARSENIC

Immacolata Antonucci

Dottoranda: Immacolata Antonucci

Relatore: Prof.ssa Simonetta Bartolucci

Coordinatore: Prof. Giovanni Sannia

CONTENTS

RIASSUNTO

I metalli pesanti sono la causa di uno dei più gravi problemi di inquinamento del nostro tempo. Anche se in piccole concentrazioni, minacciano la salute umana e l'ambiente perché non sono biodegradabili. Le persone sono sempre state esposte ai metalli pesanti nell'ambiente (elementi metallici di pesticidi e agenti terapeutici, contaminazione metallica di cibo e acqua, etc.), soprattutto negli ultimi anni, con l'impiego dei metalli nelle applicazioni industriali; l'inquinamento causato dai metalli pesanti è anche legato alla combustione di materiale plastico, prodotti in PVC, scarichi di automobili, fumo di sigarette, batterie e rifiuti urbani. Pertanto, è importante essere informati circa le concentrazioni di metalli pesanti ed adottare misure di protezione contro la sovraesposizione. Attualmente, tra i vari inquinanti diffusi in massa nell'ambiente, i metalli pesanti sono tra i composti più nocivi; i gruppi sulfidrilici (SH), che normalmente si trovano negli enzimi si legano facilmente ai metalli pesanti, ed il risultante complesso metallo-zolfo inattiva l'enzima.

La tossicità dei metalli pesanti può provocare un danneggiamento o una riduzione della funzione del sistema nervoso centrale, danni alla composizione del sangue, ai polmoni, ai reni, al fegato e ad altri organi vitali. L'esposizione a lungo termine può portare a lenta progressione di processi degenerativi fisici, muscolari e neurologici che imitano il morbo di Alzheimer, il morbo di Parkinson, la distrofia muscolare, e la sclerosi multipla. Il ripetuto contatto a lungo termine con alcuni metalli o loro composti può anche causare il cancro (International Occupational Safety and Information Centre Salute, 1999).

Pertanto, è chiaro che il controllo dell'inquinamento delle acque e dei suoli, principalmente vicino a zone industriali o a zone contaminate, è uno dei principali obiettivi ambientali. Diversi metodi chimici sono stati sviluppati per quantificare i metalli pesanti e cercare di ridurre la loro concentrazione in siti inquinati, ma il problema persiste vista la necessità di smaltire i rifiuti trattati e ogni, probabilmente anche più tossico, sottoprodotto chimico; così tenendo conto dei progressi delle biotecnologie, sarebbe interessante cercare di sviluppare un biosensore batterico o una tecnica di bonifica a base biologica.

I biosensori sono costituiti da un "elemento biologico" che riconosce il composto di interesse dando luogo ad un fenomeno chimico o chimico fisico; la loro classificazione avviene in base alla biomolecola di riconoscimento, ad esempio biosensori enzimatici a biosensori a cellule.

Un biosensore può essere utilizzato come metodo rapido e sensibile per rilevare e quantificare specie tossiche; i biosensori si basano sull'analisi dell'espressione di un gene reporter che è controllato da un promotore sensibile ad un particolare composto tossico. L'uso di biosensori come sistema di monitoraggio ambientale ha diversi vantaggi, tra cui specificità, velocità, portabilità, facilità d'uso, la segnalazione in tempo reale e, inoltre, consente misurazioni tossicologiche. D'altra parte, la *bioremediation* sfrutta la versatilità metabolica dei microrganismi per degradare inquinanti pericolosi, per cui i microrganismi potrebbero essere stimolati o appositamente sviluppati per degradare/trasformare una sostanza tossica in prodotti non tossici, o ridurre le concentrazioni a livelli bassi anche direttamente nel sito inquinato.

La grande diversità genetica dei microrganismi spiega la loro grande versatilità metabolica. Inoltre, la loro abbondanza, i loro tassi di crescita elevati e la loro suscettibilità ad acquisire geni attraverso il trasferimento genico orizzontale, permette loro di evolvere rapidamente e di adattarsi alle mutevoli condizioni dell'ambiente,

anche per ambienti estremi che non permettono la proliferazione di altri organismi viventi. I microrganismi hanno una grande varietà di meccanismi di difesa contro i metalli presenti nell'ambiente naturale e hanno sviluppato sistemi basati su regolatori trascrizionali metallo-sensori che regolano la trascrizione di geni che codificano proteine responsabili della disintossicazione dal metallo, del sequestro, dell'efflusso e dell'assorbimento.

I microrganismi che mostrano tali caratteristiche possono essere un punto di partenza per la costruzione di biosensori per il monitoraggio dell'inquinamento ambientale. La costruzione di un biosensore richiede, da un lato, lo studio della biochimica alla base della tolleranza dell'inquinante da parte dalla cellula, e dall'altro, un sistema genetico facilmente gestibile. Il ceppo ricombinante potrebbe essere rappresentato da un sistema genetico costituito da un promotore inducibile, sensibile a composti tossici, fuso ad un gene reporter che codifica una proteina facilmente rilevabile. Una varietà di promotori ben caratterizzati è disponibile per le manipolazioni genetiche (promotori di vari metalli pesanti, aldeidi aromatiche, idrocarburi, pesticidi, salicilati, etc.). I geni reporter più comunemente usati sono: *lacZ*, che codifica la β-galattosidasi, la cui attività enzimatica può essere determinata da una reazione colorimetrica; il gene della luciferasi (gene *lux*) o il gene per la *Green Fluorescent Protein* (GFP), che possono essere rilevati rispettivamente mediante tecniche di bioluminescenza e spettrofluorimetriche.

I biosensori quindi stanno emergendo come metodi nuovi e sicuri per rilevare gli inquinanti ambientali come l'arsenico. Essi non sono destinati a sostituire completamente i metodi chimici ma possono offrire un monitoraggio rapido ed in loco anche di tracce del composto target, in paragone a metodologie cromatografiche analitiche non portatili. I biosensori permettono misure quantitative o semi-quantitative del target, grazie a elementi di riconoscimento biologici (cellule, anticorpi, DNA, RNA, enzimi o recettori proteici) accoppiati a trasduttori fisici. Ad oggi, i biosensori batterici sono per la maggior parte basati sull'utilizzo di microrganismi mesofili, quelli termofili però sono buoni candidati per la costruzione di biosensori cellulari ed enzimatici più stabili e forti. I vantaggi dell'utilizzo di organismi termofili sono collegati alla loro elevata resistenza alla temperatura e agli agenti caotropici o ai detergenti spesso presenti nei rifiuti industriali e nelle acque di scarico. Questi microrganismi rappresentano quindi una risorsa considerevole nello sviluppo di nuovi processi biotecnologici.

Per realizzare un biosensore è preliminare l'identificazione di elementi responsivi alla sostanza che si vuole rilevare, quindi il principale obiettivo di questa tesi è stato caratterizzare a livello molecolare il meccanismo di resistenza all'arsenico di *Thermus thermophilus* e la realizzazione di biosensori cellulari ed enzimatici per rilevare l'inquinamento da arsenico nei terreni e nelle acque; un altro obiettivo è stato l'identificazione di nuovi microrganismi arsenico-tolleranti e la caratterizzazione del loro meccanismo di resistenza.

Il batterio termofilo gram negativo *T. themophilus* HB27 è in grado di crescere in presenza di arsenato e arsenito in un intervallo di concentrazioni letali per altri organismi; i putativi geni di resistenza non sono stati trovati in un singolo operone di resistenza ma associati a geni cromosomali apparentemente non collegati funzionalmente, questi sono: un arsenato reduttasi, un regolatore trascrizionale ed una proteina di membrana di trasporto; l'arsenato reduttasi *Tt*ArsC è stata precedentemente caratterizzata.

Per la realizzazione del biosensore, è stato ricercato nel genoma di *T. themophilus* il regolatore trascrizionale che può fungere da metallo-sensore; il regolatore

2

trascizionale *Tt*SmtB, appartenente alla famiglia ArsR/SmtB, è stato identificato e caratterizzato funzionalmente. L'analisi trascrizionale mediante RT-PCR del gene *TtsmtB* e dei geni vicini ha dimostrato che è espresso come terzo in un operone a cinque geni (*TTC0351-TTC0352-TTC0353-TTC0354-TTC0355*) codificanti putative proteine con non ovvia relazione funzionale, eccetto per *TTC0354* che codifica per una putativa ATPasi trasportante cationi con un motivo per il riconoscimento dei metalli pesanti, che potrebbe mediare l'efflusso attivo dell'arsenito.

Analisi di qRT-PCR hanno mostrato variazioni nei profili trascizionali di *TTC0351*, primo gene dell'operone, di *TTC0353* e *TTC0354* in seguito al trattamento con arsenato e arsenito, confermando il loro coinvolgimento nella risposta all'arsenico e suggerendo che *Tt*SmtB possa essere il regolatore.

È interessante notare che, pur essendo un cluster genico, elementi consensus di promotori sono stati identificati non solo a monte di *TTC0351*, ma anche come promotori interni a monte dei geni *TTC0353* e *TTC0354*, suggerendo che questi geni potrebbero anche essere trascritti singolarmente e regolati distintamente per garantire che relativi livelli di espressione possano variare in condizioni di crescita diverse.

Il promotore del gene *TTC0354* contiene inoltre la sequenza corrispondente al sito consensus palindromico di legame per proteine appartenenti alla famiglia ArsR/SmtB, sovrapposto agli elementi basali della trascrizione; ciò suggerisce che la sua espressione potrebbe essere regolata attraverso una modulazione del legame del metallo sensore *Tt*SmtB al DNA. A questo proposito, *Tt*SmtB è stato clonato ed espresso in forma ricombinante in *E. coli*, purificato all'omogeneità e caratterizzato funzionalmente.

In vitro, la proteina ricombinante *Tt*SmtB è in grado di legare tutti i promotori individuati con diversa affinità; in particolare il complesso tra *Tt*SmtB ed il suo stesso promotore è appena rilevabile, suggerendo una bassa affinità di legame. *Tt*SmtB lega invece il promotore *TTC0354* in maniera sequenza specifica, cooperativa (n Hill = 2.5) e con elevata affinità (K_d = 0.27 µM), ma in presenza di arsenato e arsenito non riesce a legarlo. Un passaggio importante nella resistenza all'arsenico è la riduzione intracellulare dell'arsenato ad arsenito da parte dell'arsenato reduttasi, che in genere è localizzata nello stesso operone del regolatore; visto che in *T. thermophilus* i geni di resistenza non sono nello stesso operone, tramite EMSA è stata confermata la capacità di *Tt*SmtB di interagire anche con il promotore di *Tt*ArsC, il cui ruolo nella resistenza all'arsenico era già stato precedentemente dimostrato dal nostro gruppo di ricerca.

Per verificare *in-vivo* la funzione di *Tt*SmtB nella regolazione dei geni collegati al meccanismo di resistenza, è stato generato un mutante di delezione del gene *TtsmtB* (*ΔsmtB),* in cui sono stati misurati i livelli di espressione dei geni *TTC0351*, *TTC0354* e *TtarsC* mediante qRT-PCR.

Nel ceppo mutante i livelli di espressione sono significativamente più alti che nel ceppo wild-type, dando una prova sperimentale del fatto che *in-vivo Tt*SmtB si lega ai suoi promotori target ostacolandone la trascrizione genica. Il gene *TtsmtB* inoltre non è essenziale per la sopravvivenza dell'organismo, infatti in assenza di arsenico il ceppo *ΔsmtB* cresce allo stesso modo del wild-type. Il mutante cresce in maniera simile al wild-type in presenza di arsenito, in presenza di arsenato invece la velocità di crescita decrementa.

E' stato quindi ipotizzato che nel ceppo *ΔsmtB* l'esposizione all'arsenito può essere bilanciata dall'aumentata espressione del gene *TTC0354* che ne permette una più rapida estrusione dalla cellula. Dall'altro lato l'effetto inibitorio dell'arsenato sulla

3

crescita cellulare, può essere superato solo dopo la riduzione dell'arsenato ad arsenito da parte di *Tt*ArsC.

E' interessante notare che la complementazione di *Tt*SmtB nel ceppo mutante aumenta la tolleranza all'arsenato e ristabilisce parzialmente la crescita ai livelli del wild-type; questi risultati sono coerenti con il ripristino dell'espressione di *Tt*SmtB, confermando il suo ruolo nella regolazione della resistenza all'arsenico.

Questi risultati hanno aperto la strada a valutare la realizzazione di un biosensore dell'arsenico basato su cellule di *T. thermophilus*.

Pertanto ci siamo interessati all'identificazione di sequenze regolatorie riconosciute da *Tt*SmtB e responsive all'arsenico, da fondere al gene reporter della β-galattosidasi. I sistemi reporter sono stati basati sulla costruzione di un ceppo di *T. thermophilus* Δ42 contenente un ibrido trascrizionale di fusione tra un promotore di *Thermus* responsivo all'arsenico ed il gene *bga*A, codificante una β-galattosidasi termostabile. Sono stati prodotti tre costrutti reporter: pMH0351prombgaA, pMH0353prombgaA e pMH0354prombgaA, contenenti a monte del gene *bga*A tre diversi promotori, target del regolatore trascrizionale *Tt*SmtB.

L'analisi dell'attività β-galattosidasica ha dimostrato che solo due dei tre testati rispondono sensibilmente all'arsenico. Il promotore *0351*, a monte dell'intero operone di *Tt*SmtB, risulta essere quello con l'attività più bassa, non inducibile in presenza di arsenico. I promotori 0353 e 0354 sono entrambi in grado di aumentare l'espressione del gene reporter in seguito a trattamento con arsenato e arsenito.

Inoltre l'attività del promotore *0354* più bassa rispetto a 0353 è stata attribuita ad una maggiore repressione da parte di *Tt*SmtB. Infatti analizzando l'attività del gene reporter nel ceppo mutante *T. thermophilus ΔsmtB*, che non esprime il regolatore trascrizionale, l'attività del promotore *0354* risulta maggiore rispetto al promotore *0353*. Pertanto il ceppo reporter *T. thermophilus* Δ42 *0354*prom è stato valutato come candidato per un biosensore per l'arsenico.

L'analisi dell'attività β-galattosidasica a differenti tempi di crescita dopo il trattamento con arsenico, ha permesso di settare il miglior intervallo per misurare la risposta del biosensore, indicando che la risposta può essere misurata con affidabilità a 30 minuti dall'aggiunta do arsenato o arsenito. I nostri dati ci hanno permesso di stabilire un limite di rilevazione pari a 0.1 mM sia di arsenato che arsenito. Una caratteristica interessante di questo biosensore è la sua natura termofila; ciò rappresenta un vantaggio notevole correlato all'elevata resistenza alla temperatura e agli agenti caotropici o detergenti spesso presenti nei rifiuti industriali o nelle acque di scarico.

Quindi, nonostante questo biosensore non abbia un limite di rilevazione elevato, può essere più versatile, stabile e forte in caso di acque fortemente contaminate.

In conclusione abbiamo costruito il primo biosensore cellulare basato sull'utilizzo di un microrganismo termofilo. I nostri risultati mostrano che il biosensore è un *tool* utile per rilevare rapidamente la presenza di arsenico in siti inquinati. Nonostante ciò, sono necessari ulteriori accorgimenti per permettere la misurazione dell'arsenico in un intervallo di concentrazioni più basso, così come in presenza di altri inquinanti chimici.

Un altro step importante di questa tesi è stato lo sviluppo di un biosensore enzimatico; è stato utilizzato l'enzima *Tt*ArsC come sonda biomolecolare per rilevare la presenza di arsenico nell'acqua. In particolar modo, *Tt*ArsC è stata adsorbita su nanoparticelle d'oro (AuNPs).

L'interazione tra *Tt*ArsC e gli ioni metallici è stata caratterizzata utilizzando tecniche ottiche, valutando quantitativamente l'interazione ed il bio-riconoscimento di arsenato ed arsenito. Questi nano-biocomplessi hanno dimostrato di essere stabili ed in grado

di legare fortemente gli ioni tossici. I dati sperimentali mostrano rilevanti cambiamenti del segnale, come ad esempio la variazione della posizione del picco *Fourier Transform-Surface Plasmon Resonance* (FT-SPR). TtArsC-AuNPs hanno una elevate sensibilità per l'arsenito, a differenza di quello che accade in natura, dove il substrato principale dell'enzima *Tt*ArsC è l'arsenato.

Su queste basi, i nanobiocomplessi TtArsC-AuNPs sono in grado di interagire con le soluzioni di ioni arsenito, virando a soluzioni blu, e soluzioni di ioni arsenato, virando a soluzioni rosa/viola, a tutte le concentrazioni testate. Questi fenomeni sono stati confermati quantitativamente, attraverso *Localized Surface Plasmon* (LSP), spostamenti degli spettri UV-vis; la caretterizzazione mediante *dynamic light scattering* (DLS) rivela che i nanobiocomplessi aggregano in presenza di ioni di arsenico. Infine, lo studio della banda LSP in presenza di ioni metallici che non sono substrati dell'enzima (Cd^{2+}, Pb^{2+} e Hg^{2+}) ha indicato che il bio-riconoscimento è altamente specifico ma non completamente selettivo.

Questi risultati indicano che TtArsC-AuNPs può trovare un'applicazione semplice ed economica nello screening delle acque.

In questo lavoro ci siamo occupati di isolare un nuovo organismo resistente all'arsenico da un campione di fango proveniente un sito geotermale vicino Napoli, chiamato Pisciarelli.

Il sequenziamento dell'rRNA del 16S lo ha identificato come *Geobacillus stearothermophilus;* i Geobacilli sono termofili Gram-positivi, formanti endospore, aerobi o anaerobi facoltativi, crescono in modo ottimale a temperature comprese tra 50°C e 60°C. Analisi bioinformatiche hanno permesso di rilevare la presenza di putativi operoni *ars* nei genomi di diversi ceppi di *G. stearothermophilus*, suggerendo la possibilità per il nostro ceppo di tollerare la presenza di arsenico. I nostri esperimenti di coltura cellulare hanno dimostrato la capacità di *G. stearothermophilus* di crescere in presenza di arseniato e arsenito in un intervallo di concentrazione paragonabili a quelle di batteri classificati come resistenti all'arsenico. Questi dati supportano l'ipotesi sulla presenza di meccanismi molecolari per affrontare la tossicità di arsenico. È stato anche riportata la possibilità di ottenere nanoparticelle d'oro da un estratto "cell-free" di *G. stearothermophilus*, ciò rientra nella cosiddetto "sintesi verde" delle nanoparticelle. Ciò rende *G.stearothermophilus* un nuovo modello di studio per lo sviluppo di tecniche di *biosensing* dell'arsenico e *bioremediation*.

I nostri risultati confermano la possibilità di utilizzare *Thermus thermophilus* come sistema biologico (cellulari o enzimatiche) per la tracciabilità di inquinanti dopo una approfondita caratterizzazione molecolare, strutturale e funzionale di tutte le componenti coinvolte e delle loro interazioni.

SUMMARY

Arsenic is an ubiquitous toxic metalloid naturally present in the soil, water and air that adversely affects human health. The abundance of arsenic in the environment has guided the evolution of multiple defence strategies in almost all microorganisms which must therefore sense the metalloid and regulate the transcription of genes coding for resistance proteins. In this sense microorganisms participate to the geochemical cycling of arsenic in their living environments, promoting or inhibiting arsenic release from sediment material. The aim of this thesis has been the characterization at molecular level of the mechanisms of arsenic resistance in *T. thermophilus* and the realization of "Cell-Based" and "Enzyme-Based" biosensors for the detection of arsenic species in soils and waters.

The thermophilic gram negative bacterium *Thermus thermophilus* HB27 is able to grow in the presence of both arsenate and arsenite in a range of concentrations which are lethal for other microorganisms. The putative resistance genes have not been found in a single resistance operon but associated to chromosomal genes apparently not functionally related. In particular we found a gene coding for a thioredoxin-coupled arsenate reductase (*Tt*ArsC) which catalyzes the reduction of pentavalent arsenate to trivalent arsenite; two genes (*TTC1447*, *TTC0354*) coding putative ArsB-like transporters; and a gene coding for a transcriptional repressor (*Tt*SmtB) sensitive to arsenic, belonging to the ArsR/SmtB family of transcriptional regulators.

TtsmtB is part of an operon containing putative internal promoters upstream of genes with no obvious functional relationship. The purified recombinant protein is a dimeric DNA binding protein able to bind *in-vitro* to target sequences and to dissociate upon arsenate and arsenite binding. Inactivation of the *TtsmtB* gene, in a *T. thermophilus* *TtsmtB*⁻ mutant strain, induces the expression of the *ars* genes among which *TtarsC* and a putative efflux protein. These results prove that *Tt*SmtB has a functional role in the regulation of the arsenic resistance.

Analysing the *TTC0351*, *TTC0353* and *TTC0354* promoter activities *in-vivo*, through β-galactosidase reporter systems, it has been developed the first whole-cell arsenic biosensor based on the use of the thermophilic microorganism *T. thermophilus*. The biosensor response could be measured with reliability within 30 minutes of arsenate or arsenite addition, and have a minimum detection limit of 0.1 mM for both arsenate and arsenite. An intriguingly feature of this biosensor rely on its thermophilic nature, hence, despite not having a higher arsenic detection limit it could be more versatile, stable and strong in case of highly contaminated waters.

Moreover, it has been developed an enzyme-based biosensor to screen for the presence of arsenic using *Tt*ArsC as biomolecular probe. *Tt*ArsC has been adsorbed on gold nanoparticles (AuNPs) and nanobiocomplexes demonstrating stability and the capacity to strongly bind the toxic ions. Interestingly, TtArsC-AuNPs interaction with arsenic can be followed by naked eye, since solutions completely change their colors. Therefore, a straightforward application in fast and low-cost screening of water can be envisaged.

Finally, *Geobacillus stearothermophilus* has been isolated from a geothermal area near Naples known as Pisciarelli, and has been identified as a new arsenic tolerant microorganism. Our results made *G. stearothermophilus* a novel model of study for the development of new arsenic biosensing and bioremediation techniques and confirm the possibility of using *Thermus thermophilus* as biological systems (cellular or enzymatic) for the traceability of pollutants after a thorough molecular, structural and functional characterization of the components involved and their interactions.

6

Chapter 1

GENERAL INTRODUCTION

1.1. Heavy metals and environmental pollution

Heavy metals have been defined as those metals with atomic number greater than that of the iron [55], with a very high density and that are common cause of environmental pollution and toxicity in biological organisms. This generic definition has been recently considered little scientific and not consistent by a IUPAC (International Union of Pure and Apllied Chemistry) report, so now we refer to heavy metals when they may encounter the following characteristics:

      density exceeding 5.0 g/cm^3
      general behavior as cations
      low solubility of their hydrates
      aptitude to form complexes
      affinity towards the sulphides

In the scientific literature the following elements are normally considered heavy metals: aluminum, iron, silver, barium, beryllium, cadmium, cobalt, chromium, manganese, mercury, molybdenum, nickel, lead, copper, tin, titanium, thallium, vanadium, zinc, and certain metalloids with property similar to those of heavy metals, such as arsenic, bismuth and selenium. Heavy metals can be differentiated in "metals essential for living organisms", that are essential to maintain a proper metabolism but with potential toxicity at high concentrations: iron, cobalt, chromium, copper, manganese, molybdenum, selenium, zinc; and "mainly toxic metals": aluminum, arsenic, beryllium, cadmium, mercury, and nickel.

Heavy metals are the cause of one of the most serious pollution problems of our time. Although in small concentrations, they threaten environment and human health because they are not biodegradable (1). As they are toxic for different biological systems at low concentrations, it is highly required to detect even small traces (2); if unrecognized or inappropriately treated, toxicity can result in significant illness and reduced quality of life. For some heavy metals, toxic levels can be just above the background concentrations naturally found in nature. People have always been exposed to heavy metals in the environment (metallic elements of pesticides and therapeutic agents, metallic contamination of food and water, etc.), particularly in recent years with the increase in the industrial applications of metals (1); therefore it is important to be informed about the heavy metals and to adopt protective measures against overexposure. Nowadays, among the various pollutants widespread in mass in the environment, heavy metals are the most harmful compounds; sulfhidryl groups (SH), normally found in enzymes that control the speed of metabolic reactions in the human body, bind easily to heavy metals, and the resulting metal-sulfur complex inactivates the entire enzyme (3). Heavy metal toxicity can result in damaged or reduced mental and central nervous function, lower energy levels, and damage to blood composition, lungs, kidneys, liver, and other vital organs. Long-term exposure may result in slowly progressing physical, muscular, and neurological degenerative processes that mimic Alzheimer's disease, Parkinson's disease, muscular dystrophy, and multiple sclerosis (4, 5). Repeated long-term contact with some metals or their compounds may even cause cancer (International Occupational Safety and Health Information Centre, 1999) (6, 7).

1.2. Microbial interaction with metals

Microorganisms, which occupy a huge variety of environments, more than three billion years ago, have developed strategies for obtaining energy from virtually every compound. They play a crucial role in sustainable development of the biosphere and in biogeochemical cycles. The abundance of microorganisms, together with their great ability for horizontal gene transfer and their high growth rates, allows them to evolve quickly and to adapt to environmentally changing conditions, even to extreme environments that do not allow proliferation of other living organisms. The great genetic diversity of microorganisms also determined by horizontal gene transfer accounts for their great metabolic versatility (8).

Microorganisms have developed a wide variety of defense mechanisms against metals present in the natural environment, and they have developed metal-responsive transcriptional regulatory proteins that regulate the transcription of genes encoding proteins responsible for metal detoxification, sequestration, efflux and uptake.
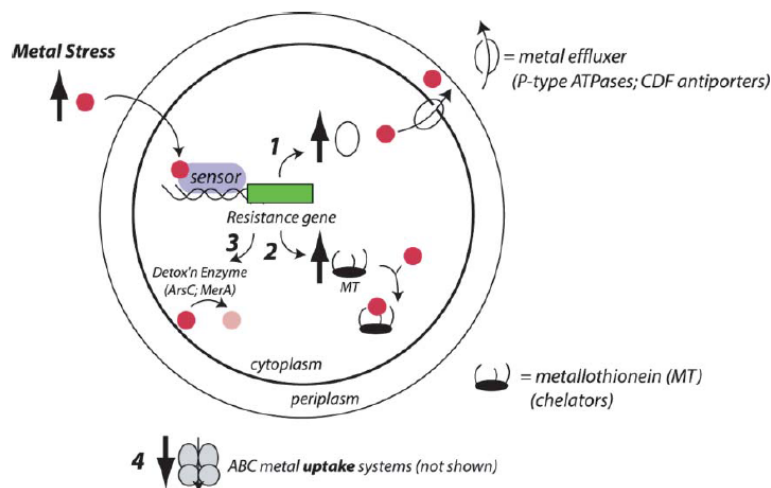

Fig.1. Cartoon representation of how a generic metal sensor protein affects resistance to toxic concentrations of a particular transition metal ion in the cytoplasm (9).

Generally, a microbial detoxification system consists, at least, of a sensor protein, which is a transcriptional regulator of the genes for resistance to metals, a detoxifying enzyme, such as a reductase, and an efflux pump to remove the metals from the cell directly. The metalloregulatory, or metal sensors proteins, directly bind a broad range of specific metal ions, which in turn, regulate allosterically (increasing or decreasing) the binding affinity to target promoters. Structural-functional studies have revealed five distinct families of metal sensors proteins: MerR, ArsR/SmtB, DtxR, Fur and NikR. The families MerR and ArsR/SmtB regulate the expression of genes needed for metal ion detoxification, efflux and sequestration; here, metal binding results in the activation (MerR) or derepression (ArsR/SmtB) of the resistance operon. In contrast, the families DtxR, Fur and NikR regulate genes coding for proteins involved in metal ion uptake; in these cases, the metal ions function as co-repressors to switch off the genes of metal uptake at defined concentrations of metal (10).

1.3. Biochemistry of arsenic

Arsenic is a metalloid of the VA group of the periodic table toxic to the environment and humans (11). In nature it is present in four different oxidation states: arsenite As(III) and arsenate As(V) are the most common, while the elemental arsenic (0) and arsenide As(-III) are rare (12-14). The main chemical-physical factors that control the speciation of arsenic are the pH and the redox potential (15). The metalloid is found in sediments, water and soil both in inorganic form, where in oxidizing conditions prevail the pentavalent arsenic ($H_2AsO_4^-$ or $HAsO_4^{2-}$) and under reducing conditions ($As(OH)_3$ or rarely $H_2AsO_3^-$) the trivalent one (16, 17), and in organic form as the monomethylarsonic acid (MMA) and dimethylarsinic acid (DMA). Disclosure of organic arsenic is lower than inorganic forms. Since arsenic has different valence states, its treatment and removal from the contaminated sites is hindered.

The main sources of arsenic are natural (mineralized areas, volcanic areas, hot springs), but its accumulation is due to human activities such as the use of pesticides, mining, waste treatment and industrial activities (18). In humans, arsenic is used to treat some forms of leukemia, but generally exposure to this metalloid causes the development of various diseases, including cancer, skin damage, gastrointestinal disease, and neuropathies (11, 19-21).

Man can take arsenic through the consumption of contaminated water and cereals grown on contaminated soil, especially rice (18, 22). In this regard it was set an arsenic maximum limit in drinking water of 10 mg/L (WHO 1996).

The arsenic toxicity depends on its chemical structure. The arsenate is a structural analogue of phosphate, it is transported across cell membranes by the specific transporters of the phosphate (Pts) or the transporter Pit (23), competing with this essential ion for many enzymatic reactions (24); it interferes with oxidative phosphorylation and with the substrate phosphorylation (25) depriving cells of their energetic reserves.

The arsenite can be transported by the aquaglyceroporins (GlfP in *E. coli*; (26)) and sometimes by sugar transporter systems, as the hexose permease in yeast (27) or glucose permease in mammalian cells (28). Moreover, it has a high affinity for thiol groups, so it can inhibit many enzymes which have cysteines in critical positions (29, 30). Therefore, due both to its increased bioavailability in environments at neutral or acid pHs, and to the protein inhibition ability, it is more toxic and dangerous of the arsenate.

Microorganisms play an important role in the biogeochemical cycling of arsenic (31) and respond in different ways to the presence of arsenic in the environment. Because of its toxicity, the organisms have developed metabolic mechanisms of resistance (13) such as chelation, partitioning, exclusion and immobilization (32). Some microorganisms actively use arsenic compounds in their metabolism as electron donors in the case of arsenite (33-35), or as a terminal electron acceptor for anaerobic respiration for the arsenate (36, 37). Others are also able to methylate the inorganic arsenic (38), or de-methylate the organic forms (12).

The arsenic methylation involves different steps in which the reduction of the pentavalent form is followed by the oxidative addition of a methyl group (29) generating an increasing series of chemical species: methyl arsenite (MMA), dimethyl arsenate (DMA-V), dimethyl arsenite (DMA-III) and trimethylarsine oxide (TMAO). The methylation reactions require S-adenosylmethionine (SAM) as a source of methyl groups. The *arsM* gene defines all the steps of the SAM-dependent methylation, it has recently been identified in more than 120 prokaryotic species (and

several archaea), and further characterized in *Rhodopseudomonas palustris* (38). The soluble methylated compounds are much less harmful than inorganic arsenic, whereby these microorganisms have a potential use in bioremediation strategies based on methylation (39-43). De-methylation reactions, necessary to complete the arsenic geochemical cycle, are not well known. Results obtained by Yoshinaga et al. (44) indicate that the de-methylation does not necessarily follow the reverse path of methylation. However, the full paths and the factors involved in de-methylation reactions are currently unknown.

The ability to oxidize the arsenite has been known from long time (45) and seems to be widely distributed among bacteria (14, 46). Some are able to use arsenite as the only energy donor, togheter with the oxygen reduction or the nitrate respiration (33, 35, 47, 48). In the most known organisms as *Rhizobium* NT-26 (49) and *Hydrogenophaga* NT-14 (50), the reaction is catalyzed by the arsenite oxidase AioAB (51), an heterodimeric molibdoenzyme of the DMSO reductase family. Recently, a new arsenite oxidase, ArxAB, was discovered in *A. ehrlichii* MLHE-1 and also found in the *Ectothiorhodospira* PHS-1 strain (52, 53); this enzyme catalyzes the anaerobic arsenite oxidation in the presence of nitrate and it also belongs to the DMSO reductase family, nevertheless it was found to be distinct from AioAB (14).

In bacteria two different activities for the arsenic reduction have been found. One is the respiratory reduction which involve the arsenate as electrons terminal acceptor. It is performed by respiratory arsenate reductase encoded from the *arr* operon, which includes *arrA* and *arrB* genes (54). The ArrAB heterodimer is a member of the DMSO reductase family. In *C. arsenatis*, the large ArrA subunit (87 kDa) contains a Mo atom and a [4Fe-4S] center, while the small ArrB subunit (29 kDa) presumably contains several other Fe-S units (55).

The second is a reduction mechanism of the arsenate in arsenite, which becomes the substrate of efflux pumps that allow the extrusion.

1.4.   Arsenic detoxification mechanism: *Ars* system

Arsenic tolerance in the bacteria is usually mediated by the gene products of *ars* operon (13, 56). Although the right operon organization varies considerably among different species, there are some key genes which are always present: the gene set which confers a basal resistance consists in the *ars*RBC operon, present in the *E. coli* genome (56) and in the *Staphylococcus aureus* plasmid pI258 (57). There is also a set of five genes *ars*RDABC, found in the *E. coli* plasmid R773 (58), that provides resistance to higher arsenic concentrations. Both operons may be found in the same microorganism, such as in *T. arsenitoxidans* 3As (59), and may contain other genes related to arsenic resistance, for example, *arsH* (6, 60) or *arsN* (61).

The gene *arsC* encodes a small cytoplasmic arsenate reductase which converts arsenate into arsenite (62), that is extruded from the cell by the action of a transmembrane transporter encoded by the *arsB* gene. In organisms that have the *arsA* gene, its gene product, an ATPase, is coupled to *arsB* and significantly increases the levels of resistance (13). The *arsR* gene encodes a trans-agent repressor belonging to the ArsR/SmtB family, involved in the metal sensing and in transcriptional regulation; the *arsD* product acts as metallochaperon assisting the transfer of arsenite to the ArsA subunit of the ArsAB complex activating it (63, 64).
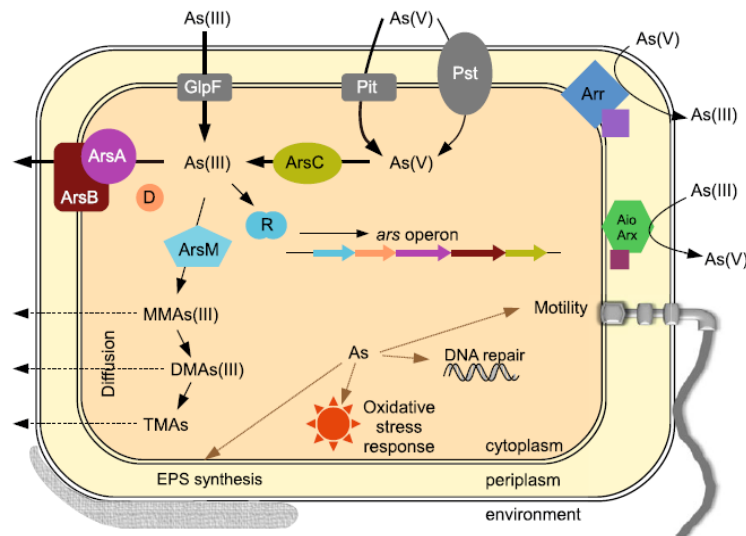
Fig. 2. Overview of bacterial interactions with arsenic. The metalloid is taken up through glycerol or phosphate transporters. Arsenate is reduced to arsenite which may then be extruded from the cell by ArsAB. Alternatively, it is methylated by ArsM, forming the volatile intermediates monomethyl arsenite (MMAs(III)), dimethyl arsenite (DMAs(III)), and trimethyl arsine (TMAs). The presence of arsenite controls expression of the ars operon and has influence on various processes including motility, EPS synthesis, DNA repair, and oxidative stress response. Arsenic outside the cytoplasm may be used for energy gain by arsenite oxidation or anaerobic respiration by arsenate reduction (65).

ArsC families

The first enzyme involved in the arsenic detoxification process is the arsenate reductase which catalyzes the conversion of the arsenate in arsenite (66, 67); in bacteria at least three distinct enzyme families are known.

The members of the first family are encoded by homologous of the *arsC* gene found on the *E. coli* R773 plasmid (R773 ArsC; (58)) and they use the couple glutaredoxin (Grx) and glutathione (GSH) as electron donor for the reduction of the arsenate (68).

The second family of arsenate reductases is related to proteins of the tyrosine phosphate phosphatase family. A characterized member is Acr2p from *Saccharomyces cerevisiae* (69).

The third family includes *S. aureus* pI258 plasmid *arsC* homologous (Sa_ArsC; (66, 67)) and use the thioredoxin for arsenate reducing (70); they are linked to the low molecular weight phosphatases family (LMWP) (71).
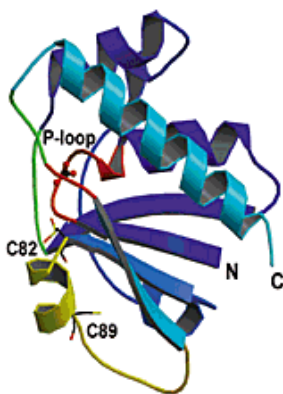

Fig. 3. Structure of *S. aureus* pI258 ArsC. Overall structure of the reduced form of arsenate reductase. The catalytic site region is shown in red, and the part of the protein involved in the redox function in yellow. The area of ArsC corresponding to the Tyr binding site in LMW PTPase is shown in green (71).

12

A well characterized member of this family is ArsC from the Gram+ *B. subtilis*. The protein conserves the three redox cysteines typical of the family and is a monomer in solution; the structure is a single αβ domain containing a central four-stranded, parallel open-twisted β-sheet flanked by α-helices on both sides (72).

Among the characterized arsenate reductases, it has been recently characterized the catalytic activity of *Tt*ArsC from the thermophilic bacterium *T. thermophilus* HB27 (73). *TtarsC* encodes a protein of 150 amino acids (16957.49 Da; pI 6.53) containing the three cysteine residues, Cys7, Cys83 and Cys90, conserved among the bacterial thioredoxin-coupled arsenate reductases and playing a key role in the catalysis. It also contains the anion binding site known as the P-loop (or the CX_5R motif) and the Asp-Pro sequence in which Asp serves as catalytically important acid–base in LMWP. *Tt*ArsC reduces arsenate to arsenite using electrons coming from the Tr–Trx system, with a catalytic mechanism involving the thiol group of the N-terminal Cys residue (Cys7); it also shows a weak phosphohydrolase activity confirming the functional correlation with ArsC from *S. aureus* pI258 (73).

Arsenite extrusion mechanism: ArsA and ArsB

In the canonical *ars* operon with three genes, the system that allows the arsenite extrusion is constituted by a secondary carrier protein ArsB (74), a protein with 12 transmembrane α-helices which constitutes the channel through which the arsenite is extruded from the cell. It acts as a secondary antiporter carrier $As(OH)_3/H^+$, using the membrane potential to extrude As(III) (75).

For the *arsRDABC* operon, there is the additional presence of ArsA and ArsD proteins that increase the effectiveness of the efflux arsenite system. It is striking that the *arsD* and *arsA* genes are always together in arsenic resistance bacterial operons and this has led to assume that the *arsRDABC* operons have evolved from *arsRBC* by inserting of the *arsD* and *arsA* genes (76, 77).

ArsA is the catalytic subunit with ATPase activity, ruled by arsenite. It contains two internal repetitions, A1 and A2, linked by a linker region of 25 amino acids, each of them presents the ATP-binding domains (NBD-nucleotide binding domain). For the ArsA activation, an interaction with As(III) is required, in fact only in response to this binding the two NBD domains come to be in contact resulting in the ATP hydrolysis (76).

ArsD is present as a homodimer and has a role of chaperone; it has a high affinity binding site for arsenite and determines its transport to the ArsAB pump, increasing the extrusion efficiency. Upon interaction between ArsD and ArsA, a conformational change is induced which, on one hand reduces the affinity of ArsD for the arsenite, on the other stabilizes the arsenite ArsA binding site, facilitating its transfer from ArsD to ArsA (77, 78).
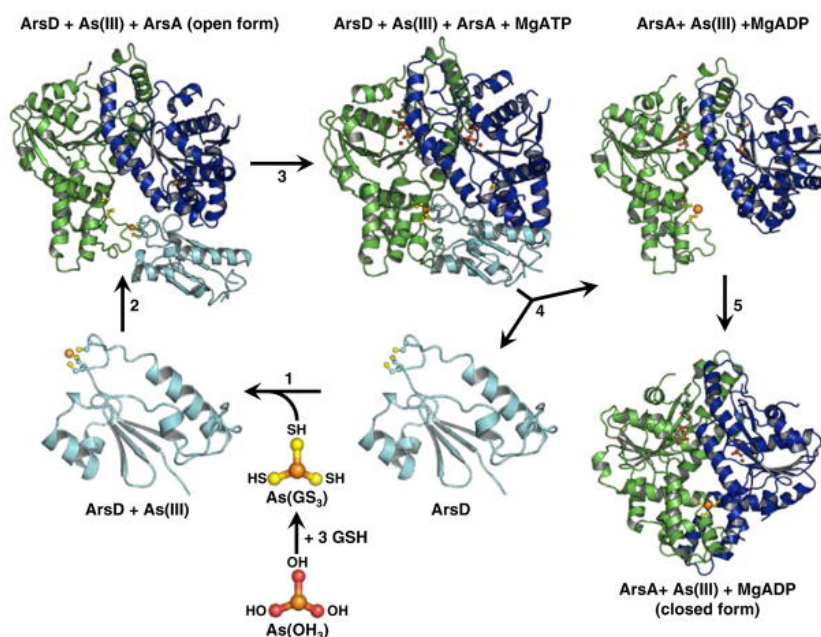
Fig. 4. Proposed reaction scheme for transfer of As(III) from ArsD to ArsA. In the cytosol As(OH)$_3$, the solution form or arsenite, reacts with 3 GSH to form As(GS)$_3$, the arsenic donor to ArsD. *Step 1* ArsD binds As(III) by exchange of the three thiols of As(GS)$_3$ for the thiols of cysteines residues Cys12, Cys13 and Cys18. Although ArsD is a dimer, the structure of the monomer of apoArsD is shown. *Step 2* As(III)-bound ArsD binds to the open form of ArsA. *Step 3* As(III) is transferred in a step-wise exchange from the three thiols of ArsD to the thiols of Cys113, Cys172 and Cys422 of ArsA. *Step 4* Transfer of As(III) results in dissociation of the ArsD-ArsA complex. *Step 5* As(III)-bound ArsA undergoes a conformational change in ArsA to the closed form concomitant with activation of ATP hydrolysis (77).

Transcriptional regulation: ArsR/SmtB family

The SmtB/ArsR family represents a class of transcriptional regulators which confers the ability to respond to stress induced by heavy metal-toxicity. The SmtB/ArsR members function exclusively as transcriptional repressors; when the apo-sensor proteins are bound to the operator/promoter (O/P) DNA, the resistance operons are repressed; metal binding strongly inhibits DNA binding (79).

The first transcriptional repressor characterized of SmtB/ArsR family belongs to the cyanobacterium *Synechococcus* PCC 7942, it is encoded by the locus *smt*, which contains an *smtA* gene coding for a metallothionein of class II and an *smtB* gene coding for an *smtA* transcriptional repressor (80).

The recombinant form of SmtB from *Synechococcus* PCC 7942 is predominant as an asymmetrical dimer. (81). The X-ray crystallographic structure of SmtB confirms that the protein crystallizes as a dimer with two putative helix-turn-helix (HTH) DNA binding domains, one in each subunit (82).

Each monomer has a α/β folding, containing five α-helices and two β-sheets arranged as follows: α1- α2- α3- αR- β1- β2- α5 (82). The region between the α3 and αR helices form the helix-turn-helix motif, which has a strong structural similarity to the domain of other transcriptional regulators including the CAP (Catabolite Activator Protein) (83).
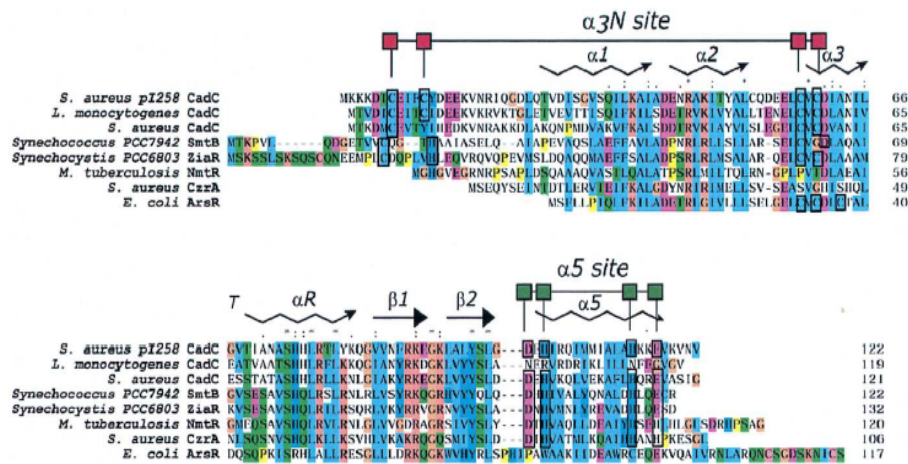
14

Fig. 5. Alignment of amino-acid sequences of ArsR/SmtB family members, with highlighted five α-helices and two β-sheets, the HTH motif and the α3N and α5 metals binding sites (79).

Residues of α1-2-5 helices of each monomer form a hydrophobic core of the dimer that is mainly useful as scaffold for the correct HTH motif orientation. α1 and α5 helices of a monomer are adjacent and antiparallel to the corresponding helices of the other monomer. These four helices shape two surfaces of the dimer, while the other two α2 helices shape each end of the hydrophobic core. αR is called recognition helix and binds the DNA major groove. In each monomer there are two antiparallel β-sheets called β1 and β2. The hairpin structure, which is formed immediately after the recognition helix, is anchored by hydrophobic interactions and hydrogen bonds. (82).

ArsR/SmtB family members have a highly conserved sequence ELCV(C/G)D at α3 helix level, defined as 'metal binding box' (82, 84) which contains residues involved in metal coordination and thus is directly involved in the detection of the metal ion. It was hypothesized that these Cys residues bind the metal by formation of metal-thiolate bonds, and then inhibit the interaction of the adjacent helix-turn-helix region with the DNA (85). This hypothesis was confirmed by the fact that the replacement of one or both of the cysteine residues with a non-binding metal residue, inhibits the ability of the arsenic to dissociate ArsR from the promoter/operator region (85). The absorption spectroscopy of As(III)-ArsR revealed that As(III) is coordinated by three cysteine residues inside of the α3 helix, two of that are clearly derived from ELCVCD motif (85).

Metal binding sites are referred as α3N and α5; some ArsR/SmtB family members own only the α3N site, such as CadC from *Listeria monocytogenes*; others have only the α5, as CzrA and NmtR; while others else contain both sites; this is the case of Smtb, ZiaR and most of the CadC. The α3N site is constituted by three or four reduced cysteines , two of them are derived from the CXC sequence within the metal binding box in the α3 helix, while the remaining residues are derived from the N-terminal region. The α5 site, however, includes four residues that derive exclusively from the α5 helix C-terminal end.

CzrA, SmtB, NmtR, and CadC share a DHHX region which binds the zinc at α5 site level and it has been observed that the binding of the metal in SmtB and NmtR triggers an allosteric response that pushes the protein to an open conformation with a lower binding affinity for the DNA (86).

All the operons regulated by metals contain sequences in their promoter for the binding of the protein; in particular one (or two) 12-2-12 imperfect inverted repeat

sequences, which are generally located close to, or overlying, the transcription start site of the regulated gene or operon. The *smt* operon is the only one with two similar repeated sequences, named "S2/S1" and "S4/S3". The S2/S1 repetition is required for the regulation of *smtA* gene expression, while the S4/S3 repetition has a minimal effect on the regulation of *smtA* expression. The alignment of inverted repeat sequences derived from: the promoter region of the *ziaR* gene in *Synechocystis*, the promoters of the *czr* gene of *S. aureus* and *nmtR* gene of *M. tuberculosis*, *cadC* of *S. aureus* and in the *E. coli ars* operon, suggested distinct consensus sequences for the α3 and α5C sensors. The 12-2-12 inverted repeat sequence, with a consensus sequence like aAtAxxTGAaca-xxtatTCAxaTxtt can be found in *smt*, *zia*, *crz* and *nmt* a; in *cadC* and *ars*, , the presence of a 6-2-6 sequence, belonging to the 12-2-12 repetition has been found (79).

Fig. 6. Comparison of the conserved 12-2-12 inverted repeat of SmtB/ArsR-regulated O/Ps. Alignment of the imperfect, hyphenated 12-2-12 inverted repeats from the *Synechococcus smt* O/P (S2/S1, S4/S3), *Synechocystis zia* O/P, *S. aureus czr* O/P, *M. tuberculosis nmt* O/P, *S. aureus* pI258 *cad* O/P, and *E. coli* R773 *ars* O/P (79).

Given the arrangement of the SmtB homodimer and of the12-2-12 inverted repeat, one would expect that a homodimer could bind to a single inverted repeat, with the recognition helix that binds the DNA major groove. Recent studies have shown that the binding occurs by two dimers to a single repetition. It is interesting to note, however, that the region containing the "S2/S1" and "S4/S3" sequences binds only two dimers, and not the four expected. This suggests that the two sites can form a loop structure, stabilized by dimer-dimer interactions (79).

1.5.   *Thermus thermophilus*

Microorganisms are increasingly being used as specific devices for sensing biologically relevant concentrations of pollutants (87), but, to date, progress in this field is limited due to incomplete biological information regarding the molecular mechanism of degradation and detoxification of environmental contaminants in many microbial communities (88). As thermophilic organisms are also part of peculiar geochemical cycles in hostile environments, they represent an interesting model system for defining the ability to cope with metal stress under rapidly changing conditions.
Thermus thermophilus is an aerobic Gram-negative thermophilic bacterium, that grows at temperatures ranging from 50° and 82°C, it is very used in laboratories due

to its high growth rates, cell yields of the cultures, and the constitutive expression of an impressively efficient natural competence apparatus (89, 90).

Between the species of *Thermus* genus, a genomic complete sequence analysis was carried on *T. thermophilus* HB8 and HB27. HB27 strain was originally isolated from a natural thermal environment in Japan by Oshima and Kazutumo; its optimal growth is at 74°C and at pH 7.0. Many thermophilic organisms are strictly anaerobic, as a result of an adaptation to the low solubility of oxygen at these temperatures. However the *Thermus* gender is an exception: *T. thermophilus* HB8, for example, can grow in anaerobic conditions by complete or partial denitrification, or using heavy metals as final acceptors of the anaerobic respiration. HB27 strain, nevertheless, cannot grow in anaerobic conditions. *T. thermophilus* cells morphologically appear as thin bacilli, which tend to form filaments able to divide by binary division. *T. thermophilus* envelope consists of four layers. As all Gram-negative bacteria, it is surrounded by an outer membrane composed primarily of phospholipids and lipopolysaccharides, and a thin layer of peptidoglycan, responsible for the structural rigidity of the cell; this last is itself surrounded by amorphous material, covalently linked to the peptidoglycan (90). *T. thermophilus* HB27 genome is composed by a chromosome (TTC) of 1.894.877 bp and a megaplasmid (TTP) of 232.605 bp, named pTT27. GC content is medially 69.4%. Regions that show a low GC content are ribosomal RNA cluster (91, 92).
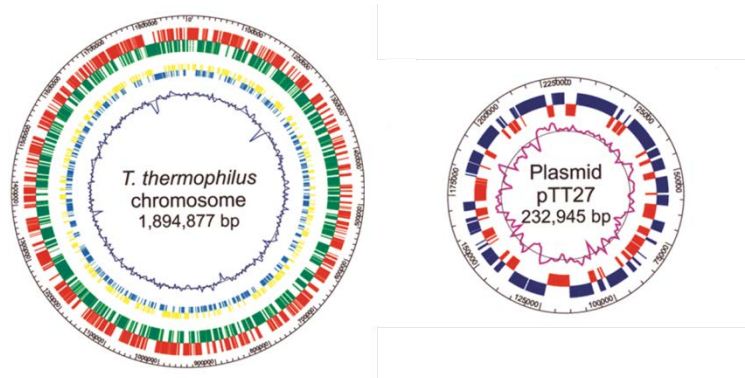
Fig. 7. Maps of *T. thermophilus* HB27 chromosome and plasmid.

T. thermophilus cells, in addition to being constitutively and highly competent for natural transformation (93), are non-discriminatory with respect to the source of the DNA externally added and this allows an efficient introduction of heterologous DNA and genetic modification. For these reasons *T. thermophilus* has been widely used as host for libraries construction of large inserts and it is considered a good candidate for the functional screening of genomic and metagenomic library at elevated temperatures. Several genetic systems have been realized for *T. thermophilus* and, to date some cosmids, fosmids, and BAC vectors with a replication origin in single copy or alternatively multi-copy inducible origins are therefore available (94).

One of the first vectors developed is the shuttle vector pMK18 obtained through the fusion of the replication origin from a natural *Thermus* sp. ATCC27737 plasmid, a gene coding for a thermostable kanamycin resistance and the pUC18 replication origin and multiple cloning site. The pMK18 plasmid showed an high transformation

efficiency (10^8-10^9 for microgram of plasmid) in *T. thermophilus* HB8 and HB27, both for natural competence and by electroporation. It was shown that *T. thermophilus* HB27 can acquire the pMK18 modified by the *E. coli* methylation system with the same efficiency with which it acquires its DNA. To demonstrate its utility as a cloning vector, the gene encoding the β subunit of a thermostable nitrate reductase was cloned. The possibility of a further transfer to *E. coli* has demonstrated its utility as a shuttle vector (95).

Genetic manipulation has also been addressed to inactivate genes (knockout); for example it has been generated a strain in which the gene coding for the malate dehydrogenase has been inactivated (Δ*mdh*). The system has also been used as a reporter to quantify the *T. thermophilus* promoters strength cloned upstream of the *mdh* gene (96).

Two versatile shuttle vectors for *T. thermophilus* and *E. coli*, based on the *T. thermophilus* pTT8 plasmid and the *E. coli* pUC13 vector have also been developed. These shuttle vectors, named pTRK1T and pTRH1T, have a gene that encodes a protein homologous to replication proteins derived from pTT8, a replicon for *E. coli*, new multiple cloning sites and a lacZα gene of the pUC13vector and also a gene that encodes a thermostable protein which confers resistance to kanamycin or hygromycin, which may be used as a selection marker in *T. thermophilus*. These shuttle vectors are useful to produce enzymes and proteins of biotechnological interest. These carriers should facilitate the procedures for cloning both in *E. coli* and in *T. thermophilus* (97).

T.thermophilus has also been used for the overexpression of thermostable and thermoactive enzymes and their improvement through directed evolution as for example the Mn-dependent catalase and the DNA polymerase (98).

The use, instead, of an expression vector containing the *T.thermophilus* β-glucosidase gene (*bgl*) as a reporter in combination with a host strain lacking the two putative β-galactosidase genes (Δ*bgl*) has allowed the study of the gene expression by assaying the β-galactosidase activity with the 2-nitrophenyl-βD-glucopyranoside as substrate at 80°C (99).

It has also been reported the use of a GFP variant as an *in vivo* tag, the *superfolder* GFP (sGFP), a variant of the green fluorescent protein that efficiently folds when it combines with misfolded proteins, and is functional *in vivo* at 70°C in *T. thermophilus* (100).

Some thermophilic bacteria belonging to the genus *Thermus*, isolated from different geothermal vents, have the ability to use arsenate for respiration (*Thermus* sp. HR13) and to rapidly oxidize arsenite (*T. aquaticus* and *T. thermophilus*), but nothing is known about their *ars* systems. A preliminary analysis of the genome of *T. thermophilus* HB27 evidenced, the presence of putative components of the arsenic detoxification system interspersed in the chromosome; in particular: the ORF *TTC1502* encoding a putative arsenate reductase (ArsC), two genes (*TTC1447*, *TTC0354*) encoding putative ArsB-like transporters and one gene encoding a transcriptional regulator belonging to the ArsR/SmtB family (*TTC0353*). It was also found a single putative *arsB* gene in the natural plasmid pTT27 (*TTP0033*) of *T. thermophilus* (66, 73).

Growth of *T.thermophilus* HB27 showed tolerance to concentrations of arsenate and arsenite up to 20 mM and 15 mM, respectively. Investigation on the molecular mechanism underlying this arsenic resistance, started from the identification, characterizationand regulation of the arsenate reductase (*Tt*ArsC) (see paragraph 1.4; (73)). These results identified *Tt*ArsC as an important component in the arsenic

resistance in *T. thermophilus* giving the first structural-functional characterization of a thermophilic arsenate reductase; a more clear vision of the *T. thermophilus ars* system, requires the study of the other components of the system, such as the putative transcriptional regulator *Tt*SmtB (encoded by *TTC0353*) and the ArsB-like transporter (encoded by *TTC0354*).

1.6.   Environmental biomonitoring

As told before, arsenic is a ubiquitous toxic metalloid that contaminates both groundwater sources (101, 102) and soils (103) worldwide. Strikingly, more than 100 million people in the world are at risk from consuming water contaminated by arsenic (104), and strategies to detect and prevent this global problem are urgently required.

There are currently two widely used methods of arsenic detection in drinking water: laboratory-based analytical methods and field-based testing methods (105). The laboratory-based analytical methods require highly trained personnel and expensive analytical machinery, such as inductively coupled plasma mass spectroscopy (ICPMS) and atomic absorption spectroscopy. Further, the delay in turnaround time between specimen collection and result availability limits their day-to-day use. Field-based testing methods are largely chemical colorimetric assays, such as the Gutzeit method, which generate toxic arsine gas by reducing

arsenic with a strong acid, that is not ideal to transport and handle in the field (105). These tests require the use of hazardous chemicals and can generate toxic byproducts. So different chemical methods have been developed to treat polluted sites, but the problem persists given the necessity to dispose the treated waste and any, probably even more toxic, chemical byproducts. Biosensors and bioreporters are beginning to emerge as safe, alternative methods to detect environmental pollutants such as arsenic (106).

A biosensor can be utilized as a rapid and sensitive method to detect and quantify such toxic species; these type of biosensors rely on the analysis of the expression of a reporter gene that is controlled by a promoter responsive to a particular toxic compound (88).
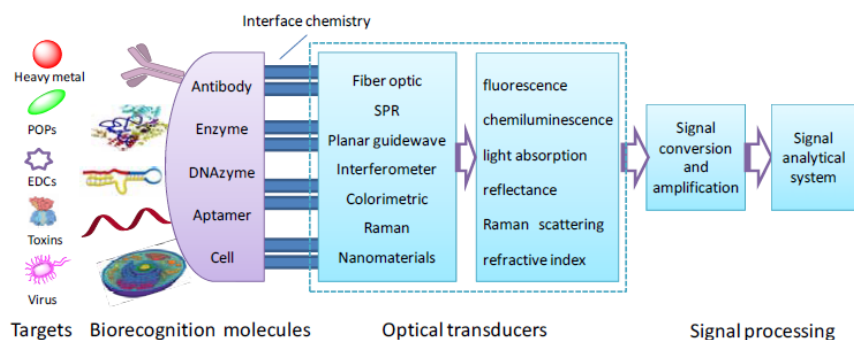

Fig. 8. Schematic representation of an optical biosensor (107).

A variety of well characterized promoters are available for genetic manipulations, for example promoters of various heavy metals (108), aromatic aldehydes (88), hydrocarbons (109), pesticides (110), and salicylates (111). The most-used reporter

genes are: *lacS*, encoding a β -galactosidase, whose enzymatic activity can be determined by a colorimetric reaction; luciferase genes (*lux*) (112) or the gene for Green Fluorescent Protein (GFP) (113), that can be detected by bioluminescience and spectrofluorimetry, respectively.

There are a lot of biotechnological bio-sensing applications; for example a whole-cell biosensor has been reported to detect aqueous concentrations of aromatic aldehydes (88). This biosensor was based on an *E. coli* Bl21DE3 strain containing: a fusion transcriptional hybrid between an aromatic aldehydes responsive archaeal promoter (*S. solfataricus adh* promoter) and the *gfp* gene; moreover, on a different compatible plasmid, the gene for the BldR sensor protein (114). This system responded to benzaldehyde, cinnamaldehyde and salicylaldehyde at millimolar concentrations (88).

Within the biosensors development , an important role is played by transcription factors (TFs), they are natural sensory proteins that have evolved to regulate gene expression in response to environmental changes or key intracellular signals that need tight control. Hence, it is not surprising that one straightforward approach to exploit TFs for high-throughput screening is to hack into the host transcription system and employ a synthetic or native condition-specific promoter to drive the expression of a reporter gene (115). In addition to the inherent regulatory potential of TFs, the high degree of modularity also makes TFs a superb starting point for biosensor development. TFs contain at least a protein interaction domain to recruit transcriptional machinery, as well as a DNA binding domain (DBD), which often resides in proximity to the metabolite-binding domain (MBD). The high degree of modularity makes it possible to engineer specifically the MBD to improve its affinity and selectivity towards a new molecule (115).

Reported arsenite-induced bacterial biosensors utilize the regulatory machinery of the arsenite-responsive transcriptional repressor ArsR to control expression of reporter genes in response to arsenite exposure, which directly take advantage of the wild-type regulatory expression machinery. In this category has been reported a color-based bacterial biosensor for measuring arsenic by eyes or measured by spectrometer. The biosensor was based on the *arsR–lacZ* recombinant gene cassette *E. coli* DH5α. It demonstrated a quantitative range of sensing from 10 to 500 μg L^{-1} of As in 3-h reaction time (116). Because the whole arsenite sensing element needs a basal level of *arsR* expression to function, the genetic background could not be avoided. The basal genetic background will reduce sensitivity and detection limit of arsenite-responsive biosensors, thus limiting their applications in in-field detection; it has been described a method to obtain a more sensitive arsenite-responsive biosensor with directed evolution. Li L. et al. (117) constructed an arsenite-inducible vector with GFP as the reporter gene, pUC18-ars-gfp; then, iteratively, multirounds of directed evolution were applied to improve the arsenite-sensing element and seek for the improved mutants. The biosensor plasmids were transformed into *E. coli* DH5α, and the performance of the final evolved mutant was examined in comparison with that of the wild-type biosensor. The evolved arsenite-responsive biosensor demonstrated an excellent performance in the detection of low trace arsenite in environmental water (117).

It has also been reported an example of tunable cell-based arsenic sensor (118); since the receptor protein both detects the target ligand and acts to activate/repress the target promoter, they expected that the concentration of receptor in the cytoplasm would determine the sensing sensitivity for the ligand as well as the transcriptional dynamic range of the cognate-inducible promoter. Thus, the density of the

intracellular receptor could function as a dial to tune continuously the sensitivity and dynamic range of the gene expression system. They used the arabinose inducible P_{BAD} promoter to express ArsR and achieve continuous tunability of ArsR density in the *E. coli* cytoplasm by externally added arabionose; the dose–response results show that the response sensitivity and dynamic range of the ArsR sensor module are both increased with the decrease of the arabinose induction level. These results confirm that the synthetic ArsR receptor-mediated sensor for $NaAsO_2$ can be significantly tuned by lowering its receptor density in the cytoplasm to meet the practical sensing limits required in real-world applications (118).

To date, bacterial biosensors are mostly based on the use of mesophilic microorganisms, but thermophilic microorganisms could be good candidates for the construction of more stable and stronger cellular or enzymatic biosensors. The advantages of using thermophilic microorganisms are related to their higher resistance to the temperature and caotropic agents or detergents often present in industrial off-loads and wastewaters.

1.7. Enzymatic biosensors: a general vision

Together with cellular biosensors to detect heavy metals, several examples of enzyme biosensors have also been described, such as the use of the inhibitory effect of mercury on the urease enzyme to obtain indirect concentration measurements of the metal (119).

The enzymatic biosensors are based on enzymes in intimate contact with the transducers. Several materials, which function as transducers, can be used for the immobilization of enzymes, such as:

- *Porous silicon* (PSi); it is an almost ideal material as transducer due to its porous structure, like a natural sponge, having a specific surface of the order of 200–500 m^2 cm^{-3} (120), moreover, PSi is an available and low cost material. PSi biosensors are generally optical biosensors which combine the advantages of simplicity of sample preparation with ease of integration into high-throughput arrays. Transduction methods include surface plasmon resonance, thin-film interference and optical waveguide technologies (121).

- *Graphene*; it has received considerable attention in the field of sensing due to its unique physicochemical properties such as large surface area to volume ratio, acceptable biocompatibility, excellent thermal and electrical conductivity, low cost, safety and ease of production. Graphene also offers a direct electron transfer between the functionalized graphene and active site of bioreceptor without involvement of any mediator and all these features make it a suitable material for electrochemical sensors (122).

- *Zinc oxide* (ZnO) *nanoparticles*; ZnO is a semiconducting material that exhibits high surface area to volume ratio, high biocompatibility, highly stability, biomimetic, less toxicity and has a good electron transferring feature. ZnO nanoparticles are good sources for immobilization of proteins due to the high isoelectric point (122).

- *Gold nanoparticles* (AuNPs); AuNPs are biocompatible and extensively employed as stable immobilizer for biomolecules. They have high specific surface area, high surface energy, high conductivity and offer numerous adsorption sites to antibodies, enzymes and proteins which make them an ideal choice for biosensors (122).

Researchers currently have a variety of immobilization methods at their disposal, including covalent attachment, entrapment, encapsulation and cross-linking. While

covalent attachment can provide an avenue to form a permanent bond between the functional groups of the protein and those of the substrate, the reactions are typically slow, laborious, and the experimental conditions required for such reactions can be detrimental to both the protein and electronic properties of the substrate. Alternatively, proteins can be entrapped within a highly cross-linked polymer matrix or encapsulated within a membrane (123).

Anyway, the mainly used method for the enzyme immobilization for all the above materials is the adsorption. Physical adsorption on a certain carrier is one of the oldest and simplest methods. Usually, enzyme adsorption implies neither additional chemical reagents nor activators; therefore, this is the least denaturing method of immobilization, which provides retention of the enzyme activity. Additionally, adsorption is commercially attractive due to its low cost if compared with other immobilization methods. Lately, use of different nanostructured materials became one of the most common approaches in immobilization techniques (124).

1.8. Aim of the work

The aim of this thesis has been centred on three main objectives:

A)   Characterization at molecular level of the mechanism of arsenic resistance in *T. thermophilus*; this objective has been achieved through the following points:

1. Identification and functional characterization of the transcriptional regulator *Tt*SmtB, belonging to ArsR/SmtB family and generation of a *T. thermophilus Ttsmtb*⁻ strain (chapter 2.1).
2. Evaluation of the interaction of *Tt*SmtB with other protein components by pull-down and mass spectrometry assays (chapter 2.2).
3. Expression of *Tt*SmtB in *T. thermophilus* HB27 (chapter 2.3).

B)   Realization of biosensors for the detection of arsenic species in soils and waters:

1. Identification and *in-vivo* analysis of responsive regulatory sequences for the realization of a "Cell-Based" biosensor based on *Tt*SmtB functionality (chapter 3.1).
2. Realization of an "Enzyme-Based" nanobiosensor based on the arsenate reductase *Tt*ArsC (73) (chapter 3.2).

C)   Identification of new arsenic tolerant microorganisms and the characterization of their resistance mechanism (chapter 4).

Our results confirm the possibility of using biological systems (cellular or enzymatic) for the traceability of pollutants after a thorough molecular, structural and functional characterization of the components involved and their interactions.

References

1.   **Verma N, Singh M.** 2005. Biosensors for heavy metals. Biometals **18:**121-129.
2.   **Bontidean I, Berggren C, Johansson G, Csoregi E, Mattiasson B, Lloyd JA, Jakeman KJ, Brown NL.** 1998. Detection of heavy metal ions at femtomolar levels using protein-based biosensors. Analytical Chemistry **70:**4162-4169.
3.   **Geng CN, Zhu YG, Hu Y, Williams P, Meharg AA.** 2006. Arsenate causes differential acute toxicity to two P-deprived genotypes of rice seedlings (Oryza sativa L.). Plant and Soil **279:**297-306.
4.   **Jain CK, Ali I.** 2000. Arsenic: Occurrence, toxicity and speciation techniques. Water Research **34:**4304-4312.
5.   **Thakur JK, Thakur RK, Ramanathan AL, Kumar M, Singh SK.** 2011. Arsenic Contamination of Groundwater in Nepal-An Overview. Water **3:**1-20.
6.   **Paez-Espino D, Tamames J, de Lorenzo V, Canovas D.** 2009. Microbial responses to environmental arsenic. Biometals **22:**117-130.
7.   **Rosen P.** 1971. Theoretical significance of arsenic as a carcinogen. J. of th. Biol. **32:**425-426.
8.   **Diaz E.** 2004. Bacterial degradation of aromatic pollutants: a paradigm of metabolic versatility. International Microbiology **7:**173-180.
9.   **Giedroc DP, Arunkumar AI.** 2007. Metal sensor proteins: nature's metalloregulated allosteric switches. Dalton Transactions**:**3107-3120.
10.   **Pennella MA, Giedroc DP.** 2005. Structural determinants of metal selectivity in prokaryotic metal-responsive transcriptional regulators. Biometals **18:**413-428.
11.   **Neubauer O.** 1947. Arsenical cancer; a review. British journal of cancer **1:**192-251.
12.   **Cullen WR, Reimer KJ.** 1989. Arsenic speciation in the environment. Chem Rev **89:**713-764.
13.   **Rosen BP.** 2002. Biochemistry of arsenic detoxification. Febs Letters **529:**86-92.
14.   **Oremland RS, Stolz JF.** 2003. The ecology of arsenic. Science **300:**939-944.
15.   **Smedley PL, Kinniburgh DG.** 2002. A review of the source, behaviour and distribution of arsenic in natural waters. Applied Geochemistry **17:**517-568.
16.   **Planer-Friedrich B, London J, McCleskey RB, Nordstrom DK, Wallschlaeger D.** 2007. Thioarsenates in geothermal waters of yellowstone national park: Determination, preservation, and geochemical importance. Environmental Science & Technology **41:**5245-5251.
17.   **Planer-Friedrich B, Suess E, Scheinost AC, Wallschlaeger D.** 2010. Arsenic Speciation in Sulfidic Waters: Reconciling Contradictory Spectroscopic and Chromatographic Evidence. Anal Chem **82:**10228-10235.
18.   **Nordstrom DK.** 2002. Public health - Worldwide occurrences of arsenic in ground water. Science **296:**2143-2145.
19.   **Nicolis I, Curis E, Deschamps P, Benazeth S.** 2009. Arsenite medicinal use, metabolism, pharmacokinetics and monitoring in human hair. Biochimie **91:**1260-1267.
20.   **Platanias LC.** 2009. Biological Responses to Arsenic Compounds. Journal of Biological Chemistry **284:**18583-18587.
21.   **Dani SU.** 2010. Arsenic for the fool: An exponential connection. Science of the Total Environment **408:**1842-1846.
22.   **Zhao F-J, McGrath SP, Meharg AA.** 2010. Arsenic as a Food Chain Contaminant: Mechanisms of Plant Uptake and Metabolism and Mitigation Strategies. Annual Review of Plant Biology, Vol 61 **61:**535-559.
23.   **Bartolucci S, Contursi P, Fiorentino G, Limauro D, Pedone E.** 2013. Responding to toxic compounds: a genomic and functional overview of Archaea. Front in Bioscienc-Landmark **18:**165-189.
24.   **Westheimer FH.** 1987. Why nature chose phosphates. Science **235:**1173-1178.
25.   **Gresser MJ.** 1981. ADP-arsenate. Formation by submitochondrial particles under phosphorylating conditions. The Journal of biological chemistry **256:**5981-5983.
26.   **Meng YL, Liu ZJ, Rosen BP.** 2004. As(III) and Sb(III) uptake by G1pF and efflux by ArsB in Escherichia coli. Journal of Biological Chemistry **279:**18334-18341.
27.   **Liu ZJ, Boles E, Rosen BP.** 2004. Arsenic trioxide uptake by hexose permeases in Saccharomyces cerevisiae. Journal of Biological Chemistry **279:**17312-17318.
28.   **Liu Z, Sanchez MA, Jiang X, Boles E, Landfear SM, Rosen BP.** 2006. Mammalian glucose permease GLUT1 facilitates transport of arsenic trioxide and methylarsonous acid. Biochemical and Biophysical Research Communications **351:**424-430.
29.   **Dombrowski PM, Long W, Farley KJ, Mahony JD, Capitani JF, Di Toro DM.** 2005. Thermodynamic analysis of arsenic methylation. Environmental Science & Technology **39:**2169-2176.

30.   **Hughes MF.** 2002. Arsenic toxicity and potential mechanisms of action. Toxicology Letters **133:**1-16.

31.   **Mukhopadhyay R, Rosen BP.** 2002. Arsenate reductases in prokaryotes and eukaryotes. Environmental Health Perspectives **110:**745-748.

32.   **di Toppi LS, Gabbrielli R.** 1999. Response to cadmium in higher plants. Environmental and Experimental Botany **41:**105-130.

33.   **Santini JM, Sly LI, Schnagl RD, Macy JM.** 2000. A new chemolithoautotrophic arsenite-oxidizing bacterium isolated from a gold mine: Phylogenetic, physiological, and preliminary biochemical studies. Applied and Environmental Microbiology **66:**92-97.

34.   **Silver S, Phung LT.** 2005. Genes and enzymes involved in bacterial oxidation and reduction of inorganic arsenic. Applied and Environmental Microbiology **71:**599-608.

35.   **Bryan CG, Marchal M, Battaglia-Brunet F, Kugler V, Lemaitre-Guillier C, Lievremont D, Bertin PN, Arsene-Ploetze F.** 2009. Carbon and arsenic metabolism in Thiomonas strains: differences revealed diverse adaptation processes. Bmc Microbiology **9**.

36.   **Macy JM, Nunan K, Hagen KD, Dixon DR, Harbour PJ, Cahill M, Sly LI.** 1996. Chrysiogenes arsenatis gen nov, sp nov; a new arsenate-respiring bacterium isolated from gold mine wastewater. International Journal of Systematic Bacteriology **46:**1153-1157.

37.   **Stolz JF, Oremland RS.** 1999. Bacterial respiration of arsenic and selenium. Fems Microbiology Reviews **23:**615-627.

38.   **Qin J, Rosen BP, Zhang Y, Wang GJ, Franke S, Rensing C.** 2006. Arsenic detoxification and evolution of trimethylarsine gas by a microbial arsenite S-adenosylmethionine methyltransferase. Proceedings of the National Academy of Sciences of the United States of America **103:**2075-2080.

39.   **Yamanaka K, Ohba H, Hasegawa A, Sawamura R, Okada S.** 1989. Mutagenicity of dimethylated metabolites of inorganic arsenics. Chemical & Pharmaceutical Bulletin **37:**2753-2756.

40.   **Yamanaka K, Hayashi H, Tachikawa M, Kato K, Hasegawa A, Oku N, Okada S.** 1997. Metabolic methylation is a possible genotoxicity-enhancing process of inorganic arsenics. Mutation Research-Genetic Toxicology and Environmental Mutagenesis **394:**95-101.

41.   **Yamauchi H, Kaise T, Takahashi K, Yamamura Y.** 1990. Toxicity and metabolism of trimethylarsine in mice and hamsters. Fundamental and Applied Toxicology **14:**399-407.

42.   **Moore AJ, Kukuk PF.** 2002. Quantitative genetic analysis of natural populations. Nature Reviews Genetics **3:**971-978.

43.   **Mass MJ, Tennant A, Roop BC, Cullen WR, Styblo M, Thomas DJ, Kligerman AD.** 2001. Methylated trivalent arsenic species are genotoxic. Chemical Research in Toxicology **14:**355-361.

44.   **Yoshinaga M, Cai Y, Rosen BP.** 2011. Demethylation of methylarsonic acid by a microbial community. Environmental Microbiology **13:**1205-1215.

45.   **Turner AW.** 1949. Bacterial oxidation of arsenite. Nature **164:**76-76.

46.   **Heinrich-Salmeron A, Cordi A, Brochier-Armanet C, Halter D, Pagnout C, Abbaszadeh-Fard E, Montaut D, Seby F, Bertin PN, Bauda P, Arsene-Ploetze F.** 2011. Unsuspected Diversity of Arsenite-Oxidizing Bacteria as Revealed by Widespread Distribution of the aoxB Gene in Prokaryotes. Applied and Environmental Microbiology **77:**4685-4692.

47.   **Huang Y, Li H, Rensing C, Zhao K, Johnstone L, Wang G.** 2012. Genome Sequence of the Facultative Anaerobic Arsenite-Oxidizing and Nitrate-Reducing Bacterium Acidovorax sp Strain NO1. Journal of Bacteriology **194:**1635-1636.

48.   **Oremland RS, Hoeft SE, Santini JA, Bano N, Hollibaugh RA, Hollibaugh JT.** 2002. Anaerobic oxidation of arsenite in Mono Lake water and by facultative, arsenite-oxidizing chemoautotroph, strain MLHE-1. Applied and Environmental Microbiology **68:**4795-4802.

49.   **Santini JM, vanden Hoven RN.** 2004. Molybdenum-containing arsenite oxidase of the chemolithoautotrophic arsenite oxidizer NT-26. Journal of Bacteriology **186:**1614-1619.

50.   **vanden Hoven RN, Santini JM.** 2004. Arsenite oxidation by the heterotroph Hydrogenophaga sp str. NT-14: the arsenite oxidase and its physiological electron acceptor. Biochimica Et Biophysica Acta-Bioenergetics **1656:**148-155.

51.   **Lett M-C, Muller D, Lievremont D, Silver S, Santini J.** 2012. Unified Nomenclature for Genes Involved in Prokaryotic Aerobic Arsenite Oxidation. Journal of Bacteriology **194:**207-208.

52.   **Zargar K, Hoeft S, Oremland R, Saltikov CW.** 2010. Identification of a Novel Arsenite Oxidase Gene, arxA, in the Haloalkaliphilic, Arsenite-Oxidizing Bacterium Alkalilimnicola ehrlichii Strain MLHE-1. Journal of Bacteriology **192:**3755-3762.

53.   **Zargar K, Conrad A, Bernick DL, Lowe TM, Stolc V, Hoeft S, Oremland RS, Stolz J, Saltikov CW.** 2012. ArxA, a new clade of arsenite oxidase within the DMSO reductase family of molybdenum oxidoreductases. Environmental Microbiology **14:**1635-1645.

54.   **Macy JM, Santini JM, Pauling BV, O'Neill AH, Sly LI.** 2000. Two new arsenate/sulfate-reducing bacteria: mechanisms of arsenate reduction. Archives of Microbiology **173:**49-57.

55.   **Krafft T, Macy JM.** 1998. Purification and characterization of the respiratory arsenate reductase of Chrysiogenes arsenatis. European Journal of Biochemistry **255:**647-653.

56.   **Carlin A, Shi WP, Dey S, Rosen BP.** 1995. The ars operon of Escherichia-coli confers arsenical and antimonial resistance. Journal of Bacteriology **177:**981-986.

57.   **Silver S.** 1998. Genes for all metals - a bacterial view of the periodic table - The 1996 Thom Award Lecture. Journal of Industrial Microbiology & Biotechnology **20:**1-12.

58.   **Chen CM, Misra TK, Silver S, Rosen BP.** 1986. Nucleotide-sequence of the structural genes for an anion pump - the plasmid-encoded arsenical resistance operon. Journal of Biological Chemistry **261:**5030-5038.

59.   **Arsene-Ploetze F, Koechler S, Marchal M, Coppee J-Y, Chandler M, Bonnefoy V, Brochier-Armanet C, Barakat M, Barbe V, Battaglia-Brunet F, Bruneel O, Bryan CG, Cleiss-Arnold J, Cruveiller S, Erhardt M, Heinrich-Salmeron A, Hommais F, Joulian C, Krin E, Lieutaud A, Lievremont D, Michel C, Muller D, Ortet P, Proux C, Siguier P, Roche D, Rouy Z, Salvignol G, Slyemi D, Talla E, Weiss S, Weissenbach J, Medigue C, Bertin PN.** 2010. Structure, Function, and Evolution of the Thiomonas spp. Genome. Plos Genetics **6**.

60.   **Muller D, Medigue C, Koechler S, Barbe V, Barakat M, Talla E, Bonnefoy V, Krin E, Arsene-Ploetze F, Carapito C, Chandler M, Cournoyer B, Cruveiller S, Dossat C, Duval S, Heymann M, Leize E, Lieutaud A, Lievremont D, Makita Y, Mangenot S, Nitschke W, Ortet P, Perdrial N, Schoepp B, Siguier P, Simeonova DD, Rouy Z, Segurens B, Turlin E, Vallenet D, Van Dorsselaer A, Weiss S, Weissenbach J, Lett M-C, Danchin A, Bertin PN.** 2007. A tale of two oxidation states: Bacterial colonization of arsenic-rich environments. Plos Genetics **3**.

61.   **Chauhan NS, Ranjan R, Purohit HJ, Kalia VC, Sharma R.** 2009. Identification of genes conferring arsenic resistance to Escherichia coli from an effluent treatment plant sludge metagenomic library. Fems Microbiology Ecology **67:**130-139.

62.   **Martin P, DeMel S, Shi J, Gladysheva T, Gatti DL, Rosen BP, Edwards BFP.** 2001. Insights into the structure, solvation, and mechanism of ArsC arsenate reductase, a novel arsenic detoxification enzyme. Structure **9:**1071-1081.

63.   **Lin Y-F, Yang J, Rosen BP.** 2007. ArsD: an As(III) metallochaperone for the ArsAB As(III)-translocating ATPase. Journal of Bioenergetics and Biomembranes **39:**453-458.

64.   **Yang J, Rawat S, Stemmler TL, Rosen BP.** 2010. Arsenic Binding and Transfer by the ArsD As(III) Metallochaperone. Biochemistry **49:**3658-3666.

65.   **Kruger MC, Bertin PN, Heipieper HJ, Arsene-Ploetze F.** 2013. Bacterial metabolism of environmental arsenic-mechanisms and biotechnological applications. Applied Microbiology and Biotechnology **97:**3827-3841.

66.   **Ji GY, Silver S.** 1992. Regulation and expression of the arsenic resistance operon from Staphylococcus-Aureus plasmid pI258. Journal of Bacteriology **174:**3684-3694.

67.   **Ji GY, Silver S.** 1992. Reduction of arsenate to arsenite by the ArsC protein of the arsenic resistance operon of Staphylococcus-aureus plasmid-pI258. Proceedings of the National Academy of Sciences of the United States of America **89:**9474-9478.

68.   **Shi J, Vlamis-Gardikas V, Aslund F, Holmgren A, Rosen BP.** 1999. Reactivity of glutaredoxins 1, 2, and 3 from Escherichia coli shows that glutaredoxin 2 is the primary hydrogen donor to ArsC-catalyzed arsenate reduction. Journal of Biological Chemistry **274:**36039-36042.

69.   **Mukhopadhyay R, Rosen BP.** 2001. The phosphatase C(X)(5)R motif is required for catalytic activity of the Saccharomyces cerevisiae Acr2p arsenate reductase. Journal of Biol. Chem. **276:**34738-34742.

70.   **Ji GY, Garber EAE, Armes LG, Chen CM, Fuchs JA, Silver S.** 1994. Arsenate reductase of Staphylococcus-aureus plasmid pI258. Biochemistry **33:**7294-7299.

71.   **Zegers I, Martins JC, Willem R, Wyns L, Messens J.** 2001. Arsenate reductase from S-aureus plasmid pI258 is a phosphatase drafted for redox duty. Nature Structural Biology **8:**843-847.

72.   **Bennett MS, Guan Z, Laurberg M, Su XD.** 2001. Bacillus subtilis arsenate reductase is structurally and functionally similar to low molecular weight protein tyrosine phosphatases. Proceedings of the National Academy of Sciences of the United States of America **98:**13577-13582.

73.   **Del Giudice I, Limauro D, Pedone E, Bartolucci S, Fiorentino G.** 2013. A novel arsenate reductase from the bacterium Thermus thermophilus HB27: Its role in arsenic detoxification. Biochimica Et Biophysica Acta-Proteins and Proteomics **1834:**2071-2079.

74.   **Rosen BP.** 1999. Families of arsenic transporters. Trends in Microbiology **7:**207-212.

75.   **Dey S, Rosen BP.** 1995. Dual-mode of energy coupling by the oxyanion-translocating ArsB protein. Journal of Bacteriology **177:**385-389.

76.   **Rosen BP, Bhattacharjee H, Zhou TQ, Walmsley AR.** 1999. Mechanism of the ArsA ATPase. Biochimica Et Biophysica Acta-Biomembranes **1461:**207-215.

77.   **Ajees AA, Yang J, Rosen BP.** 2011. The ArsD As(III) metallochaperone. Biometals **24:**391-399.

78.   **Lin Y-F, Walmsley AR, Rosen BP.** 2006. An arsenic metallochaperone for an arsenic detoxification pump. Proceedings of the National Academy of Sciences of the United States of America **103:**15617-15622.

79.   **Busenlehner LS, Pennella MA, Giedroc DP.** 2003. The SmtB/ArsR family of metalloregulatory transcriptional repressors: structural insights into prokaryotic metal resistance. Fems Microbiology Reviews **27:**131-143.

80.   **Morby AP, Turner JS, Huckle JW, Robinson NJ.** 1993. SmtB is a metal-dependent repressor of the Cyanobacterial metallothionein gene SmtA - identification of a Zn inhibited DNA-protein complex. Nucleic Acids Research **21:**921-925.

81.   **Kar SR, Adams AC, Lebowitz J, Taylor KB, Hall LM.** 1997. The cyanobacterial repressor SmtB is predominantly a dimer and binds two Zn2+ ions per subunit. Biochemistry **36:**15343-15348.

82.   **Cook WJ, Kar SR, Taylor KB, Hall LM.** 1998. Crystal structure of the cyanobacterial metallothionein repressor SmtB: A model for metalloregulatory proteins. J of Mol Biology **275:**337-346.

83.   **Schultz SC, Shields GC, Steitz TA.** 1991. crystal-structure of a CAP-DNA COMPLEX - the DNA is bent by 90-degrees. Science **253:**1001-1007.

84.   **Shi WP, Wu JH, Rosen BP.** 1994. Identification of a putative metal-binding site in a new family of metalloregulatory proteins. Journal of Biological Chemistry **269:**19826-19829.

85.   **Shi WP, Dong J, Scott RA, Ksenzenko MY, Rosen BP.** 1996. The role of arsenic thiol interactions in metalloregulation of the ars operon. Journal of Biological Chemistry **271:**9291-9297.

86.   **Chakravorty DK, Wang B, Lee CW, Giedroc DP, Merz KM, Jr.** 2012. Simulations of Allosteric Motions in the Zinc Sensor CzrA. Journal of the American Chemical Society **134:**3367-3376.

87.   **Lei Y, Chen W, Mulchandani A.** 2006. Microbial biosensors. Anal Chimica Acta **568:**200-210.

88.   **Fiorentino G, Ronca R, Bartolucci S.** 2009. A novel E-coli biosensor for detecting aromatic aldehydes based on a responsive inducible archaeal promoter fused to the green fluorescent protein. Applied Microbiology and Biotechnology **82:**67-77.

89.   **Averhoff B.** 2009. Shuffling genes around in hot environments: the unique DNA transporter of Thermus thermophilus. Fems Microbiology Reviews **33:**611-626.

90.   **Cava F, Hidalgo A, Berenguer J.** 2009. Thermus thermophilus as biological model. Extremophiles **13:**213-231.

91.   **Henne A, Bruggemann H, Raasch C, Wiezer A, Hartsch T, Liesegang H, Johann A, Lienard T, Gohl O, Martinez-Arias R, Jacobi C, Starkuviene V, Schlenczeck S, Dencker S, Huber R, Klenk HP, Kramer W, Merkl R, Gottschalk G, Fritz HJ.** 2004. The genome sequence of the extreme thermophile Thermus thermophilus. Nature Biotechnology **22:**547-553.

92.   **Lioliou EE, Pantazaki AA, Kyriakidis DA.** 2004. Thermus thermophilus genome analysis: benefits and implications. Microbial Cell Factories **3**.

93.   **Koyama Y, Hoshino T, Tomizuka N, Furukawa K.** 1986. Genetic-transformation of the extreme thermophile Thermus-thermophilus and of other Thermus spp. J of Bacteriology **166:**338-340.

94.   **Leis B, Angelov A, Liebl W.** 2013. Screening and Expression of Genes from Metagenomes. Advances in Applied Microbiology, Vol 83 **83:**1-68.

95.   **de Grado M, Castan P, Berenguer J.** 1999. A high-transformation-efficiency cloning vector for Thermus thermophilus. Plasmid **42:**241-245.

96.   **Kayser KJ, Kilbane JJ.** 2001. New host-vector system for Thermus spp. based on the malate dehydrogenase gene. Journal of Bacteriology **183:**1792-1795.

97.   **Fujita A, Misumi Y, Koyama Y.** 2012. Two versatile shuttle vectors for Thermus thermophilus-Escherichia coli containing multiple cloning sites, lacZ alpha gene and kanamycin or hygromycin resistance marker. Plasmid **67:**272-275.

98.   **Hidalgo A, Betancor L, Moreno R, Zafra O, Cava F, Fernandez-Lafuente R, Guisan JM, Berenguer J.** 2004. Thermus thermophilus as a cell factory for the production of a thermophilic Mn-dependent catalase which fails to be synthesized in an active form in Escherichia coli. Applied and Env. Microb. **70:**3839-3844.

99.   **Ohta T, Tokishita S-i, Imazuka R, Mori I, Okamura J, Yamagata H.** 2006. beta-glucosidase as a reporter for the gene expression studies in Thermus thermophilus and constitutive expression of DNA repair genes. Mutagenesis **21:**255-260.

100.   **Cava F, Angel de Pedro M, Blas-Galindo E, Waldo GS, Westblade LF, Berenguer J.** 2008. Expression and use of superfolder green fluorescent protein at high temperatures in vivo: a tool to study extreme thermophile biology. Environmental Microbiology **10:**605-613.

101.   **Mukherjee A, Das D, Mondal SK, Biswas R, Das TK, Boujedaini N, Khuda-Bukhsh AR.** 2010. Tolerance of arsenate-induced stress in Aspergillus niger, a possible candidate for bioremediation. Ecotoxicology and Environmental Safety **73:**172-182.

102.   **Pokhrel D, Viraraghavan T.** 2006. Arsenic removal from an aqueous solution by a modified fungal biomass. Water Research **40:**549-552.

103.   **Canovas D, de Lorenzo V.** 2007. Osmotic stress limits arsenic hypertolerance in Aspergillus sp P37. Fems Microbiology Ecology **61:**258-263.

104.   **de Mora K, Joshi N, Balint BL, Ward FB, Elfick A, French CE.** 2011. A pH-based biosensor for detection of arsenic in drinking water. Analytical and Bioanalytical Chemistry **400:**1031-1039.

105.   **Choe S-I, Gravelat FN, Al Abdallah Q, Lee MJ, Gibbs BF, Sheppard DC.** 2012. Role of Aspergillus niger acrA in Arsenic Resistance and Its Use as the Basis for an Arsenic Biosensor. Applied and Environmental Microbiology **78:**3855-3863.

106.   **Diesel E, Schreiber M, van der Meer JR.** 2009. Development of bacteria-based bioassays for arsenic detection in natural waters. Analytical and Bioanalytical Chemistry **394:**687-693.

107.   **Long F, Zhu A, Shi H.** 2013. Recent Advances in Optical Biosensors for Environmental Monitoring and Early Warning. Sensors **13:**13928-13948.

108.   **Hillson NJ, Hu P, Andersen GL, Shapiro L.** 2007. Caulobacter crescentus as a whole-cell uranium biosensor. Applied and Environmental Microbiology **73:**7615-7621.

109.   **Paitan Y, Biran I, Shechter N, Biran D, Rishpon J, Ron EZ.** 2004. Monitoring aromatic hydrocarbons by whole cell electrochemical biosensors. Analytical Biochemistry **335:**175-183.

110.   **Chouteau C, Dzyadevych S, Durrieu C, Chovelon JM.** 2005. A bi-enzymatic whole cell conductometric biosensor for heavy metal ions and pesticides detection in water samples. Biosensors & Bioelectronics **21:**273-281.

111.   **Huang WE, Wang H, Zheng HJ, Huang LF, Singer AC, Thompson I, Whiteley AS.** 2005. Chromosomally located gene fusions constructed in Acinetobacter sp ADP1 for the detection of salicylate. Environmental Microbiology **7:**1339-1348.

112.   **Mitchell RJ, Gu MB.** 2004. Construction and characterization of novel dual stress-responsive bacterial biosensors. Biosensors & Bioelectronics **19:**977-985.

113.   **Liao VHC, Chien MT, Tseng YY, Ou KL.** 2006. Assessment of heavy metal bioavailability in contaminated sediments and soils using green fluorescent protein-based bacterial biosensors. Environmental Pollution **142:**17-23.

114.   **Fiorentino G, Ronca R, Cannio R, Rossi M, Bartolucci S.** 2007. MarR-like transcriptional regulator involved in detoxification of aromatic compounds in Sulfolobus solfataricus. Journal of Bacteriology **189:**7351-7360.

115.   **Zhang J, Jensen MK, Keasling JD.** 2015. Development of biosensors and their application in metabolic engineering. Current Opinion in Chemical Biology **28:**1-8.

116.   **Huang C-W, Wei C-C, Liao VH-C.** 2015. A low cost color-based bacterial biosensor for measuring arsenic in groundwater. Chemosphere **141:**44-49.

117.   **Li L, Liang J, Hong W, Zhao Y, Sun S, Yang X, Xu A, Hang H, Wu L, Chen S.** 2015. Evolved Bacterial Biosensor for Arsenite Detection in Environmental Water. Environmental Science & Technology **49:**6149-6155.

118.   **Wang B, Barahona M, Buck M.** 2015. Amplification of small molecule-inducible gene expression via tuning of intracellular receptor densities. Nucleic Acids Research **43:**1955-1964.

119.   **Nayak M, Kotian A, Marathe S, Chakravortty D.** 2009. Detection of microorganisms using biosensors-A smarter way towards detection techniques. Biosensors & Bioelectronics **25:**661-667.

120.   **De Stefano L, Rotiroti L, Rendina I, Moretti L, Scognamiglio V, Rossi M, D'Auria S.** 2006. Porous silicon-based optical microsensor for the detection of L-glutamine. Biosensors & Bioelectronics **21:**1664-1667.

121.   **Li J, Sailor MJ.** 2014. Synthesis and characterization of a stable, label-free optical biosensor from TiO2-coated porous silicon. Biosensors & Bioelectronics **55:**372-378.

122.   **Kumar S, Ahlawat W, Kumar R, Dilbaghi N.** 2015. Graphene, carbon nanotubes, zinc oxide and gold as elite nanomaterials for fabrication of biosensors for healthcare. Biosensors & Bioelectronics **70:**498-503.

123.   **Bhakta SA, Evans E, Benavidez TE, Garcia CD.** 2015. Protein adsorption onto nanomaterials for the development of biosensors and analytical devices: A review. Analytica Chimica Acta **872:**7-25.

124.   **Dudchenko OY, Pyeshkova VM, Soldatkin OO, Akata B, Kasap BO, Soldatkin AP, Dzyadevych SV.** 2016. Development of Silicalite/Glucose Oxidase-Based Biosensor and Its Application for Glucose Determination in Juices and Nectars. Nanoscale research letters **11:**59-59.

Chapter 2

CHARACTERIZATION OF THE ARSENIC RESISTANCE MECHANISM IN *THERMUS THERMOPHILUS*

2.1. **An ArsR/SmtB family member involved in the regulation of arsenic resistance genes in *Thermus thermophilus* HB27.**

2.2. **A pull-down assay for the identification of *Tt*SmtB molecular interactors.**

2.3. ***Tt*SmtB expression in *Thermus thermophilus* HB27.**

SUMMARY

This chapter focuses on the characterization at molecular level of the mechanisms of arsenic resistance in *Thermus thermophilus* through molecular, structural and functional study of the components involved and their interactions.
This study was structured in three main points:

1) Structural and functional characterization of *Tt*SmtB, a transcriptional regulator belonging to ArsR/SmtB family.
   Its functional role in the regulation of the arsenic resistance was proved analysing the *Tt*SmtB ability to bind *in-vitro* the identified target sequences, and generating a *T. thermophilus TtsmtB⁻* strain.

2) Evaluation of the interaction of *Tt*SmtB with other cellular protein components. The *Tt*SmtB molecular interactors have been identified in the presence and in the absence of arsenic by pull-down and mass spectrometry assays.

3) Expression of *Tt*SmtB in *T. thermophilus* HB27.
   This has been achieved by cloning the *TtsmtB* gene under the control of the *Pnar* promoter into the bi-functional *E. coli-Thermus* sp. vector pMKE2. The transcriptional regulator expression has been evaluated by western blot analysis.

2.1 An ArsR/SmtB family member involved in the regulation of arsenic resistance genes in *Thermus thermophilus* HB27

Immacolata Antonucci[1], Danila Limauro[1], Patrizia Contursi[1], Ana Luisa Ribeiro[2], Immacolata Del Giudice[1], José Berenguer[2], Simonetta Bartolucci[1] and Gabriella Fiorentino[1*]

1 Dipartimento di Biologia, Università degli Studi di Napoli Federico II,Complesso Universitario Monte S. Angelo, Naples, Italy

2 Centro de Biología Molecular Severo Ochoa (CSIC-UAM). Campus Universidad Autónoma de Madrid, 28049, Madrid, Spain

[*]Corresponding author: fiogabri@unina.it

ABSTRACT

The thermophilic gram negative bacterium *Thermus thermophilus* HB27 is able to grow in the presence of arsenic and contains arsenic resistance genes interspersed in the chromosome; *TtsmtB* encodes a transcriptional regulator belonging to the ArsR/SmtB family and is part of an operon containing putative internal promoters upstream of genes with no obvious functional relationship. The purified recombinant protein is a dimeric DNA binding protein able to bind *in vitro* to target sequences and to dissociate upon arsenate and arsenite binding. Inactivation of the *TtsmtB* gene induces the expression of the *ars* genes among which *TtarsC*, the arsenate reductase, and a putative efflux protein. These results prove that *Tt*SmtB has a functional role in the regulation of the arsenic resistance.

INTRODUCTION

Arsenic is an ubiquitous toxic metalloid naturally present in the soil, water and air that adversely affects human health. Depending on the redox potential of the environment, it can be found in two biologically active forms: the trivalent arsenite, AsIII, highly toxic for human health or the less-toxic pentavalent arsenate, AsV.

Arsenite enters the cell through aquaglyceroporins; since it has a high affinity for sulfur it exerts its toxicity through binding to dithiols in proteins and in glutathione (GSH) contributing to protein inactivation and ultimately generating reactive oxygen species (ROS) (1, 2). On the other hand arsenate, as a phosphate analogue, enters the cells through phosphate transporters and its toxicity is mediated by replacing phosphate in essential biochemical reactions (3, 4).

The abundance of arsenic in the environment has guided the evolution of multiple defence strategies in almost all microorganisms which must therefore sense the metalloid and regulate the transcription of genes coding for resistance proteins. Despite being toxic, some microorganisms also use arsenic as electron acceptor in anaerobic respiratory chains or as electron donor for chemolythotrophic growth, and even for anoxigenic photosynthesis (5, 6). Other microorganisms are able to methylate inorganic arsenic or de-methylate the organic forms (7).

In many prokaryotes arsenic resistance is mainly linked to the presence of plasmid or chromosomally encoded *ars* operons with a variable number of genes; in the simplest system resistance is achieved through cytoplasmic reduction of AsV to AsIII by arsenate reductase, active extrusion of AsIII by a membrane protein and regulation by ArsR, a trans-acting repressor of the ArsR/SmtB family (8, 9); two additional genes encoding ArsA, a second component of the arsenite transporter with ATPase activity and ArsD, a metallochaperon, can increase the effectiveness of the arsenite efflux system (10, 11).

Arsenate reductases use the thioredoxin, glutaredoxin or mycoredoxin systems as electron donors (12). Arsenite export is mediated by two families of proteins: ArsB proteins, that have been found only in bacteria (10), and Acr3 proteins, with representatives in bacteria, fungi and plants (13).

Regarding transcriptional regulators different families of metal-sensing proteins (identified by the family HTH_5 of Pfam database) have been described in bacteria, with ArsR/SmtB being the most extensively studied and named after its founding members, *E. coli* ArsR and *Synechoccus* PCC 7942 SmtB (14, 15). The members of the ArsR/SmtB family have many common features, but display a great diversity in metal-sensing motifs and metal binding mechanisms. They share a dimeric quaternary structure with helix-turn-helix (HTH) or winged HTH DNA binding domain and a highly conserved motif, ELCV(C/G)D, defined as the metal binding box, located in the HTH region (16, 17); metal binding at this region interferes with DNA binding. The SmtB DNA-binding site contains an imperfect 12-2-12 inverted repeat (or a half of this site) located within the operator-promoter region or overlapping the transcriptional start site; since binding to the metal alleviate transcriptional repression, these factors act as de-repressors (18). Despite conservation of the metal binding motif, the metal selectivity and the binding mode vary, because the conserved Cys residues may form metal-thiolate bonds but with different geometry and coordination (19).

With all of the activities above described, microbes participate to the geochemical cycling of arsenic in their living environments, promoting or inhibiting arsenic release from sediment material. In this context, thermophilic microorganisms affect the

bioavailability of arsenic compounds in a wide variety of hydrothermal habitats. However, information regarding the molecular mechanisms of arsenic resistance in these habitats is still scarce (20).

The thermophilic gram negative bacterium *Thermus thermophilus* HB27 is able to grow in the presence of both arsenate and arsenite in a range of concentrations which are lethal for other microorganisms (21). The putative resistance genes have not been found in a single resistance operon but associated to chromosomal genes apparently not functionally related. In a recent work we demonstrated the involvement of a thioredoxin-coupled arsenate reductase (*Tt*ArsC) in the resistance mechanism and hypothesized that arsenic dependent induction of *TtarsC* could be mediated by factors such as ArsR/SmtB transcriptional regulators (21).

In the present study we investigate on the role of the protein *Tt*SmtB in the regulation of the arsenic resistance mechanism in *T. thermophilus* HB27 through genetic and biochemical analyses.

MATERIALS AND METHODS

Plasmids, bacterial strains, and growth conditions. *T. thermophilus* HB27 wild type strain was purchased from the DSMZ and grown aerobically at 70°C in TM medium without or with $NaAsO_2$ and KH_2AsO_4 (Sigma) at the final concentrations of 8 mM and 12 mM, respectively as described (21).

T. thermophilus ΔsmtB::kat and *TtsmtB* complemented strain were grown aerobically at 70 °C in TM medium containing kanamycin (30 µg/ml). A frozen (-80 °C) stock of both *T. thermophilus ΔsmtB::kat* and *TtsmtB* complemented strain was streaked on a TM plate (solidified by the addition of 1,6 % Agar) containing kanamycin (30 µg/ml) and incubated for 48 h at 70 °C. Single colonies that appeared on the plate were inoculated into TM liquid medium supplied with the antibiotic and shaken at 70 °C overnight.

For RT-PCR and qRT-PCR experiments, cultures of *T. thermophilus* HB27 and *ΔsmtB::kat* were grown in TM medium (50 ml); when the cell density reached 0.5 OD_{600nm} , they were harvested at 0 and 60 min after the addition of 8 mM $NaAsO_2$ or 12 mM KH_2AsO_4, immediately spun down, and pellets kept at -80 °C.

For the calculation of the generation time, *T. thermophilus* HB27, *ΔsmtB::kat* and *TtsmtB* complemented strain were grown at 70 °C for 20 hours, and generation times calculated within the exponential phase by the equation: $T_g = t/n$, whereas: t = time frame of exponential growth phase; $n = (\log_{10} N_t - \log_{10} N_0) / \log_{10}2$. N_t = number of cells at time t; N_0 = number of cells at time 0. Number of cells was calculated assuming that $1 OD_{600nm}$ corresponds to 1×10^8 cells (22).

E. coli strains were grown in Luria Bertani (23) medium at 37 °C with 50 µg/ml kanamycin and/or 33 µg/ml chloramphenicol as required.

Strain genotypes and sources are summarized in Table S1.

DNA and RNA extraction. Genomic DNA was prepared following reported procedures (24). Total RNA was extracted using a RNAeasy Mini Kit (Qiagen). The extracted RNA samples (20 µg) were then diluted to 0.2 mg/ml for DNAse treatment with the Ambion® TURBO™ DNase according to the manufacturer's instructions.

End-point reverse transcription RT-PCR. RT-PCR reactions were carried out on 2 µg of DNAseI-treated RNAs using SuperScript III Reverse Transcriptase (Invitrogen) as already described (21). Specific oligonucleotides (*0352rv*, *0353rv*, *0354rv* and *0355rv*) were designed based on *T. thermophilus* HB27 gene sequences using

Primer3Plus and used as primers for the RT reactions. PCR reactions were performed using the following primer pairs: *0351fw* and *0352rv*; *0352fw* and *0353rv*; *0353fw* and *0354rv;* *0354fw* and *0355rv* by 35 amplification cycles of 94°C for 1 min, a specific annealing temperature for each primer set for 1 min, 72°C for 1 min, and a final extension at 72°C for 10 min. The products of each PCR were detected by agarose gel electrophoresis. The primer sequences are reported in Table S2.

Construction of *T. thermophilus ΔsmtB::kat.* To obtain a *smtB* deletion mutant of *T. thermophilus* HB27 the chromosomal *TTC0353* (*TtsmtB*) gene was replaced with the kanamycin nucleotidyltrasferase gene (*kat*) cassette by double homologous recombination. Two regions upstream and downstream of *TTC0353* (arm UP and arm DW) were amplified by PCR using *T. thermophilus* HB27 genomic DNA as template. For arm UP, the forward primer (UP fw SmtB *Eco*RI) and the reverse primer (New UP rv SmtB *Xba*I) contained *Eco*RI and *Xba*I sites, respectively. For arm DW, the forward primer (New DW fw SmtB *Xba*I) and the reverse primer (DW rv SmtB *Hind*III) contained *Xba*I and *Hind*III sites. The resulting products (909-bp arm UP and 1014-bp arm DW) were digested, purified, ligated in vitro (in 1:1 molar ratio) and cloned into pUC19, giving the pUC19*ΔsmtB* vector. In this plasmid, at the *Xba*I site it was inserted the *kat* cassette extracted from pUC19-*kat* after *Xba*I digestion. The resulting vector was named pUC19*ΔsmtB::kat*. The orientation of *kat* gene-insert was confirmed by restriction analysis. The pUC19*ΔsmtB*::*kat* plasmid was used in linear form to transform *T. thermophilus* HB27 (25), adding 200 ng of DNA to 0.5 mL of cells in their exponential growth phase (0.3 − 0.5 OD_{600nm}). After four hours of incubation, the cells were plated on TM plates containing kanamycin (30 µg/mL) and incubated for 48 h at 70 °C.

The replacement of the *TtsmtB* gene was verified by PCR on the genomic DNA of the transformants; in particular three primer sets (Table S2) were used: one pair (*0351promfw*/*0351promrv*) amplified a region in both deleted and wild-type strains; another one (*0352fw*/*0353rv*) amplified a region only in the wild type strain; the last pair (*smtBfw*/*smtBrv*) amplified a fragment of 1125 bp corresponding to the *kat* gene in the mutant strain compared to the *smtB* gene of 372 bp in the wild-type.

The *kat* substitution insertion at the correct site was further confirmed by DNA sequencing.

Complementation of the mutant strain *T. thermophilus ΔsmtB::kat.* To perform the complementation of *T. thermophilus ΔsmtB::kat,* the strain was transformed with the pMKpnqo-*TtsmtB* vector. This plasmid was realized starting from pMKpnqobgaA, a derivative of pMKEbgaA vector, (26) in which the *bgaA* gene was substituted by the 372-bp *TtsmtB* between the *Nde*I/*Hind*III sites. This plasmid was used to transform the mutant strain. The acquisition and the expression of the DNA were verified by PCR on the transformant DNAs, using a primer pair (*smtBfw*/*smtBrv*) which amplified a fragment of 372 bp corresponding to the *TtsmtB* gene, and by RT-PCR on the transformant DNAseI-treated RNA, using a primer pair (*smtBrealfw/0353rv*) which amplified a fragment of 107 bp inside the *TtsmtB* gene (Table S2).

qRT-PCR. To determine whether *TtsmtB* gene expression (*TTC0353*) was induced by arsenic, and to verify the expression of *TTC0351*, *TTC0354* and *TtArsC* (*TTC1501*) in the *ΔsmtB* strain, qRT-PCR reactions were performed using the Step-ONE plus Real time PCR system (Applied Biosystems) and the SYBR Select Master Mix kit (Applied Biosystems). Total RNA extracted from *T. thermophilus* HB27 and

ΔsmtB cells (treated or not with arsenite or arsenate as described above) was digested with Turbo DNase, RNase free. The cDNAs were synthetized using a mixture of the proper reverse primer (*0351realrv*, *0353rv*, *0354realrv* or *arsCrealrv*) and the 16S reverse primer (*16Sthrv*), used as internal control. The specific cDNAs synthesized were amplified using the following primers: *0351realfw* and *0351realrv*; *smtBrealfw* and *0353rv*; *0354realfw* and *0354realrv*; *arsCrealfw* and *arsCrealrv* or *16Sthfw* and *16Sthrv* (Table S2). The oligonucleotides were designed using Primer Express 2.0 software (ABI Biosystems) and amplified a 112-bp *TTC0351*- specific product, a 107-bp *TtsmtB*-specific product, a 89-bp *TTC0354*-specific product and a 100-bp *TtarsC*-specific product. For the amplification of the specific cDNAs 25 ng from the RT-reaction mixture were used, whereas 5 ng were used to amplify the 16S fragment. DNA contamination was tested by the inclusion of a control without reverse transcriptase for each RNA sample. Two independent experiments were performed, and each sample was always tested in triplicate. PCR amplification followed a standard protocol, with a 15 s denaturation phase at 95 °C, and a specific annealing temperature for each primer set for 30 s for 40 cycles. The amplification data were analyzed using the Step-ONE software (Applied Biosystems). Induction folds were calculated by the comparative Ct method. The relative expression ratio of the target gene, *TtsmtB* or *TTC0354*, vs. that of the 16S rRNA gene was calculated by the equation: $RQ = 2^{-\Delta\Delta Ct}$, whereas $\Delta\Delta Ct = \Delta Ct$ reference-ΔCt target and $\Delta Ct = Ct$ gene of interest-Ct reference gene (27).

Computational methods. *Promoter identifications*- The promoter regions upstream of *TTC0351*, *TTC0353*, *TTC0354* and *TtarsC* (*TTC1502*) (21) were identified using bioinformatic tools for promoters search available at http://www.softberry.com/berry.phtml?topic=bprom&group=programs&subgroup=gfin db, http://www.fruitfly.org/seq_tools/promoter.html and manual alignments.
As the promoter consensus sequences they were considered those reported in Setostyanova et al. (28).
Protein analyses- To establish relations of similarity between the *Tt*SmtB protein sequence and protein sequences in the SwissProt Data Bank, the BLAST program was used (29). The protein sequence alignments were generated using CLUSTALW (30). Predictions of the secondary and tertiary protein structures were obtained through the use of Psipred and ESyPred3D programs available through http://www.expasy.org/.

Cloning, expression and purification of *TtsmtB*. The gene encoding *TtsmtB* (*TTC0353*) from *T. thermophilus* HB27 was amplified by PCR on genomic DNA, using Taq DNA polymerase (Thermo Scientific) and the primers containing the *Nde*I (*smtBfw*) and *Hind*III (*smtBrv*) sites at the 5' and 3' ends, respectively. Amplified fragments were purified, digested with appropriate restriction enzymes, and cloned in the *Nde*I/*Hind*III-digested pET28b(+) vector (Novagen). For protein expression, *E. coli* BL21-CodonPlus(DE3)-RIL cells transformed with pET28/*TtsmtB* were grown in LB medium containing kanamycin (50 µg/ml), chloramphenicol (33 µg/ml) and 0.25 mM $ZnSO_4$. When the culture reached 0.7 OD_{600nm}, protein expression was induced by the addition of 0.5 mM isopropyl-1-thio-β-D-galactopyranoside (IPTG) and the bacterial culture was grown for 16 h at 22 °C. Cells were harvested and lysed by sonication in 50 mM Tris-HCl, pH 7, as described (31). The recombinant protein was purified to homogeneity through two different steps: a heat treatment of the cell extract (65 °C for 10 min) followed by HiTrap Heparin chromatography (5 ml; GE

Healthcare) connected to an AKTA Explorer system (GE Healthcare). The fractions containing *Tt*SmtB were pooled, concentrated by ultrafiltration, dialyzed for 16 h at 4 °C against 50 mM Tris-HCl, pH 7.0, 0.15 M NaCl. To maintain the cysteines in the reduced state 1 mM DTT was added at each passage, and an inhibitor cocktail was also added to prevent protease activity.

To determine the native molecular mass of *Tt*SmtB, the purified protein was applied to an analytical Superdex PC75 column (0.3 cm x 3.2 cm) connected to the AKTA Explorer system and equilibrated in 50 mM Tris-HCl, pH 7, 0.2 M NaCl. The column was calibrated using a set of gel filtration markers (low range, GE Healthcare), including bovine serum albumin (67.0 kDa), ovalbumin (43.0 kDa), chymotrypsinogen A (25.0 kDa), and RNase A (13.7 kDa).

*Tt*SmtB protein was stored at -80 °C in single-use aliquots.

Circular Dichroism Measurements. CD spectra were recorded by using a Jasco J-815 CD spectrometer, equipped with a Peltier-type temperature control system (PTC-423S/15 model). Cells with path lengths of 0.1 cm were used in the far-UV region. CD spectra were recorded as described (32), with a time constant of 4 s, a 2 nm bandwidth, and a scan rate of 20 nm/min; the signal was averaged over at least three scans and baseline corrected by subtraction of a buffer spectrum. Spectra were analyzed for secondary structure using CD Deconvolution PRO and Dichroweb softwares (33). CD measurements were carried out using protein concentration of about 15 μM in a 25 mM Na-P, pH 7.0 buffer.

Electrophoretic mobility shift assay. To determine the binding of *Tt*SmtB to the putative promoter regions of *TTC0351, TTC0353, TTC0354,* and *TtarsC* an electrophoretic mobility shift assay (EMSA) was performed. The promoter regions were amplified by PCR using *0350drprex* and *0351prshort rv, 0353prshort fw* and *R0353 NdeI, New 0345 pr fw* and *R0354 NdeI, ArsCprfw* and *ArsCprrv* primer pairs (Table S2) giving 78-bp, 84-bp, 82-bp, and 78-bp fragments, respectively. EMSA reactions were set up as described in Fiorentino et al. (34); briefly, a final volume of 15 μl contained 15.000 cpm of ^{32}P-radiolabeled DNA, 0.5 μM of proteins in binding buffer (25 mM Tris-HCl, pH 8.0, 50 mM KCl, 10 mM MgCl$_2$, 1 mM dithiothreitol, 5% glycerol). The mixtures were incubated at 60 °C for 20 min and loaded onto a non-denaturing 6% polyacrylamide gel (Bio-Rad) in 1X TBE at 80 V. The gels were dried and analyzed by phosphor imaging using Quantity One software (Bio-Rad).

Sequence specific binding to *TTC0354* promoter was evaluated in a competition assay using competitors in a molar ratio of 1:200 and 1:400. As aspecific DNA a 150-bp coding region from *S. solfataricus* was amplified with *VP2 fw* and *VP2 rv* primers (35).

To quantify the interaction between *Tt*SmtB and *TTC0354* promoter the DNA was incubated with increasing amounts of the protein (0.2 - 2 μM the complexes were separated and the gels were processed and visualized as described above. To determine the dissociation constant (K$_d$) densitometric data were obtained with Quantity One (Bio-Rad) and manipulated to calculate the fractional complex formation (that is the ratio between the density of the retarded band and the total density, reported in percent). These values were analyzed by fitting the binding isotherm to the Hill equation in GraphPad Prism 6.0, and were derived from the average of two independent experiments.

In order to determine if arsenite and arsenate were ligands for *Tt*SmtB and their possible effect on binding to the target *TTC0354* promoter, 0.5 μM of protein was

pre-incubated with NaAsO$_2$ or KH$_2$AsO$_4$ at two different molar ratio (1:50 and 1:200, considering *Tt*SmtB as a dimer).

RESULTS

Identification in *T. thermophilus* HB27 of the *TTC0353* transcriptional unit, putative promoter elements and regulation by arsenic. The genomic context of *TTC0353* (*TtsmtB*) represented in Fig. 1 includes a putative cluster from *TTC0351* to *TTC0355*, with the upstream and downstream genes (*TTC0350* and *TTC0356*) with opposite orientation. *TTC0351*, encoding a putative cell wall endopeptidase of 388 amino acids, is separated from *TTC0352* by 134 bp. *TTC0352* and *TTC0355* encode homologues to the two subunits of pyridoxal 5'-phosphate (PLP) synthase, an important enzyme for *de novo* biosynthesis of PLP coenzyme. *TTC0354*, separated from *TTC0353* by 32 bp, encodes a putative cation-transporting ATPase containing a heavy metal associated (HMA) motif. In order to examine if a single transcript was formed with contiguous upstream and downstream genes, as suggested by bioinformatics, a RT-PCR analysis was performed using total RNA extracted from cells grown in TM medium; each reaction primer set spanned the junctions between two adjacent genes. In particular, with the above-mentioned RNAs, the reverse transcription reaction was obtained using alternatively: the primer *0352rv* (B in Fig. 1A), annealing to a sequence in the *TTC0352* gene at +138 from the putative start codon; the primer *0353rv* (D in Fig. 1A), annealing to a sequence in the *TTC0353* gene at +194; the primer *0354rv* (F in Fig. 1A), annealing to a sequence in the *TTC0354* gene at +125; or the primer *0355rv* (H in Fig. 1A), annealing from position +45 in the corresponding gene. The four cDNAs obtained were then used in PCR reactions with primers *0351fw*, *0352fw*, *0353fw* and *0354fw* (A, C, E and G in Fig. 1A), respectively. From all primer pairs fragments of the expected size were obtained (427 bp from *0351fw/0352rv*; 221 bp from *0352fw/0353rv*; 295 bp from *0353fw/0354rv*; 635 bp from *0354fw/0355rv*) (Fig. 1B). These results suggest that the four genes are co-transcribed as a polycistronic messenger. Investigation on the occurrence of similar gene associations in annotated bacterial genomes through Blast analysis, showed an identical organization in diverse *T.thermophilus* strains (HB8, SG09) but also in *T. oshimai* and *T. scotoductus,* suggesting conservation of such cluster in *Thermus* genus.
Transcription could initiate from a promoter putatively located in the 557 bp intergenic region between *TTC0350* and *TTC0351*.
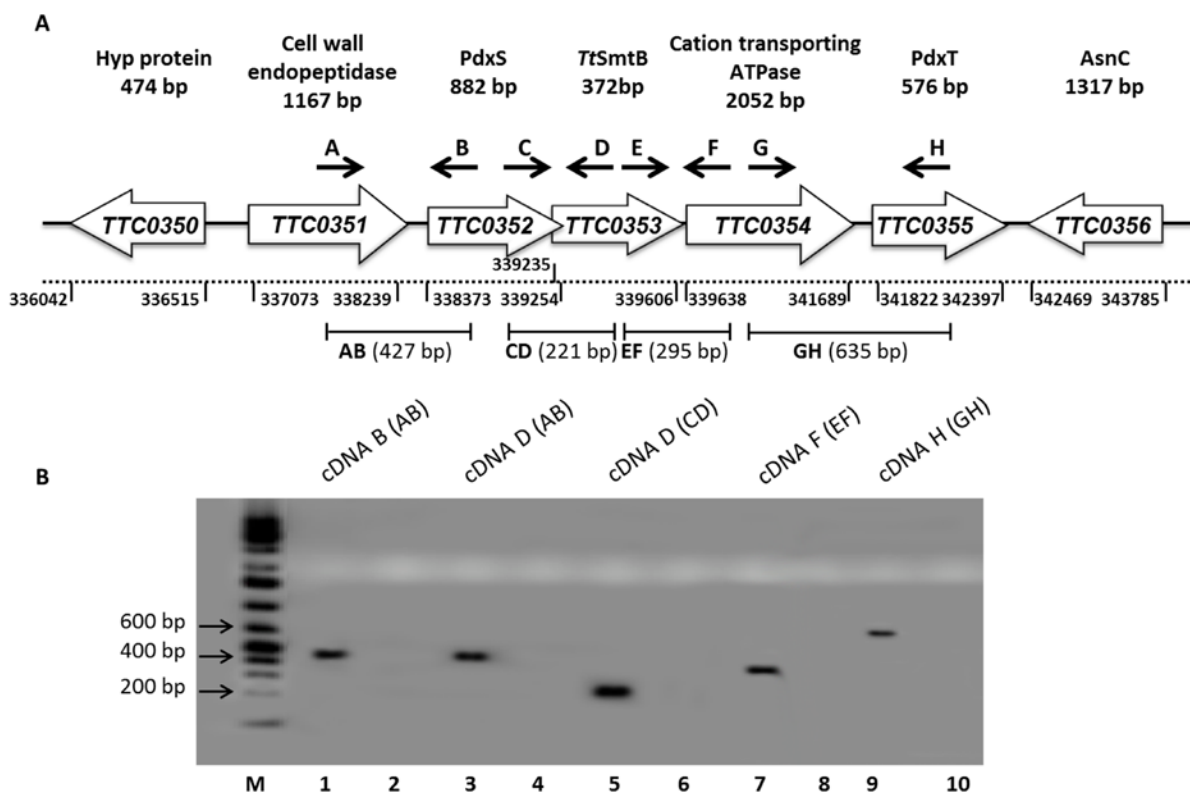
Fig.1. A. Schematic representation of the genomic environment of *TtsmtB*. Arrows above ORFs depict annealing positions and orientation of the primers used.
B. Identification of the transcriptional unit. Agarose gel of RT-PCR products. All the RT-PCR products have the expected size (AB: 427 bp, CD: 221 bp, EF: 295 bp, GH: 635 bp). M: molecular weight marker; lanes 2, 4, 6, 8, 10: negative controls obtained using as template digested RNAs incubated without reverse transcriptase; lane 1: AB fragment from the *TTC0352* cDNA; lane 3: AB fragment from the *TTC0353* cDNA; lane 5: CD fragment from the *TTC0352* cDNA; lane 7: EF fragment from the *TTC0354* cDNA; lane 9: GH fragment from the *TTC0355* cDNA.

Since the prediction on the functions of the genes in the operon did not suggest a shared role in arsenic challenge, a search for basal promoters and *Tt*SmtB binding sites was carried on in the intergenic regions using both available tools for promoter search and a "handmade" analysis (see Materials and Methods) (28). As shown in Fig. 2A, -35 and -10 consensus were found upstream of *TTC0351*, *TTC0353* and *TTC0354*, suggesting the presence of internal promoters and/or independent transcription. *TTC0353* stop codon and *TTC0354* start codon are distant 32 bp from each other; interestingly the region located between putative basal promoter elements of *TTC0354* contains the palindromic sequence (6-2-6) TTGACCAGTTGCTCAA matching the consensus of the ArsR/SmtB binding site (Fig. 2B) (18). This suggests that the intergenic region between *TTC0353* and *TTC0354* could be the regulatory target of *Tt*SmtB.

A   0351prom

cgcccc**ttgcct**tttggggcggggcccctgg**taaaat**gcgggcggctttagaggcctcctggaggtgaagcttgcgg**ttg**

0353prom

agccca**tggtgg**gcatcaacctggaccagc**tcaagg**aggaggaaaggc**ttg**

0354prom

aaacac**ttgacc**agttgctcaatgatgc**taccct**gggggc**atg**

B
0354prom   AACAC**TTGACCA** GT TGCTCAAATGATGC**TACCCT**
                         ||||| | | | ||||
SmtB consensus   ATANN**TGANNA** NN TNN**TCANN**TAT
binding site   6-2-6
                   —————————————————————————
                           12-2-12

Fig.2. A. *TTC0351*, *TTC0353*, *TTC0354* putative promoters with likely locations of consensus elements shown in bold. **B**. Identification of the consensus *ArsR/SmtB* DNA binding site within *TTC0354* promoter.

To verify if *TTC0351*, *TTC0353* and *TTC0354* expressions were arsenic dependent, qRT-PCR was carried out on RNAs obtained from cells treated for one hour with arsenic compounds, in comparison with untreated cells. As shown in Fig. 3, three-fold in *TTC0351* expression and two-fold increases of *TtsmtB* were observed in cells exposed to arsenate and a four-fold *TTC0354* induction was measured in arsenite treated cells. Such differences in the expression levels strongly suggest the activation of internal promoters under treatment conditions.
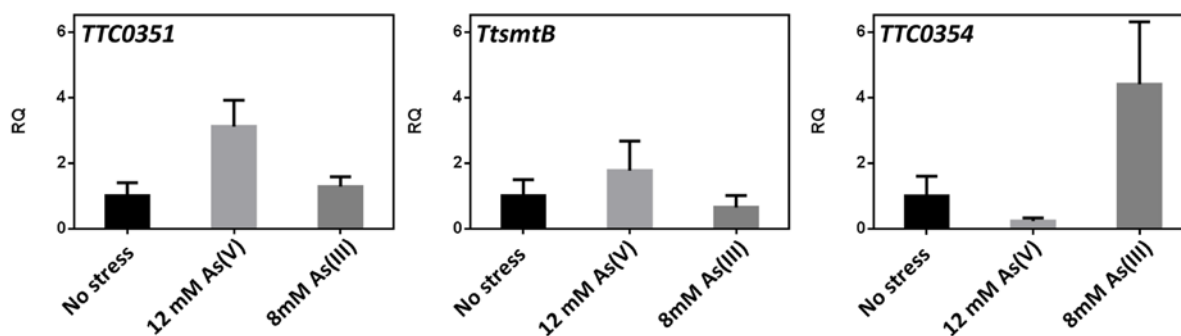
Fig.3. qRT-PCR expression analysis of *TTC0351*, *TtsmtB* (*TTC0353*) and *TTC0354*, after treatment for 60 minutes with arsenate and arsenite at sub-inhibitory concentrations (12 mM and 8 mM).

Taken together these results suggest: i) co-transcription as a single polycistronic messenger under basal conditions (the one we tested); ii) the presence of putative arsenic responsive promoters upstream of *TTC0354* that could determine different gene expression regulation; iii) the involvement of *TTC0351*, *TTC0353* and *TTC0354* in arsenic response, supporting the hypothesis of complex regulation mechanisms.

Cloning, expression purification and characterization of *Tt*SmtB. The *TTC0353* gene encodes a putative protein of 123 amino acids (predicted molecular weight of 13508.79 Da and a pI of 8.54) belonging to the ArsR/SmtB transcriptional regulator family. In fact, it has a conserved HTH DNA binding motif and a conserved ELCV(C/G)D metal binding box both located in the α-4 helix. Alignments with homologues also showed 50% identity with a structurally characterized transcriptional repressor from *Synechococcus* Pcc7942 (36). The conservation of the metal binding box and of a cysteine residue (Cys10) at the N-terminus involved in metal binding strongly suggest a key role for this protein in metal sensing. Secondary structure predictions revealed an organization in 6 α helices and 1 β-sheet, comparable to that found in ArsR/SmtB regulators (18) (Fig S1). To demonstrate that *Tt*SmtB was indeed a transcriptional regulator, the gene was cloned in pET28b(+) plasmid, producing the *Tt*SmtB protein fused to a N-terminal His-tag after expression in *E. coli* BL21- Codon Plus(DE3)-RIL. The sequence of the cloned fragments confirmed the correct fusion of *Tt*SmtB to the His-tag and it was shown to be identical to the original annotated sequence (http://www.ncbi.nlm.nih.gov/gene/2776273).

The purification protocol developed for the recombinant protein consisted in a heat treatment of the cell extract followed by HiTrap heparin chromatography (Fig. 4A). From 1l culture about 40 mg of pure protein were obtained. Addition of zinc in the culture medium and induction at 22 °C improved the yield of purified protein of about threefold and increased its stability over time.

Far-UV circular dichroism spectra were recorded to determine the secondary structure composition of *Tt*SmtB. Spectra showed a typical circular dichrogram of a helical protein with negative maxima at 208 and 222 nm and one positive peak at 195 nm (Fig.4B), indicative of a predominantly folded structure with an α-β content. Gel filtration experiments were conducted to assess the dimeric state of *Tt*SmtB in solution (data not shown).
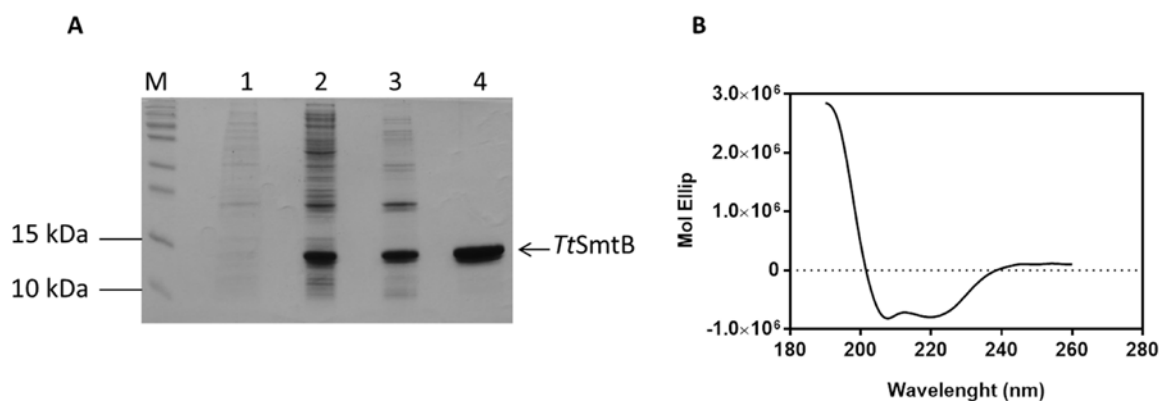

Fig.4 Analysis of recombinant *Tt*SmtB. **A**. SDS-PAGE of the purification steps: lane M: molecular mass marker; lane 1: cell extract from non-induced cells; lane 2: crude extract; lane 3: heat-treated cell extract; lane 4: fraction from Heparin chromatography. **B**. Far-UV CD spectrum of 15 μM *Tt*SmtB.

To verify if the protein was able to recognize different putative regulatory regions we performed EMSA assays. In particular, the 78-bp, 84-bp, 82-bp and 78-bp intergenic regions upstream of *TTC0351, TTC0353, TTC0354* and *TtarsC,* respectively were incubated with 0.5 μM of purified recombinant protein. Fig. 5A shows that the protein is able to bind to all the selected regions even though with different features; in fact the strongest binding is shown towards *TTC0354* (lane 4) and the lowest toward its

own putative promoter (lane 2) where the retarded band is hardly detectable. Interestingly, the proteins also bind to *TtarsC* putative cis-acting sequences (lane 8). There is a SmtB consensus binding site upstream of *TTC0354*, the putative cation exporting membrane ATPase, so further analyses were performed to better characterize the interaction of *Tt*SmtB with this region. At first we assessed if *Tt*SmtB binding to the promoter was specific; the *TTC0354 prom-Tt*SmtB complexes dissociated in the presence of an excess of cold specific probe (Fig. 5B, lanes 3-4) and were conserved in the presence of an excess of non-specific DNA (Fig. 5B, lanes 5-6), demonstrating binding specificity. Titration with increasing amounts of *Tt*SmtB indicated that the protein binds to this region in a concentration-dependent manner; furthermore, at saturating concentrations, the protein determined a shift with decreased mobility, suggesting either that other binding sites with different affinities could exist in the DNA sequence analyzed or that multiple dimers could associate to the cognate DNA. The profile obtained by fitting densitometric data to a binding curve with a Hill slope gave an overall apparent equilibrium dissociation constant (K_d) of 0.27 ± 0.07 µM and provided a Hill coefficient of 2.5 (Fig. 5C, 5D), suggesting that DNA binding is cooperative, as reported for other characterized SmtB family members (37, 38). To analyze if arsenic had an effect on the DNA binding ability by *Tt*SmtB, we performed EMSAs in which complex formation was tested after preincubation of the protein with increasing concentrations of arsenate and arsenite. The results reported in Fig. 5E, 5F demonstrate that the interaction of arsenate and arsenite to *Tt*SmtB, hampers binding to the *TTC0354* promoter although with different behaviour.
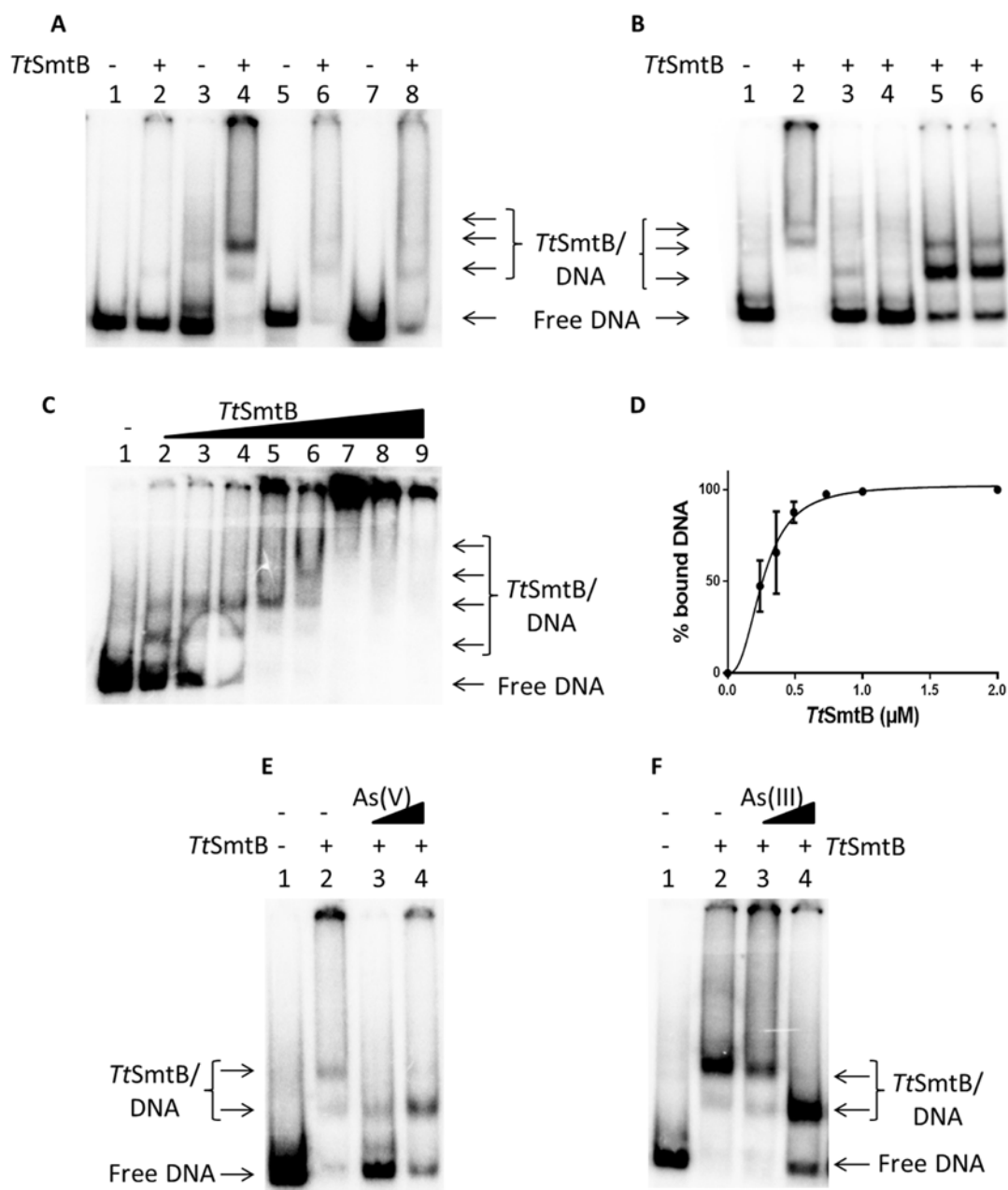
41

Fig.5. Mobility shift assays.

A. Binding of *Tt*SmtB to the *TTC0353* (lane 2), *TTC0354* (lane 4), *TTC0351* (lane 6) and *TtarsC* (lane 8) putative promoters. Lanes 1, 3, 5, 7: free probes.

B. Competition assay: EMSA were performed using *TTC0354 prom* (1 nM) both in the absence (lane 2) and in the presence of 200x and 400x of unlabeled specific (lanes 3,4) or aspecific competitor (lanes 5,6) using 0.5 µM *Tt*SmtB.

C. Titration of *TTC0354 prom* with increasing concentrations of *Tt*SmtB: lane 1, labeled DNA fragment; lanes 2-9, DNA probe incubated with *Tt*SmtB at concentrations ranging from 0.2 to 2 µM.

D. Densitometric data from EMSA obtained as described in Materials and Methods plotted vs the concentration of the protein. Error bars represent the standard deviation for each point derived from two experiments.

E. Binding of *Tt*SmtB to the *TTC0354* prom without (lane 2) and with 50x and 200x arsenate (lanes 3, 4).

F. Binding of *Tt*SmtB to the *TTC0354* prom without (lane 2) and with 50x and 200x arsenite (lanes 3, 4).

42

Construction, isolation and confirmation of *smtB⁻* mutants *(ΔsmtB)*. To evaluate the *in vivo* role of *TTC0353* in the regulation of the arsenic resistance mechanism, a *smtB⁻* mutant was obtained.
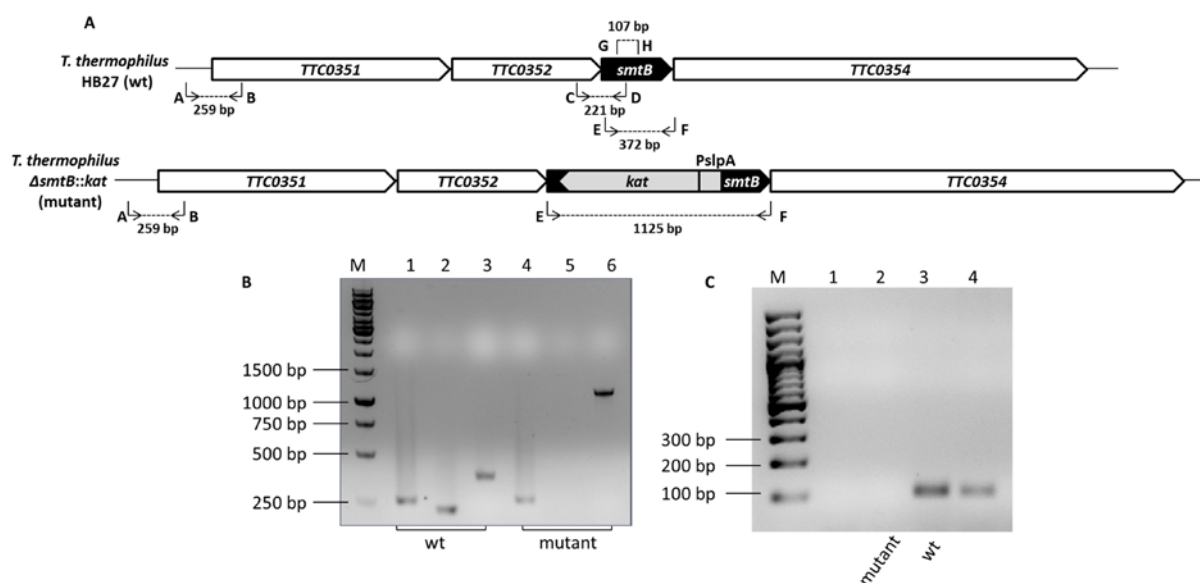

Fig.6.
A. Schematic representation of the genomic environment of *TtsmtB* and of its replacement with the *kat* cassette. Arrows above depict annealing positions and orientation of the primers used.
B. Identification *T. thermophilus ΔsmtB::kat* by PCR analysis. M: molecular weight marker; lanes 1-4 AB fragment from genomic DNA of *T. thermophilus* HB27 and *ΔsmtB::kat* respectively; lanes 2-5 CD fragment from genomic DNA of *T. thermophilus* HB27 and *ΔsmtB::kat* respectively; lanes 3-6 EF fragment from genomic DNA of *T. thermophilus* HB27 and *ΔsmtB::kat* respectively.
C. RT-PCR analysis of the *TtsmtB* gene. M: molecular weight marker; lane 1 negative control; lane 2 PCR on *TTC0353* cDNA from *T. thermophilus ΔsmtB::kat*; lane 3 PCR on *TTC0353* cDNA from *T. thermophilus* HB27; lane 4 positive control (genomic DNA of *T. thermophilus* HB27).

The *Ttsmtb* gene was inactivated by inserting in its coding sequence a kanamycin resistance gene (Fig 6A). The screening of the recombinants grown in TM medium containing kanamycin was carried out by PCR using genomic DNA and the CD primer pair (see Fig. 6A). 0353rv anneals in the deleted region so the absence of an amplification band is expected in the Δ*smtB* strain (Fig. 6B lanes 2 and 5). As a positive control, a 298 bp region was amplified in both wild type and Δ*smtB*, using the primer set 0351promfw, 0351promrv (Fig. 6 lanes 1 and 4). To confirm the correct insertion of the *kat* cassette in the genome, genomic DNA from wild type and Δ*smtB* was amplified using primers EF (see Fig. 6A) that amplified the *TtsmtB* gene or the *kat* gene in the wild type and mutant strains respectively (Fig. 6B lanes 3 and 6). The substitution between the two genes was confirmed by DNA sequencing.
RT-PCR indicated expression of the *TtsmtB* gene only in the wild type strain, indicating that the gene was inactivated in the mutant (Fig 6C).

Function of *Ttsmtb* in arsenic resistance. In the absence of arsenic, Δ*smtB* and wild type grew in a similar manner, suggesting that the gene was not essential for *T. thermophilus* survival. In order to test if Δ*smtB* strain was resistant to arsenic, its growth in the presence of arsenate and arsenite was verified and compared to that of the wild type. Interestingly, the mutant showed a decrease in growth rate in arsenate containing media (Tab. 1) although reaching the same final OD of the wild type.

43

To verify if the genes encoded in the operon were repressed by *Tt*SmtB we performed qRT-PCR on Δ*smtB* cDNAs compared to expression in the wild type strain in the absence of arsenic. Hence, as target genes we included *TTC0351* and *TTC0354*; furthermore, we wanted also to verify *TtarsC* expression in a *smtB⁻* background since we have previously demonstrated its role in the arsenic resistance mechanism. The results are reported in Fig.7: four-fold increase in the expression of *TTC0351*, three-fold in *TTC0354* expression and two-fold in *TtarsC* expression could be observed in Δ*smtB* compared to the wild type strain.
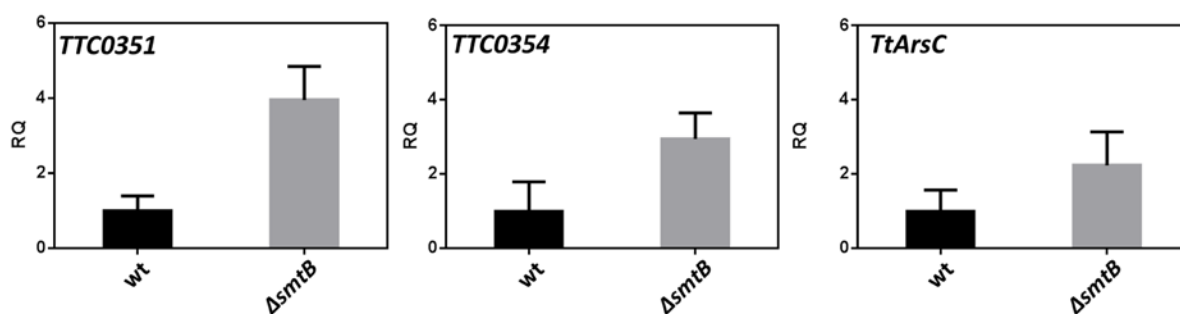

Fig.7. qRT-PCR expression analysis of *TTC0351*, *TTC0354* and *TtArsC*, in *T. thermophilus* HB27 (wt) and *T. thermophilus* Δ*smtB*::*kat* (Δ*smtB*).

These results suggest a direct involvement of *Tt*SmtB in arsenic sensing through the derepression of the entire operon as well as of the other target genes.

Analysis of *TtsmtB* complemented strain. To evaluate the effect of *Tt*SmtB on Δ*smtB* growth the *TtsmtB* gene was cloned in the pMKpnqobgaA, a plasmid under the control of a constitutive promoter (See Materials and Methods). Δ*smtB* cells were transformed with the recombinant vector and the expression of the heterologous gene was verified by RT-PCR (Fig. 8).
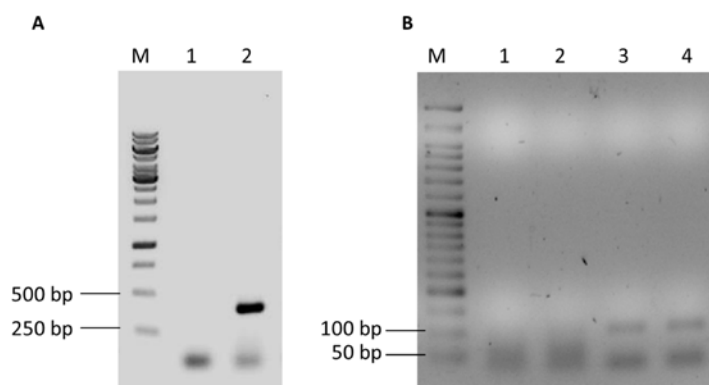

Fig. 8. Complementation of Δ*smtB*::*kat*.
A. PCR analysis of *TtsmtB* complemented strain. M: molecular weight marker; lane 1 negative control; lane 2: genomic DNA of *TtsmtB* complemented strain.
B. RT-PCR analysis *TtsmtB* complemented strain. M: molecular weight marker; lane 1 negative control; lane 2 *TTC0353* cDNA from *T. thermophilus* Δ*smtB*::*kat*; lane 3 *TTC0353* cDNA from *TtsmtB* complemented strain; lane 4 genomic DNA of *T. thermophilus* HB27.

Then growth was analyzed under control and treatment conditions. As can be inferred from the generation times, expression of *TtsmtB* in the mutant increased its

growth rate in arsenate growing cells (Table 1), further supporting its role in the arsenate sensing.

TABLE 1

	wild type	**Δ*smtB::kat***	***TtsmtB* complemented strain**
As free medium	1,32±0,1	1,22±0,08	1,38±0,07
12 mM As(V)	1,86±0,3	4,42±0,9	3±0,2
8 mM As(III)	4,84±1	5,89±1	6,03±1

Generation times (hour) of wild type *T. thermophilus* HB27, *ΔsmtB::kat* and *TtsmtB* complemented strain, grown without or with arsenate As(V) and arsenite As(III) at sub-inhibitory concentrations.

DISCUSSION

Thermophilic microorganisms are good models to explain the ability to cope with metal stress because they play important roles in arsenic bioavailability in thermal environments (39). Thus, knowledge of their physiology may be critical to monitoring the biogeochemical cycle of such metalloid and limiting its toxic effect. In the thermophilic Gram negative bacterium *T. thermophilus* HB27 we characterized the thermostable arsenate reductase *Tt*ArsC as a protein able to reduce pentavalent arsenate to trivalent arsenite in the cells (21, 40).

In this study, we further examined the arsenic resistance mechanism in this thermophile and defined the role of *TtsmtB* (*TTC0353*) as the transcriptional regulator sensitive to arsenic.

The search on the genome for arsenic resistance pathways led to the identification of *TTC0353* as a gene encoding a putative transcriptional repressor belonging to the ArsR/SmtB family. Transcriptional analysis by RT-PCR of *TtsmtB* and its neighboring genes showed that the gene was expressed in third position of an operon of five genes (*TTC0351-TTC0352-TTC0353-TTC0354- TTC0355*) encoding putative proteins with no obvious functional relation, except for *TTC0354*. This gene encodes a putative cation-transporting ATPase with a heavy-metal-associated domain that could mediate the active efflux of arsenite. qRT-PCR analysis showed the variation in the transcription profiles of *TTC0351*, the first gene of the operon, as well as of *TTC0353* and *TTC0354* upon arsenate and arsenite treatment (see Fig. 3) confirming their involvement in arsenic response and suggesting that *Tt*SmtB could be the true regulator.

Interestingly, despite being a gene cluster, basal promoter consensus elements were identified by homology search not only upstream of *TTC0351* but also as internal promoters i.e. upstream of *TTC0353* and *TTC0354* suggesting that these genes could also be singularly transcribed and distinctly regulated in order to ensure that relative expression levels of the various genes could vary under diverse growth conditions (41). Furthermore, *TTC0354* promoter contained sequences corresponding to the consensus palindromic SmtB binding site overlapping basal transcription elements (Fig. 2B) (18), strongly indicating that *TTC0354* expression could be regulated through modulation of DNA binding by the metal sensor *Tt*SmtB.

45

In *Bacteria*, the placement of the binding sites of transcription repressors relative to promoter elements is the primary determinant affecting transcription initiation. The location of the SmtB binding site overlapping the basal consensus elements suggests a negative regulatory role, i.e. as repressor, of these *cis*-acting elements also in agreement with previously characterised ArsR/SmtB family members (15).

To investigate on this latter point, *Tt*SmtB was cloned and expressed in recombinant form in *E. coli*, purified to homogeneity and functionally characterized. *In vitro*, recombinant *Tt*SmtB bound to all the promoters that we identified with different features; in particular, a hardly detectable complex was formed between *Tt*SmtB and its own promoter suggesting lower transcriptional repression exerted on it. This result is in agreement with the importance of maintaining steady and constant levels of the metal sensor *Tt*SmtB to efficiently respond to fluctuation of arsenite/arsenate intracellular concentration.

Furthermore, *Tt*SmtB bound to *TTC0354* promoter sequence site-specifically, in a cooperative manner (n Hill = 2.5) and with high affinity (K_d of 0.27 µM); it was not able to interact with such DNA sequence in the presence of both arsenate and arsenite (in a range of concentration that could be of physiological significance) suggesting that *in vivo* the transcription of this gene could be repressed under basal conditions and activated upon increase in intracellular arsenate/ite concentration.

A key step in the arsenic resistance is the intracellular reduction of arsenate to arsenite by arsenate reductases which are usually encoded in the same operon of the regulator (12); since in *T. thermophilus* resistance genes have not been found in a single operon, we confirmed through EMSA the ability of *Tt*SmtB to act also on the promoter of *Tt*ArsC whose role in arsenic challenge had already been proved (21).

Altogether these results give insights in the mechanisms of metal-regulated gene expression in thermophilic microorganisms; on the other hand *Tt*SmtB is the first thermostable ArsR/SmtB member and represents a good model system to shed light on the biochemical mechanisms of metal specificity and metal induced allostery in this class of regulators.

To verify *in vivo* the function of *Tt*SmtB in the regulation of arsenic related genes, a *smtB*⁻ mutant (*ΔsmtB*) was obtained and the expression levels of *TTC0351*, *TTC0354* and *TtarsC* were measured by qRT-PCR. In the mutant strain, gene expression levels were significantly higher than in the wild type (Fig. 7) giving experimental evidence that *in vivo Tt*SmtB is bound to its target promoters hampering gene transcription.

The results also proved that the gene is not essential for *T. thermophilus* survival as the *ΔsmtB* strain grew alike the wild type in arsenic free media; interestingly, whereas the mutant grew similarly to the wild type in the presence of arsenite, it showed a decreased growth rate in arsenate-containing medium. It can be hypothesized that in the *ΔsmtB* strain the exposition to arsenite could be counteracted by the increased expression of *TTC0354* allowing a faster extrusion from the cell. On the other hand, the inhibitory effect of arsenate on cell growth can be overcome only after the catalytic reduction to arsenite by *Tt*ArsC which precedes the transport outside the cell. Similar findings were observed in a *Synechocystis* sp. strain PCC 6803 mutant lacking *arsR* gene (42). Interestingly, complementation of *Tt*SmtB in the *ΔsmtB* strain increased the arsenate tolerance and partially recovered growth to the wild-type levels (Table 1); these results are consistent with the restored *TtsmtB* expression (Fig. 8), confirming its role in the regulation of arsenic resistance.

The role of *Tt*SmtB and its regulative sequences in arsenic sensing adds a new tile in the puzzle of the molecular mechanism of *T. thermophilus* arsenic resistance and

represents an important progress either for the development of effective, safe and stable whole-cell arsenic biosensors or for the exploitation of novel bioremediation processes.

ACKNOWLEDGMENTS

REFERENCES

1.   **Meng YL, Liu ZJ, Rosen BP.** 2004. As(III) and Sb(III) uptake by G1pF and efflux by ArsB in Escherichia coli. Journal of Biological Chemistry **279:**18334-18341.
2.   **Liu ZJ, Boles E, Rosen BP.** 2004. Arsenic trioxide uptake by hexose permeases in Saccharomyces cerevisiae. Journal of Biological Chemistry **279:**17312-17318.
3.   **Tawfik DS, Viola RE.** 2011. Arsenate Replacing Phosphate: Alternative Life Chemistries and Ion Promiscuity. Biochemistry **50:**1128-1134.
4.   **Kamerlin SCL, Sharma PK, Prasad RB, Warshel A.** 2013. Why nature really chose phosphate. Quarterly Reviews of Biophysics **46:**1-132.
5.   **Kulp TR, Hoeft SE, Asao M, Madigan MT, Hollibaugh JT, Fisher JC, Stolz JF, Culbertson CW, Miller LG, Oremland RS.** 2008. Arsenic(III) fuels anoxygenic photosynthesis in hot spring biofilms from Mono Lake, California. Science **321:**967-970.
6.   **van Lis R, Nitschke W, Duval S, Schoepp-Cothenet B.** 2013. Arsenics as bioenergetic substrates. Biochimica Et Biophysica Acta-Bioenergetics **1827:**176-188.
7.   **Qin J, Rosen BP, Zhang Y, Wang GJ, Franke S, Rensing C.** 2006. Arsenic detoxification and evolution of trimethylarsine gas by a microbial arsenite S-adenosylmethionine methyltransferase. Proceedings of the National Academy of Sciences of the United States of America **103:**2075-2080.
8.   **Wysocki R, Clemens S, Augustyniak D, Golik P, Maciaszczyk E, Tamas MJ, Dziadkowiec D.** 2003. Metalloid tolerance based on phytochelatins is not functionally equivalent to the arsenite transporter Acr3p. Biochemical and Biophysical Research Communications **304:**293-300.
9.   **Jacobson T, Navarrete C, Sharma SK, Sideri TC, Ibstedt S, Priya S, Grant CM, Christen P, Goloubinoff P, Tamas MJ.** 2012. Arsenite interferes with protein folding and triggers formation of protein aggregates in yeast. Journal of Cell Science **125:**5073-5083.
10.   **Rosen BP.** 1999. Families of arsenic transporters. Trends in Microbiology **7:**207-212.
11.   **Lin Y-F, Walmsley AR, Rosen BP.** 2006. An arsenic metallochaperone for an arsenic detoxification pump. Proceedings of the National Academy of Sciences of the United States of America **103:**15617-15622.
12.   **Rosen BP.** 2002. Biochemistry of arsenic detoxification. Febs Letters **529:**86-92.
13.   **Indriolo E, Na G, Ellis D, Salt DE, Banks JA.** 2010. A Vacuolar Arsenite Transporter Necessary for Arsenic Tolerance in the Arsenic Hyperaccumulating Fern Pteris vittata Is Missing in Flowering Plants. Plant Cell **22:**2045-2057.
14.   **Morby AP, Turner JS, Huckle JW, Robinson NJ.** 1993. SMTB IS A METAL-DEPENDENT REPRESSOR OF THE CYANOBACTERIAL METALLOTHIONEIN GENE SMTA - IDENTIFICATION OF A ZN INHIBITED DNA-PROTEIN COMPLEX. Nucleic Acids Research **21:**921-925.
15.   **Wu J, Rosen BP.** 1991. THE ARSR PROTEIN IS A TRANS-ACTING REGULATORY PROTEIN. Molecular Microbiology **5:**1331-1336.
16.   **Shi WP, Wu JH, Rosen BP.** 1994. IDENTIFICATION OF A PUTATIVE METAL-BINDING SITE IN A NEW FAMILY OF METALLOREGULATORY PROTEINS. Journal of Biological Chemistry **269:**19826-19829.
17.   **Cook WJ, Kar SR, Taylor KB, Hall LM.** 1998. Crystal structure of the cyanobacterial metallothionein repressor SmtB: A model for metalloregulatory proteins. Journal of Molecular Biology **275:**337-346.
18.   **Osman D, Cavet JS.** 2010. Bacterial metal-sensing proteins exemplified by ArsR-SmtB family repressors. Natural Product Reports **27:**668-680.
19.   **Guerra AJ, Giedroc DP.** 2012. Metal site occupancy and allosteric switching in bacterial metal sensor proteins. Archives of Biochemistry and Biophysics **519:**210-222.

20.   **Donahoe-Christiansen J, D'Imperio S, Jackson CR, Inskeep WP, McDermott TR.** 2004. Arsenite-oxidizing Hydrogenobaculum strain isolated from an acid-sulfate-chloride geothermal spring in Yellowstone National Park. Applied and Environmental Microbiology **70:**1865-1868.

21.   **Del Giudice I, Limauro D, Pedone E, Bartolucci S, Fiorentino G.** 2013. A novel arsenate reductase from the bacterium Thermus thermophilus HB27: Its role in arsenic detoxification. Biochimica Et Biophysica Acta-Proteins and Proteomics **1834:**2071-2079.

22.   **Powell EO.** 1956. Growth rate and generation time of bacteria, with special reference to continuous culture. Journal of general microbiology **15:**492-511.

23.   **Miller JH.** 1972. Experiments in Molecular Genetics. Cold Spring Harbor, N. Y.

24.   **Fiorentino G, Del Giudice I, Bartolucci S, Durante L, Martino L, Del Vecchio P.** 2011. Identification and Physicochemical Characterization of BldR2 from Sulfolobus solfataricus, a Novel Archaeal Member of the MarR Transcription Factor Family. Biochemistry **50:**6607-6621.

25.   **Koyama Y, Hoshino T, Tomizuka N, Furukawa K.** 1986. GENETIC-TRANSFORMATION OF THE EXTREME THERMOPHILE THERMUS-THERMOPHILUS AND OF OTHER THERMUS SPP. Journal of Bacteriology **166:**338-340.

26.   **Moreno R, Zafra O, Cava F, Berenguer J.** 2003. Development of a gene expression vector for Thermus thermophilus based on the promoter of the respiratory nitrate reductase. Plasmid **49:**2-8.

27.   **Pfaffl MW.** 2001. A new mathematical model for relative quantification in real-time RT-PCR. Nucleic Acids Research **29**.

28.   **Sevostyanova A, Djordjevic M, Kuznedelov K, Naryshkina T, Gelfand MS, Severinov K, Minakhin L.** 2007. Temporal regulation of viral transcription during development of Thermus thermophilus bacteriophage phi YS40. Journal of Molecular Biology **366:**420-435.

29.   **Altschul SF, Madden TL, Schaffer AA, Zhang JH, Zhang Z, Miller W, Lipman DJ.** 1997. Gapped BLAST and PSI-BLAST: a new generation of protein database search programs. Nucleic Acids Research **25:**3389-3402.

30.   **Larkin MA, Blackshields G, Brown NP, Chenna R, McGettigan PA, McWilliam H, Valentin F, Wallace IM, Wilm A, Lopez R, Thompson JD, Gibson TJ, Higgins DG.** 2007. Clustal W and clustal X version 2.0. Bioinformatics **23:**2947-2948.

31.   **Pedone E, Fiorentino G, Pirone L, Contursi P, Bartolucci S, Limauro D.** 2014. Functional and structural characterization of protein disulfide oxidoreductase from Thermus thermophilus HB27. Extremophiles **18:**723-731.

32.   **Fiorentino G, Del Giudice I, Petraccone L, Bartolucci S, Del Vecchio P.** 2014. Conformational stability and ligand binding properties of BldR, a member of the MarR family, from Sulfolobus solfataricus. Biochimica Et Biophysica Acta-Proteins and Proteomics **1844:**1167-1172.

33.   **Whitmore L, Wallace BA.** 2008. Protein secondary structure analyses from circular dichroism spectroscopy: Methods and reference databases. Biopolymers **89:**392-400.

34.   **Fiorentino G, Ronca R, Cannio R, Rossi M, Bartolucci S.** 2007. MarR-like transcriptional regulator involved in detoxification of aromatic compounds in Sulfolobus solfataricus. Journal of Bacteriology **189:**7351-7360.

35.   **Fusco S, Aulitto M, Bartolucci S, Contursi P.** 2015. A standardized protocol for the UV induction of Sulfolobus spindle-shaped virus 1. Extremophiles **19:**539-546.

36.   **VanZile ML, Cosper NJ, Scott RA, Giedroc DP.** 2000. The zinc metalloregulatory protein Synechococcus PCC7942 SmtB binds a single zinc ion per monomer with high affinity in a tetrahedral coordination geometry. Biochemistry **39:**11818-11829.

37.   **Mandal S, Chatterjee S, Dam B, Roy P, Das Gupta SK.** 2007. The dimeric repressor SoxR binds cooperatively to the promoter(s) regulating expression of the sulfur oxidation (sox) operon of Pseudaminobacter salicylatoxidans KCT001. Microbiology-Sgm **153:**80-91.

38.   **Chauhan S, Kumar A, Singhal A, Tyagi JS, Prasad HK.** 2009. CmtR, a cadmium-sensing ArsR-SmtB repressor, cooperatively interacts with multiple operator sites to autorepress its transcription in Mycobacterium tuberculosis. Febs Journal **276:**3428-3439.

39.   **Paez-Espino D, Tamames J, de Lorenzo V, Canovas D.** 2009. Microbial responses to environmental arsenic. Biometals **22:**117-130.

40.   **Politi J, Spadavecchia J, Fiorentino G, Antonucci I, Casale S, De Stefano L.** 2015. Interaction of Thermus thermophilus ArsC enzyme and gold nanoparticles naked-eye assays speciation between As(III) and As(V). Nanotechnology **26**.

41.   **Napolitano M, Rubio MA, Camargo S, Luque I.** 2013. Regulation of Internal Promoters in a Zinc-Responsive Operon Is Influenced by Transcription from Upstream Promoters. Journal of Bacteriology **195:**1285-1293.

42.   **Maria Sanchez-Riego A, Lopez-Maury L, Javier Florencio F.** 2014. Genomic Responses to Arsenic in the Cyanobacterium Synechocystis sp PCC 6803. Plos One **9**.

2.2 A pull-down assay for the identification of *Tt*SmtB molecular interactors

As demonstrated in chapter 2.1, *Tt*SmtB was located in an operon of five genes with putative internal promoters, whose expression was differently regulated.

Since *Tt*SmtB should be their regulator, this could hypothetically interact with other proteins to regulate them; to investigate on this point a pull-down assay was performed to identify its molecular interactors.

This study was done in collaboration with Dr. Andrea Carpentieri (Department of Chemistry, University of Naples "Federico II").

Material and methods

Bacterial strains, plasmids, and growth conditions

Cultures of *T. thermophilus* HB27 were grown in TM medium (350 ml); when the cell density reached 0.5 OD_{600nm} , they were harvested at 0 and 60 min after the addition of 8 mM $NaAsO_2$ or 12 mM KH_2AsO_4, immediately spun down. Harvested cells were lysed by sonication (10'cycle: 30''on/30''off) in 20 mM Na_3PO_4 pH 7.5; an inhibitor cocktail was also added to prevent protease activity in the obtained protein extracts.

For the production of *Tt*SmtB, *E. coli* BL21-CodonPlus(DE3)-RIL cells transformed with pET28*/TtsmtB* (*E. coli* BL21-*Tt*SmtB) were grown as described in chapter 2.1.

Immobilized Metal Affinity Chromatography (IMAC) and Pull-down assay

The recombinant *Tt*SmtB was immobilized on a Ni^{2+}-NTA (nitrilotriacetic acid) resin by IMAC. Briefly, *E. coli* BL21-*Tt*SmtB protein extract, prepared as described before, was incubated for 16 h at 4 °C under stirring conditions, in order to enhance the interaction and the binding of the *Tt*SmtB histidines tail with the nickel ions of the resin. The Ni^{2+}-NTA resin functionalized with *Tt*SmtB (Ni^{2+}-NTA/*Tt*SmtB) was then washed three times with the equilibration buffer (20 mM Na_3PO_4, 0,5 M NaCl, 20 mM imidazole; pH 7.5) to remove the excess of unbound protein.

Ni^{2+}-NTA/*Tt*SmtB resin was incubated for 16 h at 4 °C under stirring conditions with the three *T. thermophilus* protein extracts (not treated and treated with arsenate and arsenite), then it was washed five times with the equilibration buffer and three times with the elution buffer (20 mM Na_3PO_4, 0,5 M NaCl, 0,5 M imidazole; pH 7.5). As negative controls samples of Ni^{2+}-NTA resin without *Tt*SmtB were incubated with the same three *T. thermophilus* protein extracts.

The eluted fractions were analyzed by SDS-PAGE and hydrolysed *in situ* for the mass spectrometry analysis.

In-situ hydrolysis and LC-MS/MS analysis

The SDS-PAGE gel was divided and cut in 78 bands, each of them decolorized and subjected to *in-situ* hydrolysis. 100 µL of 0,1 M ammonium bicarbonate (AMBIC) and 130 µL of acetonitrile (ACN) were used for the decolouration. For the hydrolysis the decoloured bands were incubated for 1,5 h at 4 °C first and then for additional 16 h at 37 °C in 10 mM AMBIC, 0,1 µg/µl trypsin. The hydrolysis reactions were stopped by adding acetonitrile and 0,1% formic acid. The samples when then filtered and dried in a Savant vacuum centrifuge.

The filtered samples were analyzed with mass spectrometry LC-MS/MS using a Q-TOF instrument. Prior to analysis, the samples were dissolved in 10 µL of 0.1% formic acid and 5 µL were directly loaded into the instrument.

The reversed-phase capillary liquid chromatography (HPLC 1200 system experiments), followed by MS analysis were performed using a binary pump system connected to a nano-spray source of the mass spectrometer. The latter is represented by an hybrid Q-TOF spectrometer (MS CHIP 6520 QTOF) equipped with chip (Agilent Technologies).

The external calibration was performed using the enolase from *Saccharomyces cerevisiae* for a mass range of 400 to 2000 m/z.

The samples, after being loaded, were preconcentrated and desalted in the enrichment column at a flow of 4 µl/min in 40 nl, with 0.2% HCOOH in 2% ACN as eluent. The samples were then fractionated on a capillary column packed with C18 resin (75 µm x 43 mm in the Agilent Technologies chip) at flow-rate of 400 nl/min by applying a linear gradient from 7 to 60% of B eluent (0,2% HCOOH in 95% ACN) in A (0,2% HCOOH in 2% ACN) in 50 minutes. A first investigation was carried out by acquiring masses between 400 and 2000 m/z, with a criteria of transition from MS analysis to that MS/MS based on the three most abundant ions.

Bioinformatics analysis

The putative *Tt*SmtB molecular interactors were identified using the Mascot software (http://www.matrixscience.com/search_form_select.html).

Results and conclusions

***In-vivo* functional characterization of *Tt*SmtB**

In order to identify the *Tt*SmtB molecular interactors in *Thermus thermophilus* HB27 a pull-down assay was carried out. The recombinant *Tt*SmtB produced in *E. coli* was immobilized on a Ni^{2+}-NTA resin taking advantage of its histidines tail. Subsequently Ni^{2+}-NTA/*Tt*SmtB resin was incubated with the protein extracts of *T. thermophilus* grown in the presence and in the absence of arsenate and arsenite. The eluted fractions of the IMAC chromatography were analyzed by SDS-PAGE.

Particularly the eluates obtained from the homogenates of *T. thermophilus* HB27, treated and not with arsenate and arsenite, which were incubated with the resin without *Tt*SmtB, were compared with the respective eluates obtained from homogenates incubated with the resin to which it was linked the transcriptional regulator. From the comparison it was possible to exclude the proteins present in both samples by the putative *Tt*SmtB molecular interactors since they were tied in an unspecific way to the resin.

Because the protein mixtures were complex and the monodimensional gel has a low resolution it was not possible to separate all proteins present in the samples and it was difficult to notice differences in the gel lanes, so the gel was cut into 78 bands which were hydrolysed in situ for the mass spectrometry analysis LC-MS/MS (fig. 1).
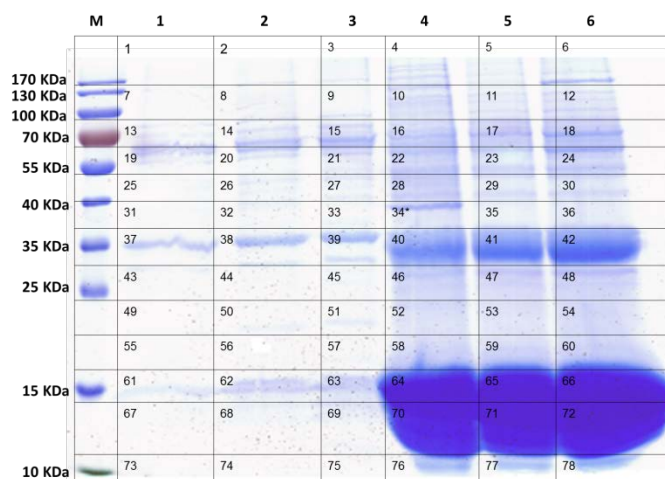
50

Fig. 1. SDS-PAGE analysis of eluates from Pull-down experiment. Lane M:Marker; lanes 1-2-3: Negative controls, eluates from resin without *Tt*SmtB attached incubated with protein extract from *T. thermophilus* not treated (lane 1), treated with arsenate (lane 2) and arsenite (lane 3); lanes 4-5-6: eluates from resin with *Tt*SmtB attached incubated with protein extract from *T. thermophilus* not treated (lane 4), treated with arsenate (lane 5) and arsenite (lane 6). The grid highlights the 78 bands cut.

Table 1. *Tt*SmtB interactors in *T. thermophilus* HB27 not treated (NT) and treated with arsenate (AsV) and arsenite (AsIII).

Band	Protein name	Accession number	*T. therm.* extract		
			NT	AsV	AsIII
5	Pyruvate dehydrogenase E1 component	Q72GP7		X	
6	Pyruvate dehydrogenase E1 component	Q72GP7			X
6	Pyrroline-5-carboxylate reductase (proC)	P54893			X
12	Hypothetical conserved protein(Resitric-modif protein Tth111, Q49LI5)	Q72GH1			X
12	Homocitrate synthase(lys20)	O87198	X	X	X
12	Hypothetical conserved protein (Thymidylate kinase,F6DGR2)	Q72JZ6			X
16	Acetolactate synthase	Q5SJ01	X		
16	2-isopropylmalate (leuA)	Q72JC9	X		
16	Transketolase	Q5SM35	X		
16	Uncharacterized protein	Q5SJM2	X		
16	Chaperone protein DnaK (Hsp70)	Q72IK5	X		X
16	Copper-exporting ATPase	Q72HW1	X		
17	Hypotetical conserved protein	Q72JZ6		X	
18	Nicotinate	Q72L13	X	X	X

51

	phosphoribosyltransferase				
18	ABC transporter ATP-binding protein	Q72HJ9			X
18	Phosphoenolpyruvate carboxykinase [ATP] (pckA)	Q72GY7			X
18	Chaperone protein DnaK (dnaK)	Q72IK5	X		X
22	2-Phosphoglycerate kinase	Q5SKZ8	X		
22	(Neo)pullulanase	Q5SI17	X	X	
22	PDH Dihydrolipoamide acetyltransferase	Q5SLV9	X	X	
22	AcetylCoA Biotin carboxylase	Q5SJ91	X		
22	60kDa chaperonin (groL)	P61490	X	X	
22	Aspartate-tRNA (Asp/Asn) ligase (aspS2)	Q5SIC2	X	X	X
22	Nicotinate phosphoribosyltransferase	Q72L13	X	X	X
23	Phosphoglycerate kinase	Q72LD8		X	
23	Acetolatate synthase	Q72JC6		X	
23	(Neo)pullulanase	Q5SI17	X	X	
23	Pyruvate dehydrogenase E2 component	Q5SLV9	X	X	
23	60kDa chaperonin (groL)	P61490	X	X	
23	Aspartate-tRNA (Asp/Asn) ligase (aspS2)	Q5SIC2	X	X	X
23	Nicotinate phosphoribosyltransferase	Q72L13	X	X	X
23	AcetylCoA Biotin carboxylase	Q5SJ91		X	
24	Dihydrolipoamide acetyltransferase	Q72GP6			X
24	Dihydrolipoyl dehydrogenase	Q72GU5			X
24	Aspartate-tRNA (Asp/Asn) ligase (aspS2)	Q72IP5	X	X	X
24	Pyridoxal 5'-phosphate synthase sub PdxS (pdxS)	Q72KG1	X		X
24	Putative dehydratase	Q72IR3	X		X
24	Hydrolase (HAD superfamily)	Q72GG4			X
28	4-OH-3-MeBut-2-en-1-yl diP synthase (ispG)	Q5SLI8	X		
28	Ribonuclease	Q5SLP1	X		
28	Heat shock protein (hslU)	Q5SKL3	X		
28	Homocitrate synthase(lys20)	O87198	X	X	X
28	Hypothetical conserved protein	Q746C0	X	X	X
28	Elongation factor Tu-B (tufB)	P60339	X	X	
29	FAD/FMN-containing dehydrogenase	Q5SMA3		X	

52

29	Homocitrate synthase (lys20)	O87198	X	X	X
29	Elongation factor Tu-B (tufB)	P60339	X	X	
29	Heat shock protein (hslU)	Q5SKL3		X	
29	Precorrin-6Y C5, 15-methyltransferase	Q746P3		X	X
29	Riboflavin biosynthesis protein RibBA (ribA)	Q72JS1		X	X
29	Hypothetical conserved protein	Q746C0	X	X	X
29	Iron-sulfur cluster-binding protein	Q72IY0		X	X
29	FAD/FMN-containing dehydrogenase	Q5SMA3		X	
30	Riboflavin biosynthesis protein RibBA (ribA)	Q72JS1		X	X
30	Precorrin-6Y C5,15-methyltransferase	Q746P3		X	X
30	Cell division protein ftsA (ftsA)	Q72JP5			X
30	Iron-sulfur cluster-binding protein	Q72IY0		X	X
30	Hypothetical conserved protein	Q746C0	X	X	X
30	tRNA (cytidine/uridine-2'-O-)-methyltransferase (trmJ)	Q72JF4	X		X
30	Two-component response regulator (hslU)	Q72JY5			X
30	Acyl carrier protein (acpP)	Q72LL3	X	X	X
34	Glycerol-3-phosphate DH [NAD (P)+] (gpsA)	P61747	X		
35	Zinc-binding dehydrogenase	Q5SL93		X	
40	Pyridoxal 5'-phosphate synthase (PdxS)	Q72KG1	X		X
40	Putative dehydratase	Q72IR3	X		X
46	Hypothetical conserved protein	Q72LF0	X	X	
46	Histidine biosynthesis bifunctional P (HisIE)	P62350	X	X	
46	30S ribosomal protein S3	P62663	X	X	
46	Uroporphyrin-III C-methyltransferase	Q746N6	X	X	
47	Hypothetical conserved protein	Q72LF0	X	X	
47	Uracil phosphoribosyltransferase	Q72J35		X	

53

47	Histidine biosynthesis biofunctional P HisIE (his1)	P62350	X	X	
47	30S ribosomal protein S3 (rpsC)	P62663	X	X	
47	Uroporphyrin-III C-methyltransferase	Q746N6	X	X	
47	tRNA(cytidine/uridine-2'-O-)-methyltransferase (trmJ)	Q72JF4	X		X
70	Hypothetical membrane spanning protein	Q72L74	X		
76	Acyl carrier protein (acpP)	Q72LL3	X	X	X
77	Acyl carrier protein (acpP)	Q72LL3	X	X	X

In table 1 *Tt*SmtB molecular interactors were reported; there were highlighted the proteins in common to the three analysed conditions, so the proteins which probably always interact with *Tt*SmtB when *T. thermophilus* was grown both in the absence and in the presence of AsV or AsIII

Interestingly, there were identified proteins which interact with the transcriptional regulator only when *Thermus* was treated with arsenic, maybe these proteins respond to particular stress conditions, as the treatments with arsenate and arsenite. Between them, particularly interesting could be the Iron-sulfur cluster-binding protein; this class of protein has a role in many redox processes, such as respiratory and photosynthetic electron transfer chains (1), so perhaps it may participate in the arsenic metabolism. Intriguingly, there were also identified proteins in common between the untreated condition and the treated with only one of the two metals.

There are ongoing proteins identification of the protein extracts in the presence of arsenite. It will be interesting to finally go to evaluate the differences in the three growth conditions to identify differentially expressed proteins and then speculate on the mechanisms in which they are involved. In this way it will be possible to develop a functional hypothesis and eventually to validate it by further methods.

Reference

1.   **Brzoska K, Meczynska S, Kruszewski M.** 2006. Iron-sulfur cluster proteins: electron transfer and beyond. Acta Biochimica Polonica 53:685-691.

2.3 *Tt*SmtB expression in *Thermus thermophilus* HB27

Thermostable enzymes have a great biotechnological potential because of their intrinsic resistant nature.

However, only a fraction of thermozymes can be overexpressed in an active form in such mesophilic hosts, so with the aim to develop a thermophilic protein expression system, *Tt*SmtB was expressed in *T. thermophilus.*

Material and methods

Bacterial strains, plasmids, and growth conditions

T. thermophilus HB27::*nar* (1) was used as hosts for expression of the *TtsmtB* gene. *E. coli*s strain DH5α [*supE44 ΔlacU169* (φ80*lacZ*ΔM15) *hsdR17 recA1 endA1 gyrA96 thi-1 relA1*] was used as host for genetic manipulation of plasmid.

Plasmid pMKE2 is a bifunctional *E. coli-Thermus* sp. vector with multiple cloning sites that allow directed cloning of genes to be expressed in *T. thermophilus* under the control of the *Pnar* promoter (1).

E. coli strains were grown in Luria-Bertani (LB) medium at 37°C. Kanamycin (30 µg/ml) was used when needed. Aerobic growth of *T. thermophilus* HB27::*nar* was carried out at 70°C with shaking (150 rpm) in TM medium . For plasmid selection, kanamycin (30 µg/ml) was added to TM plates. Transformation of *T. thermophilus* was achieved with naturally competent cells as described previously. Transformation of *E. coli* was performed as described previously.

Overexpression of *Tt*SmtB in *Thermus thermophilus*

To overexpress *Tt*SmtB in *T. thermophilus, TtsmtB* gene was cloned into pMKE2 vector. *TtsmtB* was *Nde*I/*Hind*III digested from pET28/*TtsmtB* vector and it was cloned into pMKE2 plasmid between the same sites; the resulting vector was pMKE2/*TtsmtB*.

This plasmid was used to transform *T. thermophilus* HB27::*nar* (as described before) and the transformants (*T. thermophilus-TtsmtB*) were selected on TM plates supplemented with kanamycin. Clones of *T. thermophilus* HB27::*nar* harboring the pMKE2/*TtsmtB* plasmid were grown aerobically at 70°C with shaking (150 rpm) in kanamycin-containing TM medium. At an optical density at 600 nm of 0.6 and 0.8, transcription from the *Pnar* promoter was activated by adding KNO_3 (0, 10, 20 and 40 mM) and simultaneously stopping the shaker. After incubation for 16 h at 70°C, cell extracts were prepared as described before. *TtsmtB* expression in *T. thermophilus* was verified by SDS-PAGE and Western Blot analysis.

Western Blot analysis

TtsmtB expression in *T. thermophilus* was verified by Western Blot analysis using an anti-*Tt*SmtB polyclonal antiboby.

A serum sample from a *Tt*SmtB-immunized rabbit was loaded onto a 1-ml HiTrap protein A column (GE Healthcare) connected to a fast-performance liquid

chromatography system (ÄKTA; GE Healthcare), and total IgGs were purified following the manufacturer's instructions. Antibody-containing fractions were pooled and dialyzed against 1x PBS buffer. Antibody integrity was checked by running 10 µg of total IgG sample on 15% SDS-PAGE.

For Western blot hybridizations, total protein samples (5 µg) were run on 15% SDS-PAGE and electrotransferred onto Immobilon polyvinylidene difluoride (PVDF) membranes (Millipore). Subsequently, membranes were (i) incubated for 1 h at room temperature in blocking solution, i.e., 1× TBS-T (50 mM Tris [pH 7.5], 150 mM NaCl, and 0.1% Tween 20) containing 5% (wt/vol) BSA (Sigma); (ii) incubated for 2 h at room temperature (or 16 h at 4°C) with total IgG sample (see above) diluted (1:25,000) in blocking solution; (iii) washed three times for 15 min with 1× TBS-T at room temperature; (iv) incubated for 1 h at room temperature with horseradish peroxidase-conjugated goat anti-rabbit IgG (Santa Cruz Biotechnology) diluted (1:1,000) in 1× TBS-T; (v) washed twice for 15 min with TBS-T; and (vi) washed once with TBS. Detection by enzyme-linked chemiluminescence was performed with an Immobilon Western chemiluminescent horseradish peroxidase (HRP) substrate kit (Millipore) and a ChemiDoc XRS+ system (Bio-Rad), according to the manufacturer's instructions. The *Tt*SmtB concentration in the analyzed samples was determined using a calibration curve, which was constructed by plotting known amounts of *Tt*SmtB (from 50 to 400 ng) against densitometric values measured using the Quantity One software (Bio-Rad).

Results and conclusions

Use of *T. thermophilus* for the *Tt*SmtB production

To understand if *T. thermophilus* could be used as cell factory for proteins production, we overexpressed *Tt*SmtB in the microorganism cloning its gene into pMKE2 vector under the control of the *Pnar* promoter. This vector was used in combination with the *T. thermophilus* HB27::*nar* mutant strain and the induction of the *Tt*SmtB expression was obtained by adding KNO_3 and inducing anaerobiosis. They were made several expression tests: overexpression induction at different growth time, 0.6 and 0.8 OD_{600nm}, and with different KNO_3 concentrations, 10, 20 and 40 mM.

By comparing 10 µg of the protein extracts, both of a not transformed *T. thermophilus* HB27::*nar,* of non-inducted *T. thermophilus-TtsmtB* and of induced *T. thermophilus-TtsmtB*, by SDS-PAGE analysis, allowed us to appreciate only a slight induction of the *Tt*SmtB expression (fig. 1).
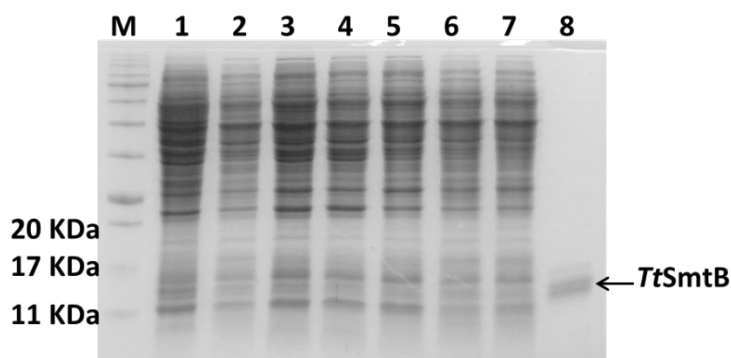
Fig. 1. SDS-PAGE analysis of the *Tt*SmtB overexpression in *T. thermophilus* HB27::*nar*. M:molecular marker; lane 1: 10 µg of *T. thermophilus* HB27::*nar* protein extract; lane 2: 10 µg of non-inducted *T. thermophilus-TtsmtB* protein extract; lane 3: 10 µg protein extract of *T. thermophilus-TtsmtB* induced at 0.6 OD_{600nm} with 40 mM KNO_3; lane 4: 10 µg protein extract of *T. thermophilus-TtsmtB* induced at 0.6 OD_{600nm} with 20 mM KNO_3; lane 5: 10 µg protein extract of *T. thermophilus-TtsmtB* induced at 0.6 OD_{600nm} with 10 mM KNO_3; lane 6: 10 µg protein extract of *T. thermophilus-TtsmtB* induced at 0.8 OD_{600nm} with 40 mM KNO_3; lane 7: 10 µg protein extract of *T. thermophilus-TtsmtB* induced at 0.8 OD_{600nm} with 20 mM KNO_3; lane 8: 3 µg of recombinant *Tt*SmtB.

To better appreciate the differences between the protein extracts form the induced *T. thermophilus-TtsmtB* cultures and to evaluate the *Tt*SmtB induction fold, western blot analysis were performed; for this purpose they were used an Anti-*Tt*SmtB polyclonal antibody and the recombinant *Tt*SmtB purified from *E. coli* BL21-*Tt*SmtB cells as positive control. Western blot analysis of 5 µg of the non-inducted and induced *T. thermophilus-TtsmtB* protein extracts, compared to 50 ng of *Tt*SmtB, showed that, except for the *T. thermophilus-TtsmtB* induction at 0.8 OD_{600nm} with 20 mM KNO_3, there was a protein expression induction (fig. 2), and that the best induction condition was at a growth time of 0.6 OD_{600nm} with 40 mM KNO_3. Interestingly, with western blot analysis it was possible to visualize also the *Tt*SmtB dimeric state.
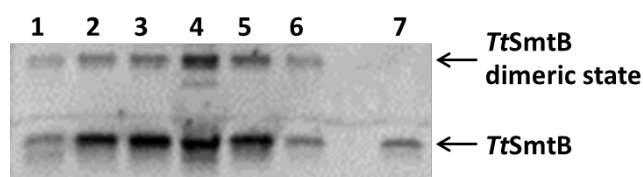

Fig. 2. Western blot analisis. Lane 1: 5 µg of non-inducted *T. thermophilus-TtsmtB* protein extract; lane 2: 5 µg protein extract of *T. thermophilus-TtsmtB* induced at 0.6 OD_{600nm} with 10 mM KNO_3; lane 3: 5 µg protein extract of *T. thermophilus-TtsmtB* induced at 0.6 OD_{600nm} with 20 mM KNO_3; lane 4: 5 µg protein extract of *T. thermophilus-TtsmtB* induced at 0.6 OD_{600nm} with 40 mM KNO_3; lane 5: 10 µg protein extract of *T. thermophilus-TtsmtB* induced at 0.8 OD_{600nm} with 40 mM KNO_3; lane 6: 10 µg protein extract of *T. thermophilus-TtsmtB* induced at 0.8 OD_{600nm} with 20 mM KNO_3; lane 7: 50 ng of recombinant *Tt*SmtB.

Having established that the best protein induction was at a growth time of 0.6 OD_{600nm} with 40 mM KNO_3, it was interesting to calculate the *Tt*SmtB induction fold; so a western blot analysis of 5 µg of the of non-inducted and chosen induced *T. thermophilus-TtsmtB* protein extracts, compared to 50, 100, 200 and 300 ng of

*Tt*SmtB was performed (fig. 3A). The *Tt*SmtB concentration in the analyzed samples was determined using a calibration curve, constructed by plotting known amounts of *Tt*SmtB (from 50 to 300 ng) against densitometric values (fig. 3B).
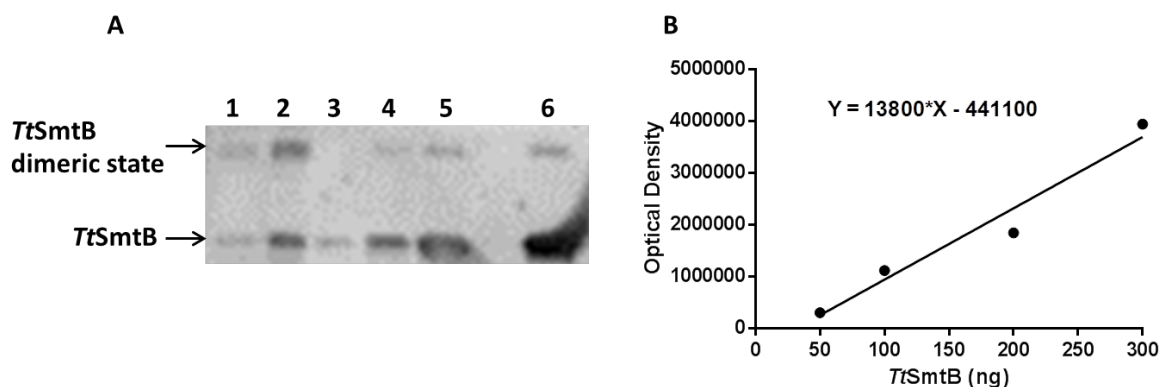

Fig. 3. A. Western blot analysis. Lane 1: 5 µg of non-inducted *T. thermophilus-TtsmtB* protein extract; lane 2: 5 µg protein extract of *T. thermophilus-TtsmtB* induced at 0.6 OD_{600nm} with 40 mM KNO_3; lanes 3-4-5-6: 50-100-200-300 ng of recombinant *Tt*SmtB. **B**. Calibration curve, constructed by plotting known amounts of *Tt*SmtB against densitometric values, the equation of the curve was shown.

By the equation (y=13800x - 441100) of the calibration curve it was calculated that the *Tt*SmtB total amount were 90.45 ng for 5 µg of non-inducted *T. thermophilus-TtsmtB* protein extract, and 141.5 ng for 5 µg of induced *T. thermophilus-TtsmtB* protein extract; moreover, that the protein induction fold was 1.6.

These experiments have confirmed our hypothesis of use of *T. thermophilus* as a system for the proteins production, but further investigations are required to improve the system and to obtain an induction fold at least comparable to those obtained with *E. coli* strains.

Reference

1.   **Moreno R, Zafra O, Cava F, Berenguer J.** 2003. Development of a gene expression vector for Thermus thermophilus based on the promoter of the respiratory nitrate reductase. Plasmid 49:2-8.

Chapter 3

DEVELOPMENT OF BIOSENSORS FOR THE DETECTION OF ENVIRONMENTAL ARSENIC

3.1. A novel *Thermus thermophilus* whole-cell biosensor for the detection of arsenic pollution.

3.2. Development of an Arsenate Nanobiosensor based on the *Tt*ArsC arsenate reductase activity to detect arsenic pollution.

SUMMARY

This chapter focuses on the development of cellular and enzymatic arsenic biosensors using the thermophilic microorganism *Thermus thermophilus* for the detection of arsenic species in soils and waters.
They have been realized two arsenic biosensors:

1) A whole-cell *T. thermophilus* biosensor.
   This objective has been achieved through the identification and *in-vivo* analysis of responsive regulatory sequences, cloning them upstream of a reporter gene coding for a thermostable β-galactosidase. The thermophilic nature of this biosensor represents a notable advantage since it could be more versatile, stable and strong in case of highly contaminated waters.

2) A *Tt*ArsC based biosensor.
   To this purpose *Tt*ArsC enzyme has been adsorbed on gold nanoparticles (AuNPs) and nanobiocomplexes demonstrating stability and capacity to strongly bind the toxic arsenic ions. *Tt*ArsC-AuNPs interaction with arsenic can be followed by naked eye since solutions completely change their colors.

3.1 A novel *Thermus thermophilus* whole-cell biosensor for the detection of arsenic pollution.

Immacolata Antonucci[1], Josè Berenguer[2], Simonetta Bartolucci[1], Gabriella Fiorentino[1*]

1 Dipartimento di Biologia, Università degli Studi di Napoli Federico II,Complesso Universitario Monte S. Angelo, Naples, Italy

2 Centro de Biología Molecular Severo Ochoa (CSIC-UAM). Campus Universidad Autónoma de Madrid, 28049, Madrid, Spain

[*]Corresponding author: fiogabri@unina.it

In preparation

ABSTRACT

Thermophilic microorganisms could be good candidates for the construction of more stable and stronger arsenic biosensors, the advantages are related to their higher resistance to the temperature and caotropic agents or detergents often present in industrial off-loads and wastewaters. Analysing the *TTC0351*, *TTC0353* and *TTC0354* promoter activities *in-vivo*, using a β-galactosidase reporter systems, it has been developed the first whole-cell arsenic biosensor based on the use of the thermophilic microorganism *T. thermophilus*. The biosensor response could be measured with reliability within 30 minutes of arsenate or arsenite addition, and have a minimum detection limit of 0.1 mM for both arsenate and arsenite.

3.1. Introduction

Arsenic is a ubiquitous toxic metalloid which contaminates both groundwater (1, 2) and soils (3) worldwide. Surprisingly, more than 100 million people in the world are at risk from consuming arsenic contaminated water (4), and strategies to detect even the smallest trace are an urgent need.

The arsenic toxicity depends on its chemical structure; the arsenate is a structural phosphate analogue, competing, inside the cell, with this essential ion for many enzymatic reactions (5). The arsenite can be transported by the aquaglyceroporins (6); moreover, it has a high affinity for thiol groups, so it can inhibit many enzymes (7). Arsenic toxicity can result in damaged or reduced mental and central nervous function, lower energy levels, and damage to blood composition, lungs, kidneys, liver, and other vital organs; moreover chronic arsenic exposure may even cause cancer (8). In this regard the WHO established an arsenic maximum limit in drinking water of 10 mg/L.

Traditionally, heavy metals discharged into the environment have been analyzed using chemical assays, which often require sample pretreatment and expensive equipment; moreover these assays require the use of dangerous chemicals and can generate even more toxic products (8).

In recent years biosensors are emerging as an alternative methods, safer then chemical detection, to detect environmental pollutants such as arsenic (9). Whole-cell bacterial biosensors employ living microorganisms with a genetic engineered sensing element to analyze pollution risk; they can detect the bioavailable concentration of metal ions along with their functionality, toxicity and genotoxicity (10). To date, reported bacterial biosensors are mostly based on the use of mesophilic microorganisms, but thermophilic microorganisms could be good candidates for the construction of more stable biosensors. The advantage of using thermophilic microorganisms is related to the higher resistance to the temperature and caotropic agents or detergents of their molecular components; such chemicals are often present in industrial off-loads and wastewaters.

The thermophilic gram negative bacterium *Thermus thermophilus* HB27 is able to grow in the presence of both arsenate and arsenite in a range of concentrations which are lethal for other microorganisms (11). The putative resistance genes have not been found in a single resistance operon but associated to chromosomal genes apparently not functionally related. In particular, we discovered a gene coding for a thioredoxin-coupled arsenate reductase (*Tt*ArsC) which catalyzes the reduction of pentavalent arsenate to trivalent arsenite (11); two genes (*TTC1447*, *TTC0354*) coding putative ArsB-like transporters, which could be involved in the extrusion of arsenite from the cell; and a gene coding for a transcriptional repressor (*Tt*SmtB), sensitive to arsenic, belonging to the ArsR/SmtB family of transcriptional regulators. *TtsmtB* is the third of an operon of five genes (*TTC0351-TTC0352-TTC0353-TTC0354-TTC0355*) encoding putative proteins with no obvious functional relation, except for *TTC0354*; interestingly*,* basal promoter consensus elements have been identified by homology search not only upstream of *TTC0351* but also as internal promoters upstream of *TTC0353* and *TTC0354.* Moreover, the generation of a *T. thermophilus* mutant lacking the *TtsmtB* gene (*T. thermophilus ΔsmtB::kat)*, has confirmed the repressor role of the transcriptional regulator (see chapter 2).

Due to its intrinsic arsenic resistance and the identification of the molecular components involved in arsenic response, here we investigate on the possibility to

use *T. thermophilus* for the realization of a whole-cell arsenic biosensor. To this purpose, in the present study, regulative sequences responsive to arsenic were searched by cloning them upstream of a reporter gene coding for a thermostable β-galactosidase in a shuttle vector able to transform a mutant strain of *T. thermophilus* lacking the β-galactosidase gene and analyzing the arsenic dependent gene expression.

3.2. Materials and methods

Table 1. Strains and genotypes

Strain	Genotype	Source
T. thermophilus Δ42	*T. thermophilus* deletion mutant of the *TTP0042* gene (β-gal⁻)	Donated by J. Berenguer
T. thermophilus Δ42 *0351*prom	*T. thermophilus* Δ42 transformed with pMH0351prombgaA, Hyg^r	This study
T. thermophilus Δ42 *0353*prom	*T. thermophilus* Δ42 transformed with pMH0353prombgaA, Hyg^r	This study
T. thermophilus Δ42 *0354*prom	*T. thermophilus* Δ42 transformed with pMH0354prombgaA, Hyg^r	This study
T. thermophilus Δ42 *0354*prshort	*T. thermophilus* Δ42 transformed with pMH0354prshortbgaA, Hyg^r	This study
T. thermophilus Δ*smtB::kat*	*T. thermophilus* HB27 deletion mutant of the *TtsmtB* gene, Kan^r	See chapter 2.1
T. thermophilus Δ*smtB::kat 0351*prom	*T. thermophilus* Δ*smtB::kat* transformed with pMH0351prombgaA, Kan^r and Hyg^r	This study
T. thermophilus Δ*smtB::kat 0353*prom	*T. thermophilus* Δ*smtB::kat* transformed with pMH0353prombgaA, Kan^r and Hyg^r	This study
T. thermophilus Δ*smtB::kat 0354*prom	*T. thermophilus* Δ*smtB::kat* transformed with pMH0354prombgaA, Kan^r and Hyg^r	This study
E. coli DH5α	F⁻ endA1 glnV44 thi-1 recA1 relA1 gyrA96 deoR nupG purB20 φ80dlacZΔM15 Δ(lacZYA-argF)U169, hsdR17($r_K^-m_K^+$), λ⁻	Invitrogen

Table 2. Oligonucleotides

Primer name	Primer sequence
F0351EcoRI	TCT<u>GAATTC</u>CTGCCAACACCAACTACGCTCTC
R0351NdeI	CTCGGAC<u>CATATG</u>CAAGCTTCAC
F0353EcoRI	TCA<u>GAATTC</u>AGCTCGTCAAGTGGGTGCAC
R0353NdeI	GCTTGG<u>CATATG</u>TTTCCTCCTC
F0354EcoRI	AAA<u>GAATTC</u>CACGAGGATGCGCCTGCTC
R0354NdeI	AGCCTT<u>CATATG</u>CCCAGGGTAGC
New 0354 pr fw	CTGTTGGCGGAGGCCCTG

3.2.1. Growth conditions

T. thermophilus Δ42 strain was grown aerobically at 70°C in TM medium as described (11).

T. thermophilus *ΔsmtB::kat* strain was grown aerobically at 70 °C in TM medium containing kanamycin (30 μg/ml). A frozen (-80 °C) stock was streaked on a TM plate (solidified by the addition of 1,6 % Agar) containing kanamycin (30 μg/ml) and incubated for 48 h at 70 °C. Single colonies that appeared on the plate were inoculated into TM liquid medium supplied with the antibiotic and shaken at 70 °C overnight.

T. thermophilus Δ42 and *ΔsmtB::kat* transformed with the reporter vectors were grown in 50 mL of TM medium containing 100 μg/ml hygromycin and/or 30 μg/ml kanamycin; when the cell density reached 0.5 OD_{600nm} aliquots (equal to 1 OD of total cells) were harvested at time 0 and 30/60/90/120 minutes after the addition of $NaAsO_2$ and KH_2AsO_4 at final concentrations of 0,1-0,5-1-5-8 mM and 0,1-0,5-1-5-12 mM, respectively. At these times, aliquots of each culture were removed and immediately spun down, and pellets were kept at -20°C.

E. coli strains were grown in Luria Bertani (12) medium at 37 °C with 100 μg/ml hygromycin as required.

Strain genotypes and sources are summarized in Table 1.

3.2.2. Construction of the reporter systems

Reporter vectors - To test whether regions upstream of *TTC0351* (336717-337080), *TTC0353* (338950-339243) and *TTC0354* (339372-339646) genes from *T. thermophilus* HB27 had promoter activities, regions were amplified by PCR using the primer pairs *F0351EcoRI* and *R0351NdeI*, *F0353EcoRI* and *R0353NdeI*, *F0354EcoRI* and *R0354NdeI*. All the primers introduced *Eco*RI and *Nde*I restriction sites so that the amplified fragments could be cloned in the pMHpnqobgaA plasmid (13) between the same sites. The resulting vectors were pMH0351prombgaA, pMH0353prombgaA and pMH0354prombgaA. The insertion and correct sequences of the PCR products were verified by DNA sequencing.

Since in a previous paper we identified regulatory sequences upstream of *TTC0354* gene matching with the consensus sequence of ArsR/SmtB binding sites, a shorter region upstream of this gene containing such sequences was amplified by PCR using

65

New 0354 pr fw and *R0354NdeI* primers and subcloned into pCR™4-TOPO® TA Vector; then it was *Eco*RI/*Nde*I digested and cloned into the same sites of the pMHpnqobgaA vector, giving the pMH0354prshortbgaA plasmid, which was used to transform *E. coli* DH5α.

All the primer sequences are shown in Table 2.

T. thermophilus transformations - pMH0351prombgaA, pMH0353prombgaA and pMH0354prombgaA vectors were uses to transform *T. thermophilus* Δ42 and *ΔsmtB::kat*; pMH0354prshortbgaA vector was transformed into *T. thermophilus* Δ42. In particular, 200 ng of DNA was added to 0,5 mL of cells in their exponential growth phase (0.3 - 0.5 OD_{600nm}). As negative control the vector pMHPnorbgaA (14), was used to transform both strains.

After four hours of incubations, the cells were plated on TM plates containing hygromycin (100 µg/mL) and/or Kanamcyn (30 µg/mL) and incubated for 24-48 h at 60°C. The selected transformants were grown as described before.

3.2.3. *In-vivo* evaluation of the β-Galactosidase activity

The promoter activities were measured with a β-Galactosidase activity assay as described by Miller in 96-well microplates (12). Briefly, the cells were suspended in 50 mM sodium phosphate pH 7.5 at the final concentration of 1 OD_{600}/mL. To 25 µl of the suspensions were added 25 µl 50 mM sodium phosphate pH 7.5 and 50 µl of SDS 0.2 % (w/v) and the mixtures were incubated for 30 minutes at 37°C; then 150 µl of the reaction buffer 80 mM sodium phosphate pH 7.5, ONPG (orto-nitrofenil-β,D galactopiranoside) 0.2 % (w/v)) were added. The micro plate was incubated for further 20 minutes at 70°C before measuring the absorbance at 550 nm and 420 nm with a Synergy H4 microplate reader (BioTeK).

The β-Galactosidase activity was calculated as Miller units (U) by the equation:

$$U = \frac{OD_{420} - (1{,}75 \times OD_{550})}{t(\text{min}) \times V(\text{mL}) \times OD_{600}}$$

Whereas: OD_{420}=OD of the chromogenic product, OD_{550}=OD of the cellular debris, t=time of reaction, V=volume of used cells and OD_{600}=OD of the cell culture (12).

The activity reported the average of two independent experiments each made in triplicate. The error bars indicate the standard deviation of the average values.

3.3.   Results

3.3.1. Characterization of the reporter systems

Previous bioinformatic analysis of the regions upstream of *TTC0351*, *TTC0353* and *TTC0354* had revealed the presence of basal promoter consensus elements, suggesting that these genes could also be singularly transcribed and distinctly regulated. To evaluate if these sequences were active *in-vivo*, they were cloned into pMHpnqobgaA vector in order to be fused in frame with the *bga*A reporter gene. The regions were amplified by PCR giving fragments of 364-bp for *0351* prom, 294-bp for *0353* prom and 275-bp for *0354* prom. The obtained plasmids pMH0351prombgaA, pMH0353prombgaA and pMH0354prombgaA were used to transform *T. thermophilus*

Δ42 cells. This strain lacks the *TTP0042* gene, coding for the endogenous β-galactosidase, to avoid interference in the enzymatic assays.

The analyzed reporter systems had a mean β-galactosidase activity of 122, 1054 and 626 Miller Units, respectively for *0351*prom, *0353*prom and *0354*prom. No activity was measured in control cells. To understand if there were differences in the expression levels at different growth stages the cells were grown and harvested at different OD_{600nm} (0.3, 0.5, 0.7 and 1) and β-galactosidase activity was assayed. Data analysis showed that the growth phase did not affect the activity of all three tested promoters (fig. 1A).

Furthermore, it was evaluated if these promoters were sensitive to arsenic treatment; β-galactosidase activity was then assayed at 0 and 60 minutes after the addition of arsenate and arsenite to the growing cells. The results showed that whereas arsenic treatment did not significantly affect *0351*prom activity, an increase in *0353*prom and *0354*prom activities was detected. Particularly, there was an increase in β-galactosidase activity upon treatment with arsenate and arsenite, of about 1.5 fold for both promoters (fig. 1B).

These data suggest the possibility to use *T. thermophilus* Δ42 *0353*prom and *T. thermophilus* Δ42 *0354*prom reporter systems for the realization of a bacterial biosensor able to detect inorganic arsenic.
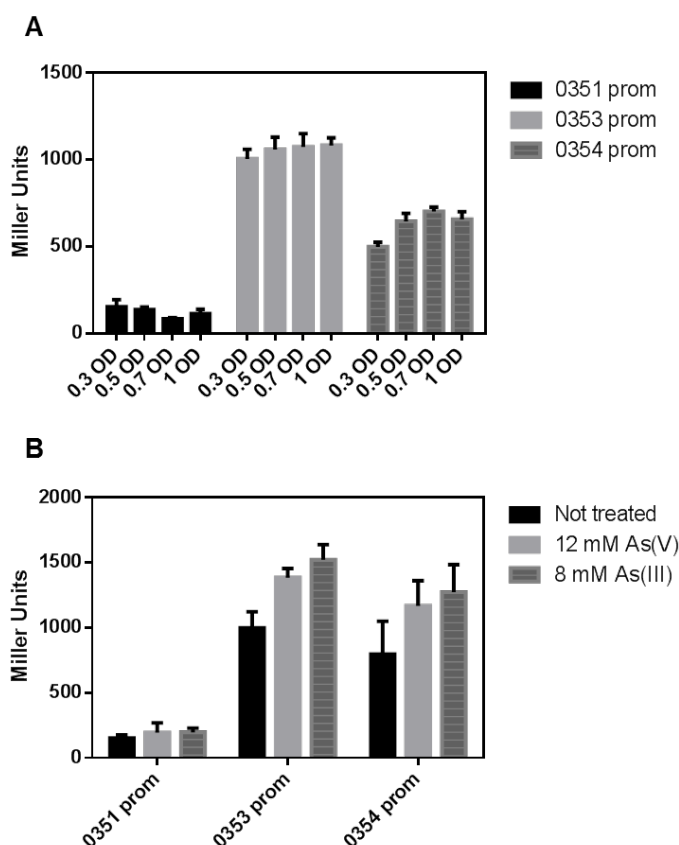
Fig. 1. (A) β-galactosidase activity expressed in Miller(0.3-0.5-0.7-1 OD_{600nm}) units of *T.thermophilus* Δ42 *0351*prom, *0353*prom, *0354*prom strains at different growth phases . **(B)** β-galactosidase activity expressed in Miller units of *T.thermophilus* Δ42 *0351*prom, *0353*prom, *0354*prom strains treated and not with 12 mM arsenate and 8 mM arsenite .

3.3.2. Analysis of the promoter activity in a *TtsmtB⁻* environment

In a previous paper (see chapter 2.1) we generated a mutant strain lacking *TtsmtB (T. thermophilus ΔsmtB::kat)* the putative transcriptional regulator involved in the regulation of arsenic resistance. In this strain arsenic related gene expression levels were significantly higher than in the wild type strain giving experimental evidence that *in vivo Tt*SmtB is bound to its target promoters hampering gene transcription.

The reporter plasmids (pMH0353prombgaA and pMH0354prombgaA) were transformed into *the ΔsmtB::kat* strain to analyze promoter activity in the absence of *TtsmtB*.

The results show that in the absence of *Tt*SmtB both reporter systems are insensitive to arsenic, confirming that *Tt*SmtB is the metal sensor with a repressor role; *0354*prom had higher activity than *0353*prom (fig. 2).
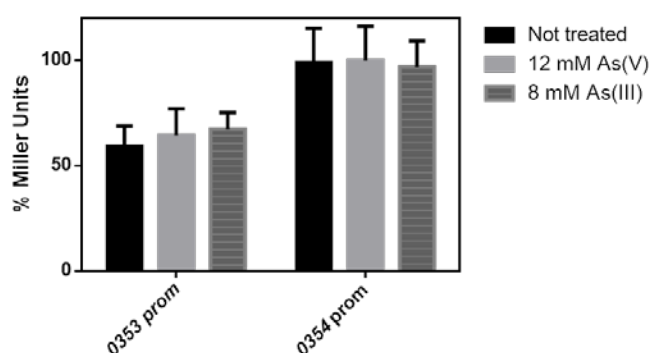
Fig. 2. β-galactosidase activity expressed in % Miller Units of *T. thermophilus ΔsmtB::kat 0353*prom and *0354*prom treated and not with 12 mM arsenate and 8 mM arsenite. % Miller Units were calculated assuming that the highest value of Miller units obtained in the assays were 100%.

These findings indicate that *in vivo Tt*SmtB repressor could be more tightly bound to *0354*prom and so that the *T. thermophilus* Δ42 *0354*prom reporter system could be more sensitive to arsenic; hence it seems a good candidate for the development of an arsenic biosensor; for this reason, other experiments were carried out on this strain.

3.3.3. Detection of β-galactosidase activity after arsenic exporure

In order to establish the best time intervals to evaluate the response to arsenic of the biosensor, β-galactosidase activity was determined after different times of arsenic exposure. A single colony was grown up to 0.5 OD_{600nm}, then arsenate and arsenite were added to induce the reporter gene expression; the β-galactosidase activity was measured at time 0 (not treated) and at 30-min intervals (for 2 hours) after the treatment. The cell growth was monitored to verify that the cell viability was not affected from arsenic treatment (fig. 3A).

As shown in fig. 3 β-galactosidase activity did not vary significantly over time, in fact the Miller Units after 30-min of treatment remained almost similar in the following 2 h (fig. 3B).
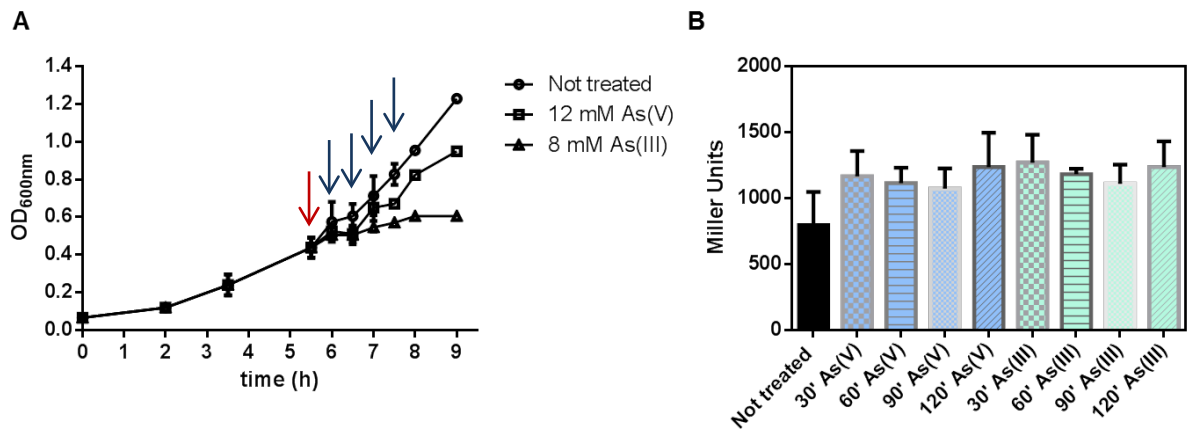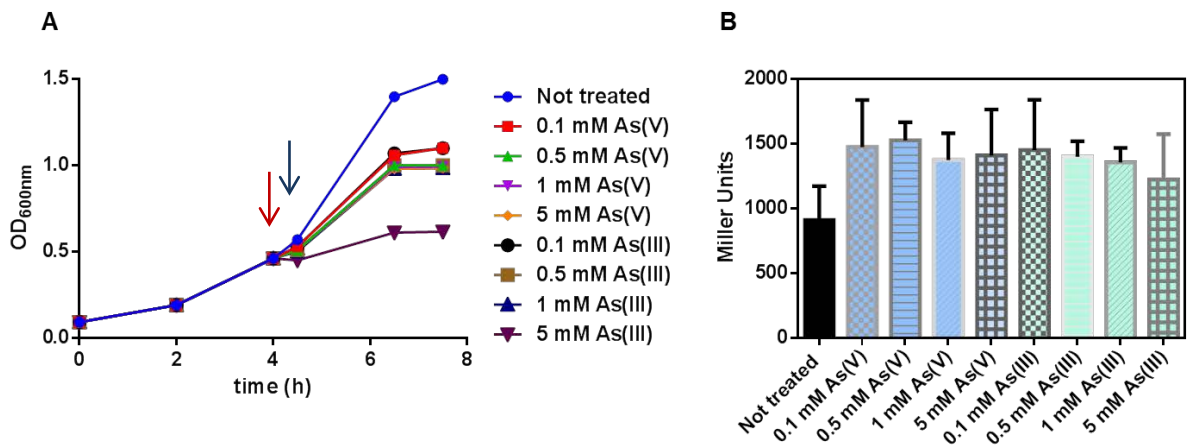
Fig.3. (A) Effect of arsenic on biosensor growth. Red arrow indicates time of arsenic addition and of the point 0 of measurement, blue arrows indicate the 30, 60, 90 and 120 minutes arsenic induction. **(B)** β-galactosidase activity with 12 mM arsenate or 8 mM arsenite for 30, 60, 90 and 120 minutes.

To establish the detection limit of the biosensor strain, a single colony was grown up to 0.5 OD_{600nm}, then arsenate and arsenite were added in a range from 0.1 mM to 5 mM. β-galactosidase activity was measured at time 0 (not treated) and at 30-min after the treatment. At this time (that from the previous experiment was established to be a proper time to detect β-galactosidase activity induction) cells retained their growth capability (fig. 4A). The results evidenced that also if there is not a dose-dependent induction, at 0.1 mM of both arsenate and arsenite the biosensor responds by increasing β-galactosidase activity (fig. 4B).

Fig.4. (A) Effect of arsenic on biosensor growth. Red arrow indicates time of arsenic addition and of the point 0 of measurement, blue arrow indicates the 30 minutes point of β-galactosidase activity mesasurement. **(B)** β-galactosidase activity expressed in Miller Units of *T.thermophilus* Δ42 *0354*prom reporter system treated and not with 0.1, 0.5, 1 and 5 mM of arsenate and arsenite for 30 minutes.

In order to verify if a linear arsenic response of the biosensor strain could be reached, it was decided to tighten the *0354*prom region from a 275-bp to a 84-bp region

centered on its basal promoter consensus elements, and to construct with it a new *T.thermophilus* Δ42 reporter system; so further experiments had to be performed to characterize the new reporter system.

3.4.   Conclusions and discussion

This study describes the construction and preliminary characterization of a β-galactosidase based biosensor for the measurement of inorganic arsenic. The biosensor was based on a *T. thermophilus* Δ42 strain containing a hybrid transcriptional fusion between a *T. thermophilus* promoter responsive to arsenic and the *bgaA* gene, coding for a thermostable β-galactosidase (13, 14).

As first step, three reporter constructs: pMH0351prombgaA, pMH0353prombgaA and pMH0354prombgaA, conferring resistance to hygromycin, were produced containing the *bga*A coding sequence under the control of different *T. thermophilus* promoters, which in a previous study were shown to be targets of the transcriptional regulator *Tt*SmtB, an ArsR/SmtB family member involved in the regulation of arsenic resistance genes.

Analysis of β-galactosidase activity demonstrated that the activity of all three tested promoters was not strictly dependent on the bacterial growth phase; moreover, two of the three tested promoter were responsive to arsenic. Interestingly, the one with the lower activity and not inducible by the presence of arsenic, was *0351*prom, the promoter upstream of the entire operon in which *TtsmtB* is located. *0353*prom and *0354*prom were able to drive increased expression of the reporter gene after arsenate and arsenite treatments.

These findings could be exploited considering that *Tt*SmtB preferably bound *0354*prom and that a DNA-protein complex between the transcriptional regulator and its own promoter (*0353*prom) was hardly detectable (see chapter 2.1, fig. 5A); so 0354prom could be mostly repressed by *Tt*SmtB. This hypothesis was proven analyzing the β-galactosidase activity into *T. thermophilus ΔsmtB::kat* transformants. In fact in this environment, that is in the absence of the arsenic sensor and in conditions of derepression, *0354*prom activity resulted to be higher than *0353*prom activity. These results led us to choose *T. thermophilus* Δ42 *0354*prom reporter strain as a candidate for an arsenic biosensor.

Analysis of β-galactosidase activity at different growth times after arsenic treatment, aimed at setting up the best time intervals to measure the response of the biosensor indicated that the response could be measured with reliability within 30 minutes after arsenate or arsenite addition. Our data allowed also to estimate a biosensor minimum detection limit of 0.1 mM for both arsenate and arsenite.

In conclusion, we constructed the first whole-cell arsenic biosensor based on the use of a thermophilic microorganism. This intriguing feature could represent a considerable advantage related to its higher resistance to temperature, and to caotropic agents or detergents often present in industrial off-loads and wastewaters.

Furthermore, our results show that the biosensors could represent a useful tool for the rapid measurement of arsenic in contaminated sites. However, further improvements are required to verify measurements in the lower range of concentrations, as well as in the presence of other chemicals besides inducer compounds.

References

1. **Mukherjee A, Das D, Mondal SK, Biswas R, Das TK, Boujedaini N, Khuda-Bukhsh AR.** 2010. Tolerance of arsenate-induced stress in Aspergillus niger, a possible candidate for bioremediation. Ecotoxicology and Environmental Safety **73:**172-182.
2. **Pokhrel D, Viraraghavan T.** 2006. Arsenic removal from an aqueous solution by a modified fungal biomass. Water Research **40:**549-552.
3. **Canovas D, de Lorenzo V.** 2007. Osmotic stress limits arsenic hypertolerance in Aspergillus sp P37. Fems Microbiology Ecology **61:**258-263.
4. **de Mora K, Joshi N, Balint BL, Ward FB, Elfick A, French CE.** 2011. A pH-based biosensor for detection of arsenic in drinking water. Analytical and Bioanalytical Chemistry **400:**1031-1039.
5. **Westheimer FH.** 1987. WHY NATURE CHOSE PHOSPHATES. Science **235:**1173-1178.
6. **Meng YL, Liu ZJ, Rosen BP.** 2004. As(III) and Sb(III) uptake by G1pF and efflux by ArsB in Escherichia coli. Journal of Biological Chemistry **279:**18334-18341.
7. **Geng CN, Zhu YG, Hu Y, Williams P, Meharg AA.** 2006. Arsenate causes differential acute toxicity to two P-deprived genotypes of rice seedlings (Oryza sativa L.). Plant and Soil **279:**297-306.
8. **Choe S-I, Gravelat FN, Al Abdallah Q, Lee MJ, Gibbs BF, Sheppard DC.** 2012. Role of Aspergillus niger acrA in Arsenic Resistance and Its Use as the Basis for an Arsenic Biosensor. Applied and Environmental Microbiology **78:**3855-3863.
9. **Diesel E, Schreiber M, van der Meer JR.** 2009. Development of bacteria-based bioassays for arsenic detection in natural waters. Analytical and Bioanalytical Chemistry **394:**687-693.
10. **Mehta J, Bhardwaj SK, Bhardwaj N, Paul AK, Kumar P, Kim K-H, Deep A.** 2016. Progress in the biosensing techniques for trace-level heavy metals. Biotechnology Advances **34:**47-60.
11. **Del Giudice I, Limauro D, Pedone E, Bartolucci S, Fiorentino G.** 2013. A novel arsenate reductase from the bacterium Thermus thermophilus HB27: Its role in arsenic detoxification. Biochimica Et Biophysica Acta-Proteins and Proteomics **1834:**2071-2079.
12. **Miller JH.** 1972. Experiments in Molecular Genetics. Cold Spring Harbor, N. Y.
13. **Cava F, Zafra O, da Costa MS, Berenguer J.** 2008. The role of the nitrate respiration element of Thermus thermophilus in the control and activity of the denitrification apparatus. Environmental Microbiology **10:**522-533.
14. **Alvarez L, Bricio C, Jose Gomez M, Berenguer J.** 2011. Lateral Transfer of the Denitrification Pathway Genes among Thermus thermophilus Strains. Applied and Environmental Microbiology **77:**1352-1358.

3.2 Development of an Arsenate Nanobiosensor based on the *Tt*ArsC arsenate reductase activity to detect arsenic pollution

The thermophilic bacterium *Thermus thermophilus* HB27 encodes chromosomal arsenate reductase (TtArsC), the enzyme responsible for resistance to the harmful effects of arsenic. We report on adsorption of TtArsC onto gold nanoparticles for naked-eye monitoring of biomolecular interaction between the enzyme and arsenic species.

Interaction of *Thermus thermophilus* ArsC enzyme and gold nanoparticles naked-eye assays speciation between As(III) and As(V)

Jane Politi[1,2], Jolanda Spadavecchia[3,4], Gabriella Fiorentino[5], Immacolata Antonucci[5], Sandra Casale[3] and Luca De Stefano[1]

[1] Institute for Microelectronics and Microsystems, Unit of Naples-National Research Council Via P. Castellino 111, 80127, Italy

[2] Department of Chemical Sciences, University of Naples 'Federico II', Via Cynthia, 80126 Naples Italy

[3] Sorbonne Universités, UPMC Univ Paris VI, Laboratoire de Réactivité de Surface, 4 place Jussieu, F-75005 Paris, France

[4] CNRS, UMR 7244, CSPBAT, Laboratoire de Chimie, Structures et Propriétés de Biomatériaux et d'Agents Thérapeutiques Université Paris 13, Sorbonne Paris Cité, Bobigny, France CNRS, Paris, France

[5] Department of Biology, University of Naples 'Federico II', Via Cynthia, 80126 Naples, Italy

E-mail: jane.politi@na.imm.cnr.it and luca.destefano@na.imm.cnr.it

Abstract

The thermophilic bacterium *Thermus thermophilus HB27* encodes chromosomal arsenate reductase (*TtArsC*), the enzyme responsible for resistance to the harmful effects of arsenic. We report on adsorption of *TtArsC* onto gold nanoparticles for naked-eye monitoring of biomolecular interaction between the enzyme and arsenic species. Synthesis of hybrid biological–metallic nanoparticles has been characterized by transmission electron microscopy (TEM), ultraviolet-visible (UV–vis), dynamic light scattering (DLS) and phase modulated infrared reflection absorption (PM-IRRAS) spectroscopies. Molecular interactions have been monitored by UV–vis and Fourier transform-surface plasmon resonance (FT-SPR). Due to the nanoparticles' aggregation on exposure to metal salts, pentavalent and trivalent arsenic solutions can be clearly distinguished by naked-eye assay, even at 85 μM concentration. Moreover, the assay shows partial selectivity against other heavy metals.

S Online supplementary data available from stacks.iop.org/NANO/26/435703/mmedia

Keywords: arsenate reductase, gold nanoparticles, biorecognition, naked eye assay

(Some figures may appear in colour only in the online journal)

1. Introduction

*Thermus thermophilus HB*27 is an extremophile organism living in arsenic-rich geothermal environments: this bacterium has developed the ability to both oxidize and reduce arsenic, thus playing an important role in its speciation and bioavailability [1, 2]. Arsenate reduction mechanisms, apparently due to convergent evolution or originating in a common ancestor and then transferred to [3, 4], can be individuated into three families: the first family has been typified as *arsC* glutathione–glutaredoxin dependent (*arsC-GSH/Grx*) and was identified in enteric bacteria (e.g. *Escherichia coli*); the second one is known as *arsC* tioredoxin dependent (*arsC-Trx*) and was found in Gram-positive bacteria (e.g. *Staphylococcus*). The last family, which includes the *ars2* gene, was amplified from *Saccharomyces cerevisiae* [5]. Microbial activities play critical roles in the geochemical cycling of arsenic because they can promote or inhibit its release from sediment material, mainly by redox reactions [6–8]. The reduction of pentavalent arsenate, As (V), to trivalent arsenite, As (III), is the major reaction causing the release of arsenic from the mineral surfaces into groundwater; in fact,

besides being more toxic, arsenite is the most mobile and common form of arsenic found in anaerobic contaminated aquifers [9]. There is a worldwide demand to sense and quantify arsenic pollution, both natural and anthropogenic, in fresh water using low-cost and easy-to-use devices, especially in developing countries.

Nanostructured materials claim a range of exciting physical and chemical properties, which make them fundamental building blocks for the next generation of instruments and devices. In particular, gold nanoparticles (AuNPs) are among the most-used nano-objects, and are exploited in many applications ranging from medical to environment monitoring. The most popular method for preparing AuNPs in water uses citrate to reduce HAuCl$_4$ under boiling conditions [10]. Therefore, several approaches have been developed to reduce Au (III) salts in water using different ligands as colloid particle stabilizers [11]. Stabilizers, usually surfactant molecules, protect particles by avoiding aggregation mechanisms and controlling their physio-chemical properties [12, 13], but these molecules are mostly toxic. Dangerous organic molecules could be substituted by some biocompatible molecules, such as polyethylene glycol (PEG), in order to prepare biocompatible PEG-stabilized AuNPs [14, 15]. Recently, great advances have been made in the use of gold nanoparticles for signaling applications, owing to their stability, chemical reactivity, non-toxic nature, strong absorption and scattering properties, and electrostatic charges that allow strong interactions with proteins and enzymes [16, 17]. For instance, biomolecule- and/or biopolymer-conjugated AuNPs are largely used as biomarkers or biodelivery vehicles, as well as for cosmetics and as anti-aging components for skin protection [18, 19].

In the following study, we report our results on the adsorption of *TtArsC* enzyme onto PEG-stabilized AuNPs (PEG-AuNPs) for monitoring its interaction with pentavalent arsenic ions (As (V)) and trivalent arsenic ions (As (III)). Both the adsorption of enzyme onto PEG-AuNPs and its interaction with As (V) and As (III) salts can be followed easily by the naked eye, since solutions completely change their colors. UV–vis spectroscopy, polarization modulation infrared reflection/adsorption (PM-IRRAS) spectroscopy, dynamic light scattering (DLS) and Fourier transform-surface plasmon resonance (FT-SPR) were used as the main characterization techniques.

2. Experimental

2.1. Chemicals

Tetrachloroauric acid (HAuCl$_4$), sodium borohydride (NaBH4), polyethylene glycol 600 diacid (PEG diacid), β-Mercaptoethylamine (cysteamine), 1, 4-phenylenediisothiocyanate (PDC), ethanol (C$_2$H$_5$OH), pyridine, dimethylformamide (DMF), 15 mM Tris-HCl, potassium metarsenite (NaAsO$_2$), potassium arsenate (KH$_2$AsO$_4$), cadmium ions solution, lead (II) methanesulfonate (C$_2$H$_6$O$_6$PbS$_2$) and mercury (II) nitrate

solution (HgN$_2$O$_6$) were purchased from Sigma Aldrich. All chemicals were used without any further purification.

2.2. Purification and preparation of TtArsC enzyme

Recombinant *TtArsC* (*TtArsC*: protein arsenate reductase from the Gram-negative bacterium *Thermus thermophilus* HB27) was purified to homogeneity using the purification procedure already described, basically consisting of a thermo-precipitation of the *Escherichia coli* cell extract followed by anion exchange and gel filtration chromatography [20]. Fractions containing purified *TtArsC* were pooled, dialyzed against 15 mM Tris-HCl, 1 mM DTT, pH 7.5 and lyophilized in aliquots of 1 mg using a freeze dryer (HetoPowerDry PL6000, Thermo Scientific). Protein aliquots for nanoparticle interaction were prepared by resuspension of the protein in 1 ml of 15 mM Tris-HCl, pH 7.5.

2.3. Synthesis of PEG-stabilized Au nanospheres (PEG-AuNPs)

Li *et al* [10] have previously reported an easy method of synthesizing AuNPs from concentrated chloroauric acid solutions by adding sodium hydroxide as a reducer agent, citrate molecules as a stabilizer of colloidal solution. We modified this protocol using PEG-diacid as stabilizer molecules by the one-step method, using it inside the mixture reaction for AuNPs solution in spite of citrate molecules [21]. Briefly, 25 ml of chloroauric acid (HAuCl$_4$) aqueous solution (2.5×10^{-4} M) was added to 0.25 ml of PEG-diacid under stirring for 10 min at room temperature. After that, 20 ml of aqueous 0.01 M NaBH$_4$ was added at once. The formation of the PEG-AuNPs solution was observed by an instantaneous color change of the pale yellow solution to typical red/rose solution after addition of the NaBH$_4$ reducing agent. The PEG-AuNPs solution, prepared as described above, was centrifuged at 15 000 rpm for 26 min three times; then the supernatant was discarded while the residue was resuspended in an equivalent amount of buffer solution (PBS pH: 7). These procedures were repeated twice in order to remove the excess PEG-diacid.

2.4. Adsorption of TtArsC onto PEG-AuNPs

The enzyme *TtArsC* was adsorbed on PEG-AuNPs by using the following procedure: 1 ml of PEG-AuNPs was added into separate tubes containing 0.05 ml of *TtArsC* (1 mg ml^{-1} in 15 mM TrisHCl, pH 7). The resulting suspension of hybrid nanoparticles, reported in the following as *TtArsC*-AuNPs, was centrifuged twice at 6000 rpm for 20 min to remove excess protein, and then the pellets were re-dispersed in 1 ml MilliQ water. This colloidal solution was sonicated for 5 min and then stirred for 1 h at room temperature.

2.5. PM-IRRAS characterization

Polarization modulation infrared reflection absorption spectroscopy (PM-IRRAS) spectra were recorded on a commercial Thermo Nexus spectrometer (Les Ulis, France). The

device was set up by focusing the external beam, using an optimal incident angle of 80°, on the sample using a mirror. Prior to this, a ZnSe grid polarizer and a ZnSe photo-elastic modulator were placed on the sample, and the incident beam was tuned between *p*- and *s*-polarizations (HINDS Instruments, PEM 90, modulation frequency = 37 kHz). Finally, the light reflected by the sample was focused onto a nitrogen-cooled MCT detector. The presented spectra result from the sum of 128 scans recorded at $8\,cm^{-1}$ resolution. Each spectrum reported represents the average of at least three measurements. The glass substrates ($11 \times 11\,mm^2$), coated by a 5 nm thick layer of chromium and a 200 nm thick layer of gold, were purchased from Arrandee (Werther, Germany). The gold-coated substrates were annealed on a butane flame to ensure a good crystallinity of the gold top layer and rinsed in a bath of absolute ethanol for 15 min before use.

Chemistry procedures based on a self-assembling monolayer of β-mercaptoethylamine (cysteamine) and a crosslinker have been described previously [22]. Briefly, the freshly cleaned gold substrates were immersed in an unstirred 10 mM ethanol solution of cysteamine at room temperature, in the dark, for 6 h. The gold substrates were then washed with ethanol and ultrapure water (Milli-Q, Millipore, France) to remove the excess thiols. The amino surface was treated following two strategies represented in scheme 1. Scheme S1 (A) shows that the amino surface was treated using 0.2% (w/v) of 1, 4-phenylenediisothio-cyanate (PDC) solution in a solution of 10% pyridine/90% dimethylformamide (DMF) for 2 h at room temperature. Then, the samples were successively washed in DMF and in ethanol and dried under a stream of nitrogen, leaving an isothiocyanate-derivatized surface. *TtArsC* was then chemically adsorbed to the isothiocyanate-covered slides by exposing the entire surface to the *TtArsC* solution for 40 min and then thoroughly rinsed twice in buffer and once in milliQ water. Scheme S1(B) shows how the amino surface was treated by EDC/NHS (80 mg/20 mg) and PEG-AuNPs modified with *TtArsC* solutions for 1 h and then rinsed with phosphate buffer solution and MilliQ water three times for 5 min. The resulting samples were used for PM-IRRAS investigations.

2.6. Transmission electron microscopy (TEM)

Transmission electron microscopy (TEM) measurements were recorded using a JEOL JEM 1011 microscope, which operates at an accelerating voltage of 100 KV. The TEM acquisitions were taken after separating the surfactant solution from the metal particles by centrifugation. Specifically, 1 ml of the nanoparticle solution was centrifuged at 14 000 rpm for 20 min. The supernatant was removed while the pellet was re-dispersed in 1 ml of water; then, a liquid droplet (10 μl) of the colloidal solution was deposited and dried on a microscope grid and finally analyzed.

2.7. Dynamic light scattering (DLS)

The size measurements were performed by dynamic light scattering (DLS) using a Zetasizer Nano ZS (Malvern

Instruments, Malvern, UK) equipped with a He-Ne laser (633 nm, fixed scattering angle of 173°, room temperature 25 °C).

2.8. UV/Vis measurements

The absorption spectra of each sample were recorded using a Jasco V-570 UV/VIS/NIR Spectrophotometer from Jasco Int. Co., Ltd, Tokyo, Japan, in the 200–800 nm range. The spectra were recorded after 30 min from the synthesis of PEG AuNPs, and from 2 min to 24 h after *TtArsC* enzyme adsorption. Finally, spectra were recorded after 10 min of *TtArsC*–AuNP interaction with each heavy metal solution.

2.9. FT-SPR

Fourier Transform-Surface Plasmon Resonance (FT-SPR) measurements were performed with an SPR 100 module from Thermo, equipped with a flow cell mounted on a goniometer. The setup was inserted in a Thermo-scientific Nexus FT-IR spectrometer, and a near-IR tungsten halogen light source was used. The incidence angle was adjusted at the beginning of each experiment with the minimal reflectivity located at $9000\,cm^{-1}$, in order to be in the highest sensitivity region of the InGaAs detector. Gold substrates for FT-SPR measurements were prepared at IMM-CNR in Lecce (Italy).

2.10. Heavy metals interaction monitoring

The interaction between *TtArsC*-AuNPs, As (V) and As (III) solutions was followed using UV–vis spectra of the *TtArsC*-AuNPs solution (50 μl of heavy metal solutions were added to 1 ml *TtArsC*-AuNPs solution) and the FT-SPR shifts of *TtArsC*-AuNPs–modified gold substrates using As (V) and As (III) at 750-325-170-85 μM. Furthermore, the interaction between *TtArsC*-AuNPs, Pb^{2+}, Cd^{2+} *and* Hg^{2+} solutions was followed using UV–vis spectra (50 μl of heavy metal solutions at 170 μM were added to 1 ml *TtArsC*-AuNPs solution).

3. Results and discussion

The interface properties of AuNPs are an interesting topic of study. In particular, the presence of chemical groups at the outer surfaces of AuNPs improves the ability of nanoparticles to interact with biological probes and consequently enhances the interaction of biosensing systems with target analytes. Coating AuNPs with a bifunctional PEG linker carrying two carboxylic groups using a one-step method [15–21] is one useful way to enhance the properties of interfaces: the so-called PEG-diacid can be used as a capping agent, an alternative approach with respect to the citrate-stabilized synthesis process [23, 24]. Furthermore, particle formation and growth can be tuned by exploiting the amphiphilic character of the PEG-diacid polymer in three steps: (1) reduction and stabilization of $HAuCl_4$ is facilitated by dicarboxylic acid-terminated PEG to form gold clusters through the exchange of electrons between them; (2) the presence of PEG-diacid molecules on gold surfaces shortens cluster dimensions and
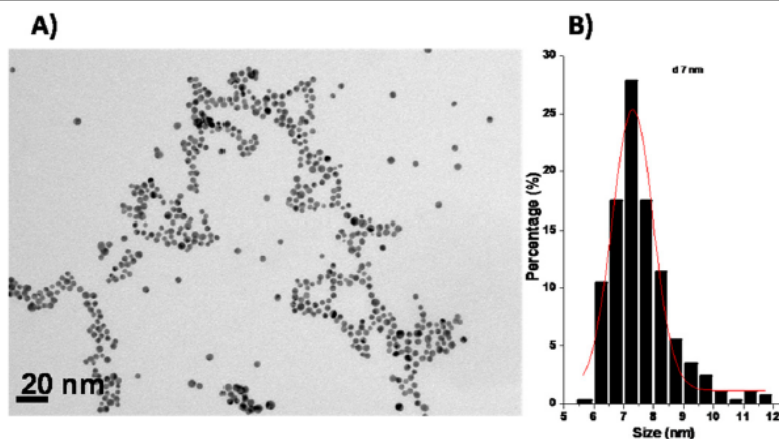
3

Figure 1. TEM images of PEG AuNPs (A) and histogram of nanoparticle size distribution (B).
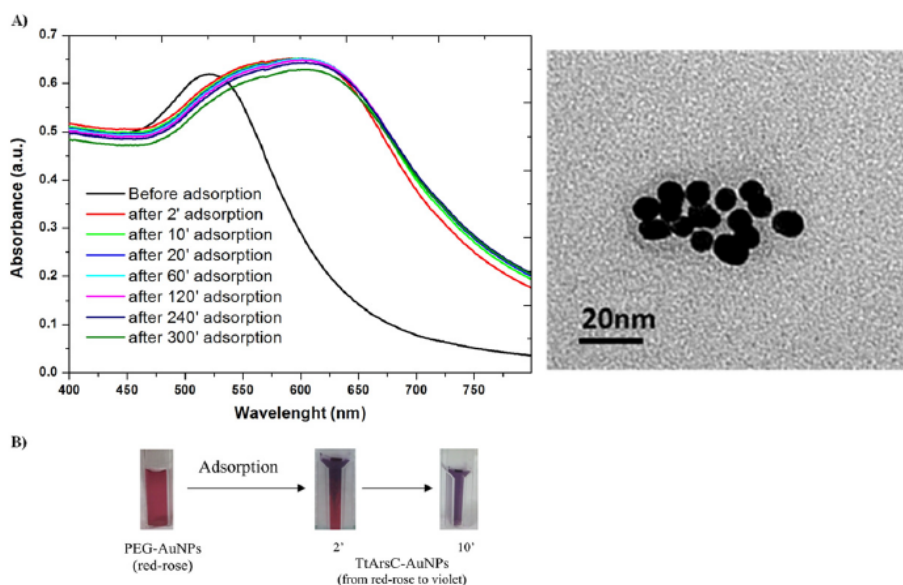

Figure 2. (A) UV–vis spectra of PEG AuNPs during adsorption of *TtArsC* enzyme as a function of time. (B) Schematic representation of nanoparticle solution change of color during adsorption of *TtArsC*.

(3) stabilizes the colloidal solution through electrostatic interactions between the carboxylic acid groups and the gold surface [15].

Figure 1(A) shows a TEM image of PEG-AuNPs after deposition on a microscope grid. The TEM picture of the PEG-AuNPs reveals fairly regular and monodispersed Au nanospheres. Figure 1(B) shows the histogram of 1623 particles: it can be fitted by a Gaussian curve with a mean size of 7 nm with a standard deviation of 2 nm. PEG-AuNPs were used as nanostructured supports for binding *TtArsC*

enzymes in the realization of an assay for biomolecular interaction. *TtArsC* enzyme adsorption onto PEG-AuNPs was monitored by the following methods: UV–Vis spectroscopy in order to monitor Localized Surface Plasmon (LSP) band shift; DLS characterizations in order to observe the aggregation/dispersion behavior of nanoparticles; TEM characterization in order to confirm the aggregation/dispersion behavior of nanoparticles; and PM-IRRAS characterizations in order to evaluate the chemical groups showed at the outer surfaces.
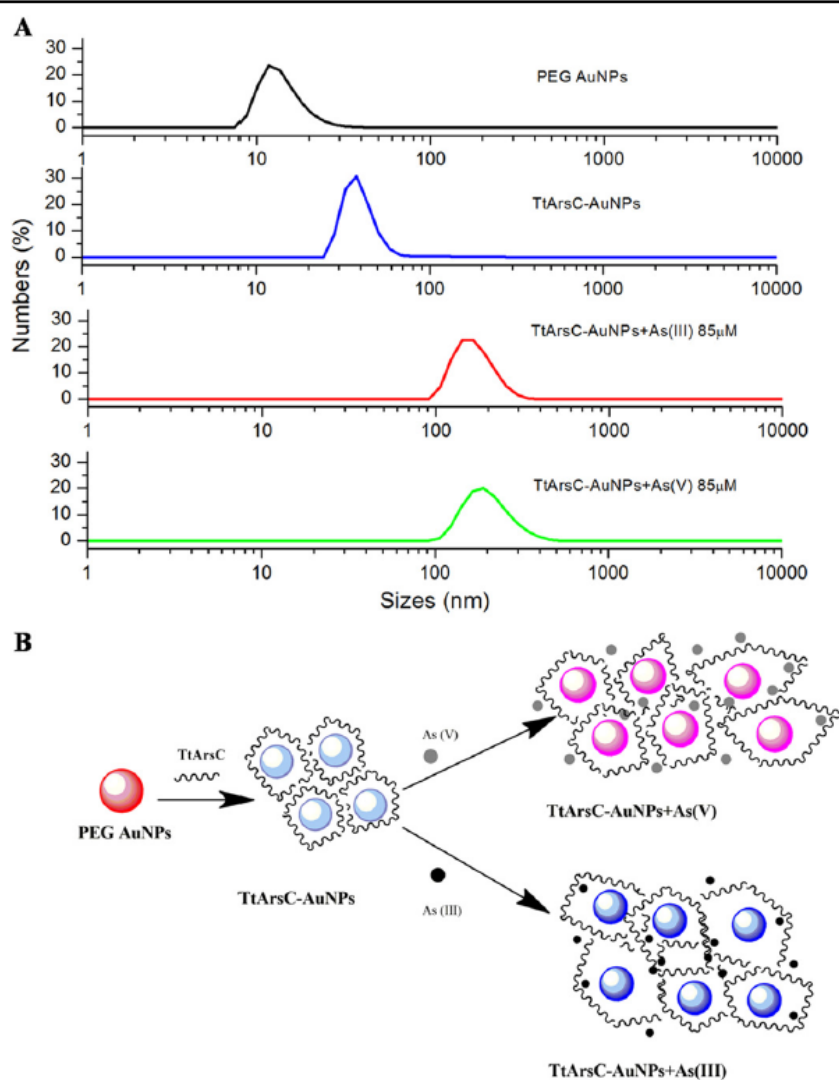
4

76

Figure 3. (A) Size change after each interaction step. (B) Schematization of aggregation process of PEG AuNPs with *TtArsC* enzyme and arsenate/arsenite ions.

Figure 2(A) (left graph) reports the LSP bands of PEG-AuNPs before and after the adsorption of enzyme molecules at equal concentrations of PEG-AuNPs in aqueous solution (10^{-4} M) as a function of time. Figure 2(A) (right image) reports the TEM image of PEG-AuNPs after adsorption to *TtArsC* (*TtArsC*-AuNPs), revealing an aggregation behavior of nanoparticles, while in figure 2(B) photographic images of the cuvettes containing the correspondent solutions are reported. The PEG-AuNP solution, before enzyme adsorption, shows an absorbance peak at 530 nm with a typical red/rose color, whereas, after mixing with the enzyme, in two minutes the color started changing and completed the reaction in about 10 min, which corresponded to a shift of the LSP peak at around 640 nm. UV–vis spectra were recorded up to 24 h after *TtArsC* adsorption, although after 5 h the hybrid biological–metal nano-complex became stable, conferring a characteristic violet color to the solution. We estimated a hydrodynamic diameter of 14 ± 5 nm for PEG-AuNPs (figure 3(A)), while *TtArsC*-AuNPs have a hydrodynamic diameter of 39 ± 13 nm, which means that the enzyme aggregated three to four PEG-AuNPs on average. A more accurate evaluation of *TtArsC* adsorption on PEG-AuNPs was confirmed by PM-IRRAS, which is particularly useful to reveal the chemical groups exposed on nanoparticles' outer
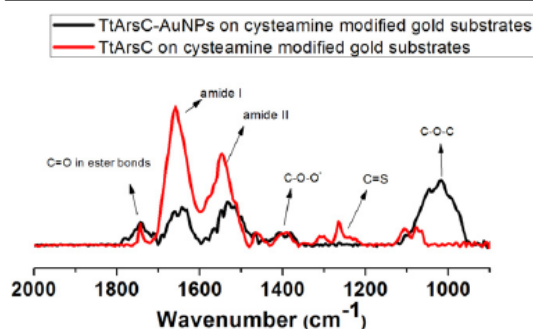
5

77

Figure 4. PM IRRAS spectra of *TtArsC* immobilized on cysteamine modified gold substrates (red line) and *TtArsC*-AuNPs on cysteamine-modified gold substrates (black line).

surfaces. Figure 4 reports, for comparison, a set of PM-IRRAS data from planar gold substrates where *TtArsC*-AuNPs (black line) and *TtArsC* alone (red line) have been covalently bonded. Figure 4 (black line) shows a peak at $1100\,cm^{-1}$ attributed to -COOH groups of PEG-diacid, and peaks at $1400\,cm^{-1}$ and $1450\,cm^{-1}$, typical of -COO- stretching vibrations.

Peaks at $1660\,cm^{-1}$ and $1530\,cm^{-1}$ are also present, representing amide II and I, respectively, which are characteristic of all proteins and enzymes. Peak at $1730\,cm^{-1}$ represent the C=O stretching mode of PEG-AuNPs immobilized onto a gold surface, thus endorsing an effective functionalization of the surface. The presence of a strong stretching band at $1100\,cm^{-1}$ together with peaks at $1450\,cm^{-1}$ and $1730\,cm^{-1}$ suggests the stabilization of the AuNPs with PEG molecules.

Figure 4 (red line) shows a peak at $1100\,cm^{-1}$ representing stretching of aliphatic ethers, a peak at $1240\,cm^{-1}$ characteristic of C=S stretching of the PDC crosslinker, and the amide I and II peaks at $1530\,cm^{-1}$ and $1660\,cm^{-1}$, respectively. The intensities of these peaks are higher with respect to the precedent case, due to rearrangement of *TtArsC* on AuNPs, where PEG-diacid functional groups interacting with the enzyme can partially mask the amide bonds. In this paper, we investigate a versatile chemistry modification that uses homobifunctional crosslinker PDC in order to achieve covalent binding of TtArsC before and after interaction with PEG-AuNPs. The isothiocyanate group present in PDC crosslinker generally act as electrophiles with a carbon atom as the electrophilic center. Electrophilic substitutions with the amino group of cysteamine lead to a stable ligand with a crosslinker that allows covalent binding of TtArsC and TtArsC-AuNPs.

Since the *TtArsC* enzyme is specialized in binding and transforming arsenic compounds, FT-SPR measurements were used to monitor the interaction between *TtArsC*-AuNPs and arsenate (As(V))/arsenite (As(III)) ions; four different concentrations were used for each salt and the details of the results are reported in figure 5. Figure S2 represents a typical shift of surface plasmon resonance from $9000\,cm^{-1}$ before interaction (black line in left graph) to $8600\,cm^{-1}$ after ion

detection (red line in left graph), and the shift of peak position as a function of time during the binding cycle followed by rinsing (right graph).

Figure 5 clearly shows that the interaction between *TtArsC*-AuNPs and arsenate/arsenite ions is concentration dependent (panels **A** and **C**); in both panels, each point reported represents the value of plasmon stabilization after interaction with arsenate/arsenite ions as a function of different concentration. The linear regression parameters obtained by OriginLab Software™ for both arsenite/arsenate ion interaction monitoring are reported in tables S1 and S2 in supplementary data. Moreover, the absolute position of the plasmon absorbance peak changes as a function of different concentrations for both arsenate and arsenite (panels B and D, respectively). Experimental data points in figures 5(B) and (D) were fitted using OriginLab Software™ by Michaelis-Mentens dose-response exponential equation:

$$y(x) = A*e^{(x/C)} + y_0 \tag{1}$$

where A represents the amplitude and C a growth constant. The first derivative of equation (1) is

$$y^1(x) = (A/C)*e^{(x/C)} \tag{2}$$

By equation (2), the sensitivity of the nanosystem in ion biorecognition can be obtained as $y^1(x_M)$ where x_M is the middle point of each data set:

$$S_{AsV} = 1.6 \pm 0.2\,cm^{-1}\,\mu M^{-1}$$

$$S_{AsIII} = 2.82 \pm 0.02\,cm^{-1}\,\mu M^{-1}$$

where S_{AsV} is the sensitivity of the system against arsenate and S_{AsIII} is the sensitivity of the system against arsenite. The estimated sensitivities reveal that the nanobiocomplexes have a higher sensitivity for As (III) ions with respect to As (V) ions, even if the natural substrates of *TtArsC* enzyme are arsenate ions. As is already known [19], the *TtArsC* enzyme has a redox system, able to link the reduction of arsenate to the consumption of dihydronicotinamide adenine dinucleotide phosphate, the so-called NADPH, by using the thioredoxin reductase/thioredoxin (Tr/Trx) system for the redox recycling with a catalytic mechanism that involves the thiol group of the N-terminal cysteine residue (Cys7). In view of our results, we can deduce that these amino acid residues, essential in redox reactions, are partially or totally masked, due to the adsorption of the enzyme onto the PEG-AuNPs' surface.

Further investigations on biorecognition at $85\,\mu M$ concentrations of both arsenite and arsenate have been performed by UV–vis measurements (see curves in figure 6). The LSP bands and the images reported also showed that, at the lowest concentration tested, a change of LSP band position and of the color of the solutions is clearly observable, thus confirming the biomolecular interaction quantified by FT-SPR measurements. Furthermore, the photographic images reported on the left of figure 6 highlight how the solution color change is a function of the arsenic ions' oxidation state: the solution of *TtArsC*-AuNPs became violet/pink on exposure to As(V), while in the case of As(III) it turned to blue. In both cases, it was clearly visible to the naked eye. Again, we
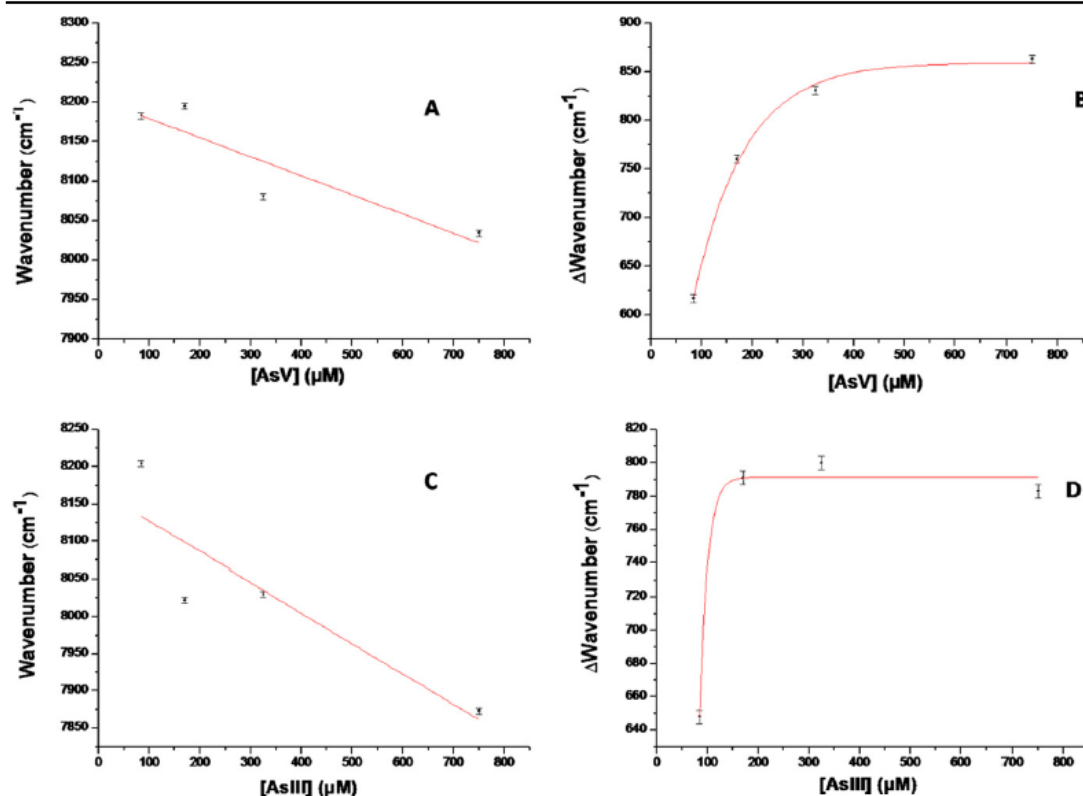
6

Figure 5. Trasmittance of SPR trend by increasing concentration of As V (A) and As III (C) solutions; shift of SPR trasmittance as a function of increasing concentration (85–170–325–750 μM) of As V (B) and As III (D) solutions.
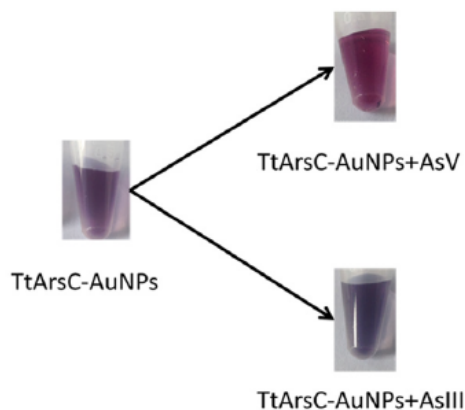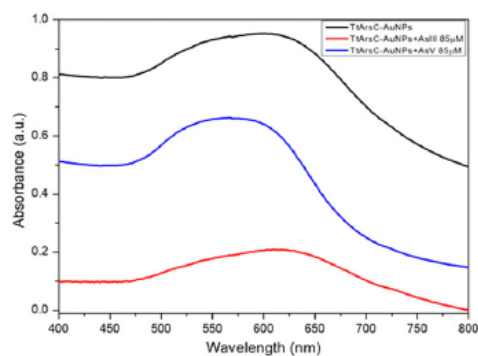

Figure 6. UV–vis spectra (vertically shifted for clarity) of *TtArsC*-AuNPs before and after interaction with arsenate and arsenite ions (right graph). Images of *TtArsC*-AuNPs color change after interaction with arsenate and arsenite ions (left scheme).

attributed this macroscopic evidence of biomolecular interaction to the nanoparticle clustering process; this is also confirmed by the DLS data in figure 3(A), specifically the fourth (red) and fifth (green) curves.

We sketched the interaction mechanism in the scheme reported in figure 3(B). Enzyme biosensing was achieved using gold nanoparticles [25]. These peptides lead to the assembly of nanoparticles due to their crosslinking by long-
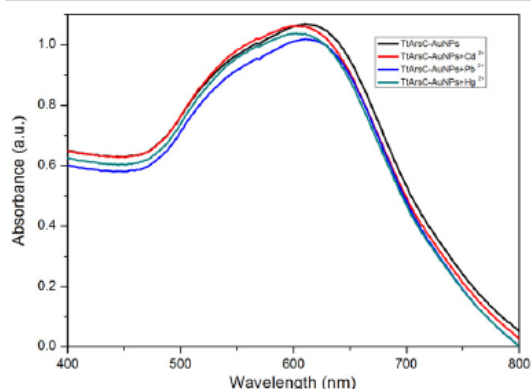
7

Figure 7. UV–vis spectra of TtArsC adsorbed on PEG AuNPs after interaction with cadmium, mercury and lead ions.

chain molecules. This aggregation–dispersion process leads to the colorimetric changes in the nanoparticle solution. Aggregation of gold nanoparticles leads to red shift in the plasmon band due to the electric dipole–dipole interaction, which in turn leads to a coupling between the plasmon oscillations of different particles [26]. The color of the gold nanoparticle solution turns from red to blue/purple due to red shift in the plasmon band. Aggregated or assembled nanoparticles display red shift in the plasmon band when compared to the isolated gold nanoparticles. This phenomenon is attributed to the coupling between the dipole modes of plasmons of different particles. As the interparticle distance is decreased, more red shift in the plasmon band is observed due to an increase in the extent of coupling.

In order to verify the interference of other heavy metal ions that are not natural substrates for the enzyme in the recognition of arsenic ions, UV–vis measurements have been performed in the presence of single ion species (Cd^{2+}, Pb^{2+} and Hg^{2+}) at a concentration of 170 μM. Figure 7 shows that in the presence of such heavy metals, there are not relevant changes in LSP position or intensity, indicating that the assay is highly specific against arsenic compounds. In order to verify whether the nanobiocomplex was also selective for As (III) and As (V), we measured the UV–vis spectra in the presence of a mixture of heavy metals. The results are reported in figure S3. We found that, despite the apparent insensitivity to other heavy metal ions that can be conjectured by data in figure 6, on exposure to a complex mix, the LSP in UV–vis spectra is quite different from the reference ones, i.e. the spectra obtained for As (III) and As(V) alone. This behavior demonstrates a lack of selectivity and prevents the use of the assay for a quantitative measurement of arsenic ions in a complex mixture. Nevertheless, since the solution always changes color in the presence of As(III) and As(V), the assay can be simply and usefully used in fast and cheap screening of water quality.

4. Conclusions

In this work, we used a novel chromosomal arsenate reductase (*TtArsC*) as biomolecular probe to screen for the presence of arsenic in water. Using optical, label-free techniques, we have characterized the interaction between *TtArsC* and arsenic ions, quantitatively evaluating interaction and biorecognition with pentavalent arsenic, As(V), and trivalent arsenic, As(III). The novel and original nanobiocomplexes demonstrated stability and the capacity to strongly bind the toxic ions. Experimental data demonstrated relevant signal changes, i.e. variation of the FT-SPR peak position (about 200 cm^{-1} also at low concentrations). *TtArsC*-AuNPs showed greater sensitivity for arsenite ions, as opposed to what happens in nature, where arsenate ions are the main substrate of *TtArsC* enzymes. On these bases, *TtArsC*-AuNP nanobiocomplexes were found to be able to interact with arsenite ions solutions, veering to blue solutions, and arsenate ions solutions, veering to violet/pink solutions, at all concentrations tested. These phenomena were confirmed quantitatively by LSP shifts in UV–vis spectra, and DLS characterization reveals that the nanobiocomplex aggregates in the presence of arsenic ions. Finally, LSP band study in the presence of metal ions that are not enzyme substrates (Cd^{2+}, Pb^{2+} and Hg^{2+}) indicated that the biorecognition is highly specific but not completely selective. A straightforward application in fast and low-cost screening of water can be envisaged.

Supplementary data

Scheme of immobilization on gold support for PM-IRRAS analysis; working principle of FT-SPR; further investigation of LSP band in UV–vis spectrum and naked-eye response of the *TtArsC*-AuNPs in the presence of complex mixtures of heavy metals are reported.

References

[1] Espino D P, Tamames J, de Lorenzo V and Cánovas D 2009 Microbial responses to environmental arsenic *Biometals* **22** 117–30
[2] Gihring T M and Banfield J F 2001 Arsenite oxidation and arsenate respiration by a new Thermus isolate *Microbiol. Lett.* **204** 335–40
[3] Jackson C R and Dugas S L 2003 Phylogenetic analysis of bacterial and archaealarsC gene sequences suggests an ancient, common origin for arsenate reductase *BMC Evol. Biol.* **3** 18

[4] Macy J M, Santini J M, Pauling B V, O'Neill A H and Sly L I 2000 Two new arsenate/sulfate-reducing bacteria: mechanisms of arsenate reduction *Arch. Microbiol.* **173** 49–57

[5] Mukhopadhyay R and Rosen B P 2002 Arsenate reductases in prokaryotes and eukaryotes *Environ. Health Perspect.* **5** 745–8

[6] Reyes C, Lloyd J R and Saltikov C W 2008 *Arsenic Contamination of Groundwater: Mechanism, Analysis, and Remediation* (Hoboken, NJ: Wiley) pp 123–46

[7] Oremland R S and Stolz J F 2005 Arsenic, microbes and contaminated aquifers *Trends Microbiol.* **13** 45–9

[8] Bartolucci S, Contursi P, Fiorentino G, Limauro D and Pedone E 2013 Responding to toxic compounds: a genomic and functional overview of Archaea *Front. Biosci.* **18** 165–89

[9] Murphy J N and Saltikov C W 2009 The ArsR repressor mediates arsenite-dependent regulation of arsenate respiration and detoxification operons of Shewanella sp. Strain ANA-3 *J. Bacteriol.* **191** 6722–31

[10] Li C, Li D, Wan G, Xu J and Hou W 2011 Facile synthesis of concentrated gold nanoparticles with low size-distribution in water: temperature and pH controls *Nanoscale Res. Lett.* **6** 1–10

[11] Huo Z, Tsung C, Huang W, Zhang X and Yang P 2008 Sub-Two Nanometer Single Crystal Au Nanowires *Nano Lett.* **7** 2041–4

[12] Li N, Zhao P, Liu N, Echeverria M, Moya S, Salmon L, Ruiz J and Astruc D 2014 'Click' chemistry mildly stabilizes bifunctional gold nanoparticles for sensing and catalysis *Chem. Eur. J.* **20** 8363–9

[13] Spadavecchia J, Apchain E, Albéric M, Fontan E and Reiche I 2014 One-step synthesis of collagen hybrid gold nanoparticles and formation on Egyptian-like gold-plated archaeological ivory *Angew. Chem. Int. Ed.* **53** 1756–89

[14] Doane T L, Cheng Y, Babar A, Hill R J and Burda C 2010 Electrophoretic mobilities of PEGylated Gold NPs *J. Am. Chem. Soc.* **132** 15624–31

[15] Spadavecchia J, Perumal R, Barras A, Lyskawa J, Woisel P, Laure W, Pradier C-M, Boukherroub R and Szunerits S 2014 Amplified plasmonic detection of DNA hybridization using doxorubicin-capped gold particles *Analyst* **139** 157–64

[16] Manson J, Kumar D, Meenan B and Dixon D 2011 Polyethylene glycol functionalized gold nanoparticles: the influence of capping density on stability in various media *Gold Bulletin* **44** 99–105

[17] Tian L, Gandra N and Singamaneni S 2013 Monitoring controlled release of payload from gold nanocages using surface enhanced Raman scattering *ACS Nano* **7** 4252–60

[18] Zhenhai G, Jianhui J, Ting Z and Daocheng W J 2011 Preparation of rhodamine B fluorescent poly(methacrylic acid) coated gelatin nanoparticles *Nanomaterials* **1** 753705

[19] Huang H J *et al* 2011 Biocompatible transferrin-conjugated sodium hexametaphosphate-stabilized gold nanoparticles: synthesis, characterization, cytotoxicity and cellular uptake *Nanotechnology* **22** 395706

[20] Del Giudice I, Limaur D, Pedone E, Bartolucci S and Fiorentino G 2013 A novel arsenate reductase from the bacterium Thermusthermophilus HB27: its role in arsenic detoxification *Biochim. Biophys. Acta* **1834** 2071–9

[21] Politi J, Spadavecchia J, Iodice M and De Stefano L 2015 Oligopeptide–heavy metal interaction monitoring by hybrid gold nanoparticle based assay *Analyst* **140** 149–55

[22] Spadavecchia J, Moreau J, Hottin J and Canva M 2009 New cysteamine based functionalization for biochip applications *Sensors Actuators* B **143** 139–43

[23] Neoh K G and Kang E T 2011 Functionalization of inorganic nanoparticles with polymers for stealth biomedical applications *Polym. Chem.* **2** 747–59

[24] Pernodet N, Fang X, Sun Y, Bakhtina A, Ramakrishnan A, Sokolov J, Ulman A and Rafailovich M 2006 Adverse effects of citrate/gold nanoparticles on human dermal fibroblasts *Small* **2** 766–73

[25] Liu J and Lu Y 2004 Adenosine-dependent assembly of aptazyme-functionalized gold nanoparticles and its application as a colorimetric biosensor *Anal. Chem.* **76** 1627–32

[26] Mirkin C A, Storhoff J J, Lazarides A A, Macic R C, Letsinger R L and Schatz G C 2000 What controls optical properties of DNA-linked gold nanoparticle assemblies? *J. Am. Chem. Soc.* **122** 4640–50

9

Chapter 4

ISOLATION AND IDENTIFICATION OF A NEW THERMOPHILIC ARSENIC RESISTANT MICROORGANISM

Isolation and identification of *Geobacillus stearothermophilus*: a new thermophilic arsenic resistant microorganism

Immacolata Antonucci[1], Simonetta Bartolucci[1], Gabriella Fiorentino[1*]

1 Dipartimento di Biologia, Univesità degli Studi di Napoli Federico II, Complesso Universitario Monte S. Angelo, Naples, Italy

*Corresponding author: fiogabri@unina.it

ABSTRACT

A novel thermophilic arsenic resistant bacterium was isolated from thermal mud located in Pisciarelli hot spring, Pozzuoli – Napoli, Italy. The isolated strain was aerobic and grew at 60 °C and at pH 7.0. Phylogenetic analysis based on 16S rRNA gene sequences identified the strain as *Geobacillus stearothermophilus*. This strain exhibited tolerance to concentration of arsenate and arsenite up to 44 mM and 0,14 mM, respectively; it owns in its genome a putative *ars* operon. These results identified *G. stearothermophilus* as a new candidate for the development of arsenic biosensing and bioremediation techniques.

4.1. Introduction

Environmental pollution in manufacturing sectors is often accompanied by the release of diverse forms of pollutants, including heavy metals and hazardous organic pollutants.

Arsenic is a toxic metalloid which is being released into the environment in a variety of ways, as coal combustion, production of pigment for paints and dyes, smelting, mining and tanning (1). Such anthropogenic influx results in increased concentration of arsenic in groundwater and soil. Geochemical cycling of arsenic can be microbially mediated in both aerobic and anaerobic systems (see capitol 1, paragraphs 1.3 and 1.4).

Biotransformation of arsenic by bacteria might offer an inexpensive, environmental-friendly substitute for arsenic remediation.

Bacteria are ubiquitous and highly diversified. They can survive in all kinds of harsh environments. Studies of the last two decades have revealed that 99% of bacteria present in the environment are still unexplored, therefore, they remain obscure for their ecological functions and unexploited for biotechnological applications (2).

Thermophilic bacteria are microbes which mostly live in hot springs due to difficulties of isolation and maintenance of pure cultures but they have not been much investigated.

They have gained worldwide importance thanks to their huge potential for the production of thermostable enzymes that have wide applications in pharmaceuticals and industries (2).

Thermostable enzymes, which have been isolated mainly from thermophilic organisms, have found a number of commercial applications because of their overall inherent stability; advances in this area have been possible with the isolation of a large number of beneficial thermophilic microorganisms from different zones of the earth and the subsequent isolation of useful enzymes (3).

In this work we aimed at the isolation and characterization of new thermophilic arsenic resistant microorganisms, in order to analyse their capability in degrading pollutants or in producing enzymes useful for detoxification.

4.2. Materials and Methods

4.2.1. Isolation

Soil, mud and waters samples were collected aseptically from the thermal site Pisciarelli (Pozzuoli, Napoli -Italy); pH and temperature were recorded. Serial dilutions of these samples were plated on nutrient agar plates in the Luria-Bertani (LB, (4)) medium, pH 7.0 and incubated at 37°C, 50°C and 75°C for 24 h. Several bacterial colonies were obtained from the mud sample grown at 50°C. Sub-samples of the thermal mud were inoculated, in the temperature range 37-70°C, into 5 mL of different media (LB and sodium phosphate buffer), at different pHs; growth was only observed in LB medium at 50°C and pH 7.0. The isolation of a pure culture was carried out by serial diluitions in LB medium.

4.2.2. Characterization and identification

The isolated microorganism was identified by 16S rRNA sequencing committed to Eurofins Genomics.

Briefly, DNA was extracted with a commercial kit according to manufacturer's manual. The 16S region was PCR amplified from sample DNA using gene specific primers and analyzed by DNA sequencing followed by data base search in the nucleotide database of the US *National Center for Biotechnology Information* (NCBI, www.ncbi.nlm.nih.gov). Comparison of the detected sequence with entries in the database finally provided the species.

4.2.3. Growth conditions

Geobacillus stearothermophilus was grown aerobically at 60°C (optimum growth temperature of the identified strain) in LB medium. A frozen (-80°C) stock of *G. stearothermophilus* cells was streaked on a LB plate (solidified by the addition of 1.5% Agar) and incubated at 60°C overnight. Single colonies that appeared on the plate were inoculated into liquid LB medium and shaken at 60°C overnight.

For the determination of Arsenic Minimal Inhibitory Concentration (MIC), arsenate (in the form of arsenic acid potassium salt anhydrous, KH_2AsO_4) and arsenite (in the form of sodium meta-arsenite, $NaAsO_2$) were added to final concentrations ranging between 3-80 mM and 0.1-5 mM, respectively, after dilution of an exponentially culture growth up 0.05 OD_{600nm}.

The MICs values were calculated by fitting (with non-linear regression) the logarithm of the arsenic concentration versus the percent growth; percent growth was calculated from OD_{600nm} measurements of cultures that were grown in different concentrations of arsenic relative to the growth of a culture without arsenic for 6 h.

4.2.4. Bioinformatic analysis

In order to search for arsenic resistance genes in *Geobacillus stearothermophilus* genome, a bioinformatic analysis was carried out through UniProt (http://www.uniprot.org/uniprot/?query=geobacillus+stearothermophilus&sort=score) and NCBI nucleotide (http://www.ncbi.nlm.nih.gov/nucleotide/) data banks.

First of all a list of proteins of *G. stearothermophilus* was downloaded from UniProt (both reviewed and unreviewed); then, they were searched "*ars* proteins". The genes coding for the proteins retrieved by the research were then analyzed on NCBI nucleotide data bank to look at the genetic environment in order to understand if they could form an hypotetic *ars* operon.

The genes which putatively form an *ars* operon are listed in the table 1.

4.3. Results

4.3.1. Isolation and identification

At the time of sampling, water and mud samples were at pH 7.0 and 40°C, while soil samples were at pH 1 and 95°C and pH 5.0 and 75°C. Growth was observed in the

"mud sample" grown in LB medium at pH 7 and 50°C. This organism was isolated by serial dilutions in LB medium and subsequently identified by 16S rRNA sequencing; the sequence detected in the sample showed 100 % homology to the NCBI sequence for *Geobacillus stearothermophilus.*

4.3.2. Identification of putative *Geobacillus stearothermophilus* "*ars* operons"

Alignment of the 16S rRNA sequence obtained against Genome Banks allowed the identification of our sample as "*Geobacillus stearothermophilus*"; from this analysis it was not possible to identify the strain.

Since databases contain genomic sequences of different *G. stearothermophilus* strains, *ars* operons were searched in all of them.

The analysis of these sequences revealed the presence of uncharacterized hypotetical *ars* genes, which could putatively be organized in an *ars* operon (Table 1). Particularly, in the *G. stearothermophilus* 10, *G. stearothermophilus* A1, *G. stearothermophilus* 53 and *G. stearothermophilus* ATCC 12980 strains could contain an *ars*RBC operon; in fact they have three neighboring genes: the first one codes for a transcriptional regulator of the ArsR/SmtB family, followed by an ArsB protein and an arsenate reductase ; this is the minimal set of genes required to confer arsenic resistance.

Indeed, in *G. stearothermophilus* NUB3621 strain there could be an *ars*RDABC operon, with the additional genes encoding ArsD and ArsA proteins, that should provide resistance to higher concentrations of arsenic (table 1); moreover, this strain contains in its genome also a putative *ars*M gene, which defines all the steps of the arsenite SAM-dependent methylation (5).

Hence, to definitely identify the strain that we isolated, further investigations, such as DNA hybridization, will be required.

Table 1.

Protein names	Gene names	Organism
ArsR family transcriptional regulator	GT50_08045	*G. stearothermophilus* 10
Arsenic resistance protein ArsB	GT50_08040	*G. stearothermophilus* 10
Protein ArsC (Arsenate reductase)	GT50_08035	*G. stearothermophilus* 10
Arsenate reductase	AA904_11755	*G.stearothermophilus* A1
Membrane protein	AA904_11745	*G.stearothermophilus* A1
ArsR family transcriptional regulator	AA904_11740	*G. stearothermophilus* A1
Arsenate reductase	GT94_07510	*G. stearothermophilus* 53
Arsenic resistance protein ArsB	GT94_07515	*G.stearothermophilus* 53
ArsR family transcriptional regulator	GT94_07520	*G. stearothermophilus* 53
Arsenate reductase	N231_13860	*G.stearothermophilus* ATCC 12980
Membrane protein	N231_13850	*G. stearothermophilus* ATCC 12980
ArsR family transcriptional regulator	N231_13855	*G.stearothermophilus* ATCC 12980
Arsenite S-adenosylmethyltransferase, ArsM	H839_08853	*G. stearothermophilus* NUB3621
Arsenical resistance operon repressor ArsD	H839_08883	*G. stearothermophilus* NUB3621
Arsenite-translocating ATPase ArsA	H839_08878	*G.stearothermophilus* NUB3621
Protein ArsC (Arsenate reductase)	H839_08888	*G.stearothermophilus* NUB3621
Arsenical-resistance protein ArsB	H839_08893	*G.stearothermophilus* NUB3621
Arsenical resistance operon repressor, ArsR	H839_08898	*G. stearothermophilus* NUB3621

4.3.3. Growth of *Geobacillus stearothermophilus* in the presence of arsenic

As a first step to understand if the strain of *G. stearothermophilus* that we isolated was arsenic resistant, cells were grown in LB medium with increasing concentration of arsenate and arsenite (Fig. 1A, 1C); as it was shown in Fig. 1 *G. stearothermophilus* tolerates the presence of arsenic into growth medium. The MICs of arsenate and arsenite were 44 mM and 0,14 mM (Fig. 1B, 1D) respectively, suggesting resistance to arsenic compounds.
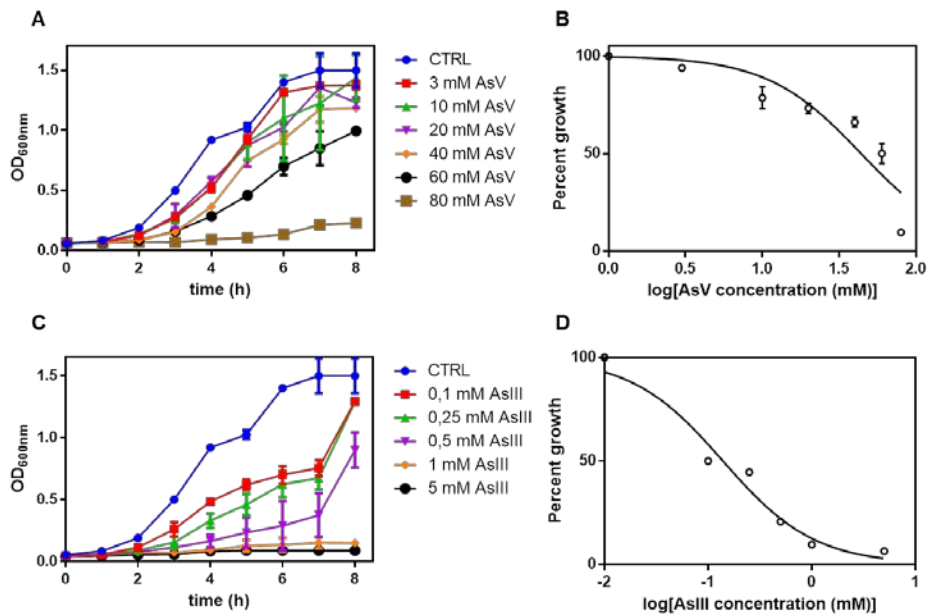

Fig. 1. Effect of arsenate and arsenite on the growth of *G. stearothermophilus*. Growth curves of T. thermophilus HB27 in the presence of increasing concentrations of arsenate (A) and arsenite (B). Legends show the arsenate and arsenite concentrations used in the experiment. MIC values were calculated by plotting the percentage of growth against the concentrations of arsenate (C) and arsenite (D). Percent growth was calculated from OD_{600nm} measurements of cultures that were grown in different concentrations of arsenic relative to the growth of a culture without arsenic for 6 h. Averages and SDs of two cultures are shown.

4.4. Conclusions and discussion

With the aim to find a new thermophilic arsenic resistant microorganism, useful for arsenic detoxification, a sampling was performed in a geothermal area near Naples, known as Pisciarelli. This is an area located close to the Solfatara crater with an intense fumarolic activity; the chemical composition of its soil samples has revealed that the main element is iron, but, as in other geothermal settings, arsenate is another important component (6). Since geothermal sites are a very interesting source of thermophilic organisms and in particular Pisciarelli is an arsenic-rich area, we hypothesized that novel thermophiles could be found able to thrive detoxifying this metal or using it for energy-yielding reactions.
From a mud sample it was isolated a microorganism growing preferentially between 50-60 °C. Subsequent 16S analysis revealed homology to the species *Geobacillus stearothermophilus.*

89

The genus *Geobacillus* was first described in 2001 by Nazina et al. (7). Geobacilli are Gram-positive, endospore-forming, aerobic or facultative anaerobic thermophiles, growing optimally at temperatures between 50°C and 60°C. They do not usually have special growth requirements and are able to utilize various carbon sources. Taking into account all of these properties, *Geobacillus* spp. could be beneficial in various biotechnological applications (8). Due to its wide growth temperature range, geobacilli, when cultivated at the proper temperature, can serve as a host for the expression of proteins derived not only from thermophiles but also from mesophiles. Several convenient shuttle vectors suitable for various geobacilli and some integration systems effective in selected *Geobacillus* strains are currently available (8).

In addition, *Geobacillus* spp. have tremendous possibility to be used as whole cell-biocatalysts. They are able to produce a large variety of enzymes required for the production of valuable bio-products (9) or for the biodegradation of pollutants (8, 10). Thus, the biotechnological potential of *Geobacillus* spp. gives an incentive to develop molecular biology techniques for analysis and genetic modification of these thermophiles.

Bioinformatic analysis have allowed us to detect the presence of putative *ars* operons in the genomes of different *G. stearothermophilus* strains, suggesting the possibility for our strain to tolerate the presence of arsenic. Our laboratory culturing experiments have demonstrated the ability of *G. stearothermophilus* to grow in the presence of arsenate and arsenite in a range of concentration comparable to those of bacteria classified as arsenic resistant (11). These data further supported evidence on the presence of molecular mechanisms for facing the toxicity of arsenic.

It has been reported the possibility to obtain gold nanoparticles from the *Geobacillus stearothermophilus* cell-free extract (12). The use of microbial cells (of which is exploited the cell-free extract) for the synthesis of nanosized materials has emerged as a novel approach for the synthesis of metal nanoparticles.

Among various metal nanomaterials, gold nanoparticles are being intensively studied and have several applications in the field of biolabeling and bioimaging, drug delivery, cancer treatment, antimicrobial and biosensors owing to their unique optical and thermal properties. It has been also reported that the smaller sized gold nanoparticles have higher thermal efficiency (12). *G. stearothermophilus* nanoparticles were found to be spherical in shape and very stable at high temperature; this was due to certain thermostable proteins secreted by the bacterium acting as capping agent (12).

G. stearothermophilus nanoparticles (NPs) production is part of the so-called "green-synthesis"; the biogenic reduction of metal precursors to produce corresponding NPs is eco-friendly, less expensive, free of chemical contaminants for medical and biological applications where purity of NPs is of major concern (13).

Giving this, *G. stearothermophilus* could be a novel model of study for the development of new arsenic biosensing and bioremediation techniques.

90

References

1. **Rehman Y, Rizvi FZ, Faisal M, Hasnain S.** 2013. Arsenic and chromium reduction in co-cultures of bacteria isolated from industrial sites in Pakistan. Microbiology **82:**428-433.
2. **Panda MK, Sahu MK, Tayung K.** 2013. Isolation and characterization of a thermophilic Bacillus sp. with protease activity isolated from hot spring of Tarabalo, Odisha, India. Iranian journal of microbiology **5:**159-165.
3. **Haki GD, Rakshit SK.** 2003. Developments in industrially important thermostable enzymes: a review. Bioresource Technology **89:**17-34.
4. **Miller JH.** 1972. Experiments in Molecular Genetics. Cold Spring Harbor, N. Y.
5. **Qin J, Rosen BP, Zhang Y, Wang GJ, Franke S, Rensing C.** 2006. Arsenic detoxification and evolution of trimethylarsine gas by a microbial arsenite S-adenosylmethionine methyltransferase. Proceedings of the National Academy of Sciences of the United States of America **103:**2075-2080.
6. **Huber R, Huber H, Stetter KO.** 2000. Towards the ecology of hyperthermophiles: biotopes, new isolation strategies and novel metabolic properties. Fems Microbiology Reviews **24:**615-623.
7. **Nazina TN, Tourova TP, Poltaraus AB, Novikova EV, Grigoryan AA, Ivanova AE, Lysenko AM, Petrunyaka VV, Osipov GA, Belyaev SS, Ivanov MV.** 2001. Taxonomic study of aerobic thermophilic bacilli: descriptions of Geobacillus subterraneus gen. nov., sp nov and Geobacillus uzenensis sp nov from petroleum reservoirs and transfer of Bacillus stearothermophilus Bacillus thermocatenulatus, Bacillus thermoleovorans, Bacillus kaustophilus, Bacillus thermoglucosidasius and Bacillus thermodenitrificans to Geobacillus as the new combinations G-stearothermophilus, G-thermocatenulatus, G-thermoleovorans, G-kaustophilus, G-thermoglucosidasius and G-thermodenitrificans. International Journal of Systematic and Evolutionary Microbiology **51:**433-446.
8. **Kananaviciute R, Citavicius D.** 2015. Genetic engineering of Geobacillus spp. Journal of Microbiological Methods **111:**31-39.
9. **Xiao Z, Wang X, Huang Y, Huo F, Zhu X, Xi L, Lu JR.** 2012. Thermophilic fermentation of acetoin and 2,3-butanediol by a novel Geobacillus strain. Biotechnology for Biofuels **5**.
10. **Shintani M, Ohtsubo Y, Fukuda K, Hosoyama A, Ohji S, Yamazoe A, Fujita N, Nagata Y, Tsuda M, Hatta T, Kimbara K.** 2014. Complete Genome Sequence of the Thermophilic Polychlorinated Biphenyl Degrader Geobacillus sp. Strain JF8 (NBRC 109937). Genome announcements **2**.
11. **Wang L, Jeon B, Sahin O, Zhang Q.** 2009. Identification of an Arsenic Resistance and Arsenic-Sensing System in Campylobacter jejuni. Applied and Environmental Microbiology **75:**5064-5073.
12. **Girilal M, Fayaz AM, Balaji PM, Kalaichelvan PT.** 2013. Augmentation of PCR efficiency using highly thermostable gold nanoparticles synthesized from a thermophilic bacterium, Geobacillus stearothermophilus. Colloids and Surfaces B-Biointerfaces **106:**165-169.
13. **Imtiyaz H, Singh NB, Singh A, Singh H, Singh SC.** 2015. Green synthesis of nanoparticles and its potential application Biotechnol Lett.

Chapter 5

GENERAL CONCLUSIONS

Environmental pollution in manufacturing sectors is often accompanied by the release of diverse forms of pollutants, including heavy metals and hazardous organic pollutants. As heavy metals accumulate in living organisms and the environment, they contribute to a wide spectrum of adverse effects, including environmental pollution and human diseases (1, 2). The carcinogenic, mutagenic, and toxicological effects of these elements have been examined to assess their effects on different organs (3, 4).

These giving justify the development of accurate and rapid methods for their detection within the framework of automatic environment monitoring.

Biosensors and bioreporters are beginning to emerge as safe, alternative methods to detect environmental pollutants such as arsenic (5). Biosensors are not intended to fully replace chemical methods but can offer rapid and on-site monitoring of even trace levels of targeted compounds in comparison with non-portable analytical chromatographic methodologies (6). Biosensors provide quantitative or semi-quantitative measurements of the target concentrations, thanks to a biological recognition element (whole cells, antibodies, DNA, RNA, enzymes, or receptor proteins) coupled to a physical transducer (7). To date, bacterial biosensors are mostly based on the use of mesophilic microorganisms, but thermophilic ones could be good candidates for the construction of more stable and stronger cellular or enzymatic biosensors. The advantages of using thermophilic biosensors are related to their higher resistance to the temperature and caotropic agents or detergents often present in industrial off-loads and wastewaters. So thermophilic microorganisms represent a valuable resource in the development of novel biotechnological products.

To realize a biosensor is preliminary the identification of responsive elements to the substance you want to detect, so the main aim of this thesis has been the characterization at molecular level of the mechanisms of arsenic resistance in *T. thermophilus* and the realization of "Cell-Based" and "Enzyme-Based" biosensors for the detection of arsenic species in soils and waters; another goal has been the identification of new arsenic tolerant microorganisms and the characterization of their resistance mechanism.

The thermophilic Gram negative bacterium *Thermus thermophilus* HB27 was able to grow in the presence of both arsenate and arsenite in a range of concentrations which are lethal for other microorganisms (8); the putative resistance genes: an arsenate reductase, a transcriptional regulator and a membrane transport protein have not been found in a single resistance operon but associated to chromosomal genes apparently not functionally related; the thioredoxin-coupled arsenate reductase *Tt*ArsC (8, 9) was previously characterized.

For the realization of the biosensor, it has been searched on *T. thermophilus* genome a transcriptional regulator which could function as metal sensor; the transcriptional regulator *Tt*SmtB belonging to ArsR/SmtB family, has been identified and functionally characterized. Transcriptional analysis by RT-PCR of *TtsmtB* and its neighboring genes showed that the gene was expressed in third position of an operon of five genes (*TTC0351-TTC0352-TTC0353-TTC0354-TTC0355*) encoding putative proteins with no obvious functional relation, except for *TTC0354*, coding a putative cation-transporting ATPase with a heavy-metal-associated domain that could mediate the active efflux of arsenite. qRT-PCR analysis showed the variation in the transcription profiles of *TTC0351*, the first gene of the operon, as well as of *TTC0353*

93

and *TTC0354* upon arsenate and arsenite treatment confirming their involvement in arsenic response and suggesting that *Tt*SmtB could be the true regulator.

Interestingly, despite being a gene cluster, basal promoter consensus elements were identified by homology search not only upstream of *TTC0351* but also as internal promoters i.e. upstream of *TTC0353* and *TTC0354* suggesting that these genes could also be singularly transcribed and distinctly regulated in order to ensure that relative expression levels of the various genes could vary under diverse growth conditions (10). Furthermore, *TTC0354* promoter contained sequences corresponding to the consensus palindromic SmtB binding site overlapping basal transcription elements (11), strongly indicating that *TTC0354* expression could be regulated through modulation of DNA binding by the metal sensor *Tt*SmtB. To investigate on this point, *Tt*SmtB was cloned and expressed in recombinant form in *E. coli*, purified to homogeneity and functionally characterized. *In vitro*, recombinant *Tt*SmtB bound to all the promoters that we identified with different features; in particular, a hardly detectable complex was formed between *Tt*SmtB and its own promoter suggesting lower transcriptional repression exerted on it. Furthermore, *Tt*SmtB bound to *TTC0354* promoter sequence site-specifically, in a cooperative manner (n Hill = 2.5) and with high affinity (K_d of 0.27 µM); it was not able to interact with such DNA sequence in the presence of both arsenate and arsenite. A key step in the arsenic resistance is the intracellular reduction of arsenate to arsenite by arsenate reductases which are usually encoded in the same operon of the regulator; since in *T. thermophilus* resistance genes have not been found in a single operon, we confirmed through EMSA the ability of *Tt*SmtB to act also on the promoter of *Tt*ArsC whose role in arsenic challenge had already been proved (8).

To verify *in vivo* the function of *Tt*SmtB in the regulation of arsenic related genes, a *smtB⁻* mutant (*ΔsmtB*) was obtained and the expression levels of *TTC0351*, *TTC0354* and *TtarsC* were measured by qRT-PCR. In the mutant strain, gene expression levels were significantly higher than in the wild type giving experimental evidence that *in vivo Tt*SmtB is bound to its target promoters hampering gene transcription. The results also proved that the gene is not essential for *T. thermophilus* survival as the *ΔsmtB* strain grew alike the wild type in arsenic free media; interestingly, whereas the mutant grew similarly to the wild type in the presence of arsenite, it showed a decreased growth rate in arsenate-containing medium. It can be hypothesized that in the *ΔsmtB* strain the exposition to arsenite could be counteracted by the increased expression of *TTC0354* allowing a faster extrusion from the cell. On the other hand, the inhibitory effect of arsenate on cell growth can be overcome only after the catalytic reduction to arsenite by *Tt*ArsC which precedes the transport outside the cell. Interestingly, complementation of *TtSmtB* in the *ΔsmtB* strain increased the arsenate tolerance and partially recovered growth to the wild-type levels; these results are consistent with the restored *TtsmtB* expression, confirming its role in the regulation of arsenic resistance. These results give insights in the mechanisms of metal-regulated gene expression in thermophilic microorganisms and accounts *Tt*SmtB as the first thermostable ArsR/SmtB member; moreover, let us to consider *T. thermophilus* as a good model system for biosensors development.

The second aim of the thesis has been the characterization of responsive regulatory sequences. Hence the putative promoters which we demonstrated to be recognized by *Tt*SmtB were fused to the β-galactosidase reporter gene. The reporter systems were based on the modification of a *T. thermophilus* Δ42 strain with a hybrid transcriptional fusion between a *T. thermophilus* promoter responsive to arsenic and

94

the *bgaA* gene, coding for a thermostable β-galactosidase. Three reporter constructs: pMH0351prombgaA, pMH0353prombgaA and pMH0354prombgaA, were produced containing the bgaA coding sequence under the control of different *T. thermophilus* promoters, which were shown to be targets of the transcriptional regulator *Tt*SmtB. Analysis of β-galactosidase activity demonstrated that the activity of all three tested promoters was not strictly dependent on the bacterial growth phase; moreover, two of the three tested promoter were responsive to arsenic. Interestingly, the one with the lower activity and not inducible by the presence of arsenic, was *0351*prom, the promoter upstream of the entire operon in which *TtsmtB* is located. *0353*prom and *0354*prom were able to drive increased expression of the reporter gene after arsenate and arsenite treatments.

These findings could be exploited considering that *Tt*SmtB preferably bound *0354*prom and that a DNA-protein complex between the transcriptional regulator and its own promoter (*0353*prom) was hardly detectable; so 0354prom could be mighty repressed by *Tt*SmtB. This hypothesis was proven analyzing the β-galactosidase activity into *T. thermophilus ΔsmtB::kat* transormants. In fact is in this environment, that in the absence of the arsenic sensor and in conditions of derepression, *0354*prom activity resulted to be higher than *0353*prom activity. These results led us to choose *T. thermophilus* Δ42 *0354*prom reporter strain as a candidate for an arsenic biosensor. Analysis of β-galactosidase activity at different growth times after arsenic treatment, aimed at setting up the best time intervals to measure the response of the biosensor indicated that the response could be measured with reliability within 30 minutes of arsenate or arsenite addition. The above data allowed only to estimate a biosensor minimum detection limit of 0.1 mM for both arsenate and arsenite.

An intriguingly feature of this biosensor rely on its thermophilic nature; this could represent a considerable advantage related to its higher resistance to temperature, and to caotropic agents or detergents often present in industrial off-loads and wastewaters.

Hence, despite not having a higher arsenic detection limit, it could be more versatile, stable and strong in case of highly contaminated waters.

In conclusion, we constructed the first whole-cell arsenic biosensor based on the use of a thermophilic microorganism. Furthermore, our results show that the whole-cell biosensor would appear a useful tool for the rapid measurement of arsenic in contaminated sites. However, further improvements are required to verify measurements in the lower range of concentrations, as well as in the presence of other chemicals besides inducer compounds.

Another important step of this thesis has been the development of an enzyme-based biosensor, it was used *Tt*ArsC as biomolecular probe to screen for the presence of arsenic in water; particularly, *Tt*ArsC was adsorbed onto gold nanoparticles (AuNPs). Using optical, label-free techniques, it was characterized the interaction between *Tt*ArsC and arsenic ions, quantitatively evaluating interaction and biorecognition with arsenate and arsenite. The novel and original nanobiocomplexes demonstrated stability and the capacity to strongly bind the toxic ions. Experimental data demonstrated relevant signal changes, i.e. variation of the FT-SPR peak position (about 200 cm^{-1} also at low concentrations). TtArsC-AuNPs showed greater sensitivity for arsenite ions, as opposed to what happens in nature, where arsenate ions are the main substrate of *Tt*ArsC enzymes. On these bases, TtArsC-AuNP nanobiocomplexes were found to be able to interact with arsenite ions solutions,

veering to blue solutions, and arsenate ions solutions, veering to violet/pink solutions, at all concentrations tested. These phenomena were confirmed quantitatively by Localized Surface Plasmon (LSP) shifts in UV–vis spectra, and dynamic light scattering (DLS) characterization reveals that the nanobiocomplex aggregates in the presence of arsenic ions. Finally, LSP band study in the presence of metal ions that are not enzyme substrates (Cd^{2+}, Pb^{2+} and Hg^{2+}) indicated that the biorecognition was highly specific but not completely selective. A straightforward application in fast and low-cost screening of water can be envisaged (9).

Our results confirm the possibility of using *T. thermophilus* as biological systems (cellular or enzymatic) for the traceability of pollutants after a thorough molecular, structural and functional characterization of the components involved and their interactions.

The last step has been the isolation of a new arsenic resistant organism from a mud sample from a geothermal area near Naples, known as Pisciarelli. 16S rRNA sequence identified it as *Geobacillus stearothermophilus;* Geobacilli are Gram-positive, endospore-forming, aerobic or facultative anaerobic thermophiles, growing optimally at temperatures between 50°C and 60°C. Bioinformatic analysis have allowed us to detect the presence of putative *ars* operons in the genomes of different *G. stearothermophilus* strains, suggesting the possibility for our strain to tolerate the presence of arsenic. Our laboratory culturing experiments have demonstrated the ability of *G. stearothermophilus* to grow in the presence of arsenate and arsenite in a range of concentration comparable to those of bacteria classified as arsenic resistant (14). These data further supported evidence on the presence of molecular mechanisms for facing the toxicity of arsenic. It has also been reported the possibility to obtain gold nanoparticles from the *Geobacillus stearothermophilus* cell-free extract (15), this is part of the so-called "green-synthesis" nanoparticles production. All these giving, make *G. stearothermophilus* a novel model of study for the development of new arsenic biosensing and bioremediation techniques.

References

1. **Jain CK, Ali I.** 2000. Arsenic: Occurrence, toxicity and speciation techniques. Water Research **34:**4304-4312.
2. **Thakur JK, Thakur RK, Ramanathan AL, Kumar M, Singh SK.** 2011. Arsenic Contamination of Groundwater in Nepal-An Overview. Water **3:**1-20.
3. **Paez-Espino D, Tamames J, de Lorenzo V, Canovas D.** 2009. Microbial responses to environmental arsenic. Biometals **22:**117-130.
4. **Rosen P.** 1971. Theoretical significance of arsenic as a carcinogen. Journal of theoretical biology **32:**425-426.
5. **Diesel E, Schreiber M, van der Meer JR.** 2009. Development of bacteria-based bioassays for arsenic detection in natural waters. Analytical and Bioanalytical Chemistry **394:**687-693.
6. **Sun J-Z, Kingori GP, Si R-W, Zhai D-D, Liao Z-H, Sun D-Z, Zheng T, Yong Y-C.** 2015. Microbial fuel cell-based biosensors for environmental monitoring: a review. Water Science and Technology **71:**801-809.
7. **Sandra P, Catherine B, T. DEC, Camille E, David P, Nicolas G, Daniel G.** 2016. A bioluminescent arsenite biosensor designed for inline water analyzer Springer-Verlag Berlin Heidelberg ed. Environ Sci Pollut Res.
8. **Del Giudice I, Limauro D, Pedone E, Bartolucci S, Fiorentino G.** 2013. A novel arsenate reductase from the bacterium Thermus thermophilus HB27: Its role in arsenic detoxification. Biochimica Et Biophysica Acta-Proteins and Proteomics **1834:**2071-2079.

9. **Politi J, Spadavecchia J, Fiorentino G, Antonucci I, Casale S, De Stefano L.** 2015. Interaction of Thermus thermophilus ArsC enzyme and gold nanoparticles naked-eye assays speciation between As(III) and As(V). Nanotechnology **26**.
10. **Napolitano M, Rubio MA, Camargo S, Luque I.** 2013. Regulation of Internal Promoters in a Zinc-Responsive Operon Is Influenced by Transcription from Upstream Promoters. Journal of Bacteriology **195:**1285-1293.
11. **Osman D, Cavet JS.** 2010. Bacterial metal-sensing proteins exemplified by ArsR-SmtB family repressors. Natural Product Reports **27:**668-680.
12. **Cava F, Zafra O, da Costa MS, Berenguer J.** 2008. The role of the nitrate respiration element of Thermus thermophilus in the control and activity of the denitrification apparatus. Environmental Microbiology **10:**522-533.
13. **Alvarez L, Bricio C, Jose Gomez M, Berenguer J.** 2011. Lateral Transfer of the Denitrification Pathway Genes among Thermus thermophilus Strains. Applied and Environmental Microbiology **77:**1352-1358.
14. **Wang L, Jeon B, Sahin O, Zhang Q.** 2009. Identification of an Arsenic Resistance and Arsenic-Sensing System in Campylobacter jejuni. Applied and Environmental Microbiology **75:**5064-5073.
15. **Girilal M, Fayaz AM, Balaji PM, Kalaichelvan PT.** 2013. Augmentation of PCR efficiency using highly thermostable gold nanoparticles synthesized from a thermophilic bacterium, Geobacillus stearothermophilus. Colloids and Surfaces B-Biointerfaces **106:**165-169.

List of Communications

Immacolata Del Giudice, Danila Limauro, Emilia Pedone, <u>Immacolata Antonucci</u>, Simonetta Bartolucci & Gabriella Fiorentino. **A novel arsenate reductase from the bacterium *Thermus thermophilus* HB27: its role in arsenic detoxification**. **Microbiology 2013**- Ischia, September 18-21, 2013.

<u>Immacolata Antonucci</u>, Danila Limauro, Immacolata Del Giudice, Josè Berenguer, Simonetta Bartolucci, Gabriella Fiorentino. **Insights in the regulation of the arsenic resistance system in *Thermus thermophilus*. Extremophiles 2014 -** Saint Petersburg, 10th International Congress on Extremphiles, September 7-11,2014.

<u>Immacolata Antonucci</u>, Francesca Anna Fusco, Danila Limauro, Immacolata Del Giudice, Josè Berenguer, Simonetta Bartolucci, Gabriella Fiorentino. **Exploiting the arsenic resistance of the thermophilic bacterium *Thermus thermophilus*. SIB 2015 -** 58th National Meeting of the Italian Society of Biochemistry and Molecular Biology. Urbino, September 14-16, 2015.

List of Publications

Jane Politi, Jolanda Spadavecchia, Gabriella Fiorentino, <u>Immacolata Antonucci</u>, Sandra Casale, Luca De Stefano. **Interaction of *Thermus thermophilus* ArsC enzyme and gold nanoparticles naked-eye assays speciation between As(III) and As(V). 2015.** Nanotechnology 2015 Oct 30;26(43):435703. doi: 10.1088/0957-4484/26/43/435703.

<u>Immacolata Antonucci</u>, Danila Limauro, Patrizia Contursi, Ana Luisa Ribeiro, Immacolata Del Giudice, José Berenguer, Simonetta Bartolucci and Gabriella Fiorentino. **An ArsR/SmtB family member involved in the regulation of arsenic resistance genes in *Thermus thermophilus* HB27.**
Submitted to Applied Environmental Microbiology.

<u>Immacolata Antonucci</u>, Josè Berenguer, Simonetta Bartolucci, Gabriella Fiorentino. **A novel *Thermus thermophilus* whole-cell biosensor for the detection of arsenic pollution.**
In preparation.

<u>Immacolata Antonucci</u>, Simonetta Bartolucci, Gabriella Fiorentino. **Isolation and identification of *Geobacillus stearothermophilus*: a new thermophilic arsenic resistant microorganism.**
In preparation.

CONSEJO SUPERIOR
DE INVESTIGACIONES
CIENTÍFICAS

CSIC

UAM

UNIVERSIDAD AUTÓNOMA
DE MADRID

CENTRO DE BIOLOGÍA MOLECULAR
"SEVERO OCHOA"

February 29, 2016

To whom it may concern,

This letter is to **certify** that Immacolata Antonucci, Ph. D. student in Industrial and Molecular Biotechnology from the University Federico II (Naples, Italy) carried out experimental works in my laboratory at the Centro de Biología Molecular Severo Ochoa (Madrid) from January 13 to April 11, 2014. Her work in this laboratory was focussed on the isolation of mutants of *Thermus thermophilus* affected in As resistance in the framework her Ph. D. Thesis project.

Signed: José Berenguer
Professor of Microbiology

Biotecnologie Industriali

SCUOLA POLITECNICA E DELLE SCIENZE DI BASE

BIO-UNIVERSE

BIOtecnologie Industriali: UNIone tra uniVERsità e impreSE "BIO-UNIVERSE"

Convegno sulle Biotecnologie Industriali in Campania
30 Gennaio 2015
Sala Azzurra - Monte Sant'Angelo, Via Cinthia, 80126 Napoli

Gli studenti della scuola di dottorato in Biotecnologie dell'Università degli Studi di Napoli Federico II (XXVII — XXVIII — XXIX ciclo) vi invitano a partecipare al primo convegno dal titolo "BIO-UNIVERSE" che si terrà il 30 Gennaio 2015, presso il Centro Congressi dell'Ateneo situato nel complesso Universitario di Monte Sant'Angelo.

Quest'iniziativa è volta ad offrire a studenti e giovani ricercatori l'opportunità di conoscere le diverse realtà imprenditoriali campane ed a mostrare il percorso da affrontare per affermar- si sia a livello accademico che aziendale. Inoltre, la manifesta- zione si propone di essere promotrice del trasferimento scien- tifico-tecnologico tra le parti.

Partendo dall'incontro con ricercatori di successo (Sessione I), passando attraverso le prime realtà industriali quali start-up e spin-off (Sessione II), si arriverà, infine, all'incontro con le aziende (Sessione III). Durante il convegno verranno analizza- ti i *case study* con le problematiche incontrate durante il per- corso che ha portato alla realizzazione delle idee progettuali, illustrandone le competenze multidisciplinari necessarie, i punti di forza, ed inoltre sottolineando come, e se, un recipro- co e costante scambio tra Università ed aziende abbia consen- tito l'affermazione commerciale delle idee.

Ore 8:30 - Registrazione

Ore 9:15 - Cerimonia di apertura
  Prof. Giovanni Sannia (Presidente della Scuola di Dottorato in Biotecnologie)
  Prof. Piero Salatino (Presidente della Scuola Politecnica e delle Scienze di Base)
  Prof.ssa Renata Piccoli (Coordinatore dei Corsi di Laurea e Laurea Magistrale in Biotecnologie Industriali)
  Dott. Salvatore Fusco (Studente della scuola di dottorato in Biotecnologie)
  Dott.ssa Angela Avitabile (Studente della scuola di dottorato in Biotecnologie)

Ore 9:30 Prof. Gennaro Marino (Professore Emerito, Federico II)
SESSIONE I - La Ricerca Applicata
  10:00 Prof. Marco Salvemini (Federico II)
  10:20 Prof.ssa Chiara Schiraldi (S.U.N.)
  10:40 Prof.ssa Vincenza Faraco (Federico II)
  11:00 Dott. Giuseppe Manco (C.N.R.)
Moderatori: Dott. Salvatore Fusco, Dott.ssa Angela Avitabile

11:20 - 12:00 Coffee Break + Sessione Poster

Ore 12:00 Prof. Roberto Vona (Ordinario di Management, Federico II)
SESSIONE II - Spin-off & Start-up
  12:30 Dott. Alfredo Ronca (FasTissues S.r.l.s.)
  12:50 Dott.ssa Cinzia Pezzella (BioPox S.r.l.)
  13:10 Dott. Luigi Mandrich (Detoxizymes S.r.l.s.)
Moderatori: Dott. Pietro Tedesco, Dott.ssa Lucia Laura Giordano

13:30 - 15:00 Pausa + Sessione Poster

Ore 15:00 Prof. Antonio Marzocchella (Professore di impianti chimici, Federico II)
SESSIONE III - L'Industria Biotecnologica e gli Sbocchi Occupazionali
  15:30 Dott.ssa Annalisa Tito (Arterra Bioscience S.r.l.)
  15:50 Dott. Andrea Aramini (Dompé S.p.A.)
  16:10 Dott.ssa Vincenza Di Palma (STMicroelectronicrs S.r.l.)
  16:30 Dott.ssa Patrizia Circelli (CiaoTech S.r.l.)
Moderatori: Dott.ssa Orsola Di Martino, Dott. Alfredo Maria Gravagnuolo

Ore 16:50 Cerimonia di chiusura
  Prof. Giovanni Sannia
  Dott.ssa Lucia Guarino (Studente della scuola di dottorato in Biotecnologie)
  Dott. Valerio Guido Giacobelli (Studente della scuola di dottorato in Biotecnologie)

Comitato organizzativo BIO-UNIVERSE: Alessandra Procentese, Alessia Gioiello, Alfredo Maria Gravagnuolo, Andrea Fulgione, Angela Avitabile, Anna Pennacchio, Annaelena Troiano, Emiliana Perillo, Fabrizia Nici, Federica Astarita, Filomena Grasso, Filomena Sannino, Flora Ianniello, Francesco Itri, **Immacolata Antonucci**, Jane Politi, Katia Pane, Lucia Guarino, Lucia Laura Giordano, Marialuisa Siepi, Marilena Esposito, Orsola di Martino, Paola Cicatiello, Pietro Tedesco, Roberta Carpine, Rosa Gaglione, Rossana Liguori, Salvatore Fusco, Salvatore Montella, Santa Errichiello, Sara Peirce, Simona Giacobbe, Stefania Passato, Valentina Madonna, Valerio Guido Giacobelli, Vincenzo Tarallo. Ringraziamenti: Marco Vastano

www.biotecnologieindustriali.unina.it — email per info e iscrizioni: progetto.biotech@yahoo.it

Interaction of *Thermus thermophilus* ArsC enzyme and gold nanoparticles naked-eye assays speciation between As(III) and As(V)

Interaction of *Thermus thermophilus* ArsC enzyme and gold nanoparticles naked-eye assays speciation between As(III) and As(V)

Jane Politi[1,2], Jolanda Spadavecchia[3,4], Gabriella Fiorentino[5], Immacolata Antonucci[5], Sandra Casale[3] and Luca De Stefano[1]

[1] Institute for Microelectronics and Microsystems, Unit of Naples-National Research Council Via P. Castellino 111, 80127, Italy

[2] Department of Chemical Sciences, University of Naples 'Federico II', Via Cynthia, 80126 Naples Italy

[3] Sorbonne Universités, UPMC Univ Paris VI, Laboratoire de Réactivité de Surface, 4 place Jussieu, F-75005 Paris, France

[4] CNRS, UMR 7244, CSPBAT, Laboratoire de Chimie, Structures et Propriétés de Biomateriaux et d'Agents Therapeutiques Université Paris 13, Sorbonne Paris Cité, Bobighy, France CNRS, Paris, France

[5] Department of Biology, University of Naples 'Federico II', Via Cynthia, 80126 Naples, Italy

E-mail: jane.politi@na.imm.cnr.it and luca.destefano@na.imm.cnr.it

Abstract

The thermophilic bacterium *Thermus thermophilus HB27* encodes chromosomal arsenate reductase (*TtArsC*), the enzyme responsible for resistance to the harmful effects of arsenic. We report on adsorption of *TtArsC* onto gold nanoparticles for naked-eye monitoring of biomolecular interaction between the enzyme and arsenic species. Synthesis of hybrid biological–metallic nanoparticles has been characterized by transmission electron microscopy (TEM), ultraviolet-visible (UV–vis), dynamic light scattering (DLS) and phase modulated infrared reflection absorption (PM-IRRAS) spectroscopies. Molecular interactions have been monitored by UV–vis and Fourier transform-surface plasmon resonance (FT-SPR). Due to the nanoparticles' aggregation on exposure to metal salts, pentavalent and trivalent arsenic solutions can be clearly distinguished by naked-eye assay, even at 85 μM concentration. Moreover, the assay shows partial selectivity against other heavy metals.

S Online supplementary data available from stacks.iop.org/NANO/26/435703/mmedia

(Some figures may appear in colour only in the online journal)

1. Introduction

*Thermus thermophilus HB*27 is an extremophile organism living in arsenic-rich geothermal environments: this bacterium has developed the ability to both oxidize and reduce arsenic, thus playing an important role in its speciation and bioavailability [1, 2]. Arsenate reduction mechanisms, apparently due to convergent evolution or originating in a common ancestor and then transferred to [3, 4], can be individuated into three families: the first family has been typified as *arsC* glutathione–glutaredoxin dependent (*arsC-*

GSH/Grx) and was identified in enteric bacteria (e.g. *Escherichia coli*); the second one is known as *arsC* tioredoxin dependent (*arsC-Trx*) and was found in Gram-positive bacteria (e.g. *Staphylococcus*). The last family, which includes the *ars2* gene, was amplified from *Saccharomyces cerevisiae* [5]. Microbial activities play critical roles in the geochemical cycling of arsenic because they can promote or inhibit its release from sediment material, mainly by redox reactions [6–8]. The reduction of pentavalent arsenate, As (V), to trivalent arsenite, As (III), is the major reaction causing the release of arsenic from the mineral surfaces into groundwater; in fact,

besides being more toxic, arsenite is the most mobile and common form of arsenic found in anaerobic contaminated aquifers [9]. There is a worldwide demand to sense and quantify arsenic pollution, both natural and anthropogenic, in fresh water using low-cost and easy-to-use devices, especially in developing countries.

Nanostructured materials claim a range of exciting physical and chemical properties, which make them fundamental building blocks for the next generation of instruments and devices. In particular, gold nanoparticles (AuNPs) are among the most-used nano-objects, and are exploited in many applications ranging from medical to environment monitoring. The most popular method for preparing AuNPs in water uses citrate to reduce $HAuCl_4$ under boiling conditions [10]. Therefore, several approaches have been developed to reduce Au (III) salts in water using different ligands as colloid particle stabilizers [11]. Stabilizers, usually surfactant molecules, protect particles by avoiding aggregation mechanisms and controlling their physio-chemical properties [12, 13], but these molecules are mostly toxic. Dangerous organic molecules could be substituted by some biocompatible molecules, such as polyethylene glycol (PEG), in order to prepare biocompatible PEG-stabilized AuNPs [14, 15]. Recently, great advances have been made in the use of gold nanoparticles for signaling applications, owing to their stability, chemical reactivity, non-toxic nature, strong absorption and scattering properties, and electrostatic charges that allow strong interactions with proteins and enzymes [16, 17]. For instance, biomolecule- and/or biopolymer-conjugated AuNPs are largely used as biomarkers or biodelivery vehicles, as well as for cosmetics and as anti-aging components for skin protection [18, 19].

In the following study, we report our results on the adsorption of *TtArsC* enzyme onto PEG-stabilized AuNPs (PEG-AuNPs) for monitoring its interaction with pentavalent arsenic ions (As (V)) and trivalent arsenic ions (As (III)). Both the adsorption of enzyme onto PEG-AuNPs and its interaction with As (V) and As (III) salts can be followed easily by the naked eye, since solutions completely change their colors. UV–vis spectroscopy, polarization modulation infrared reflection/adsorption (PM-IRRAS) spectroscopy, dynamic light scattering (DLS) and Fourier transform-surface plasmon resonance (FT-SPR) were used as the main characterization techniques.

2. Experimental

2.1. Chemicals

Tetrachloroauric acid ($HAuCl_4$), sodium borohydride ($NaBH4$), polyethylene glycol 600 diacid (PEG diacid), β-Mercaptoethylamine (cysteamine), 1, 4-phenylenediisothiocyanate (PDC), ethanol (C_2H_5OH), pyridine, dimethylformamide (DMF), 15 mM Tris-HCl, potassium metarsenite ($NaAsO_2$), potassium arsenate (KH_2AsO_4), cadmium ions solution, lead (II) methanesulfonate ($C_2H_6O_6PbS_2$) and mercury (II) nitrate

solution (HgN_2O_6) were purchased from Sigma Aldrich. All chemicals were used without any further purification.

2.2. Purification and preparation of TtArsC enzyme

Recombinant *TtArsC* (*TtArsC*: protein arsenate reductase from the Gram-negative bacterium *Thermus thermophilus* HB27) was purified to homogeneity using the purification procedure already described, basically consisting of a thermo-precipitation of the *Escherichia coli* cell extract followed by anion exchange and gel filtration chromatography [20]. Fractions containing purified *TtArsC* were pooled, dialyzed against 15 mM Tris-HCl, 1 mM DTT, pH 7.5 and lyophilized in aliquots of 1 mg using a freeze dryer (HetoPowerDry PL6000, Thermo Scientific). Protein aliquots for nanoparticle interaction were prepared by resuspension of the protein in 1 ml of 15 mM Tris-HCl, pH 7.5.

2.3. Synthesis of PEG-stabilized Au nanospheres (PEG-AuNPs)

Li *et al* [10] have previously reported an easy method of synthesizing AuNPs from concentrated chloroauric acid solutions by adding sodium hydroxide as a reducer agent, citrate molecules as a stabilizer of colloidal solution. We modified this protocol using PEG-diacid as stabilizer molecules by the one-step method, using it inside the mixture reaction for AuNPs solution in spite of citrate molecules [21]. Briefly, 25 ml of chloroauric acid ($HAuCl_4$) aqueous solution (2.5×10^{-4} M) was added to 0.25 ml of PEG-diacid under stirring for 10 min at room temperature. After that, 20 ml of aqueous 0.01 M $NaBH_4$ was added at once. The formation of the PEG-AuNPs solution was observed by an instantaneous color change of the pale yellow solution to typical red/rose solution after addition of the $NaBH_4$ reducing agent. The PEG-AuNPs solution, prepared as described above, was centrifuged at 15 000 rpm for 26 min three times; then the supernatant was discarded while the residue was resuspended in an equivalent amount of buffer solution (PBS pH: 7). These procedures were repeated twice in order to remove the excess PEG-diacid.

2.4. Adsorption of TtArsC onto PEG-AuNPs

The enzyme *TtArsC* was adsorbed on PEG-AuNPs by using the following procedure: 1 ml of PEG-AuNPs was added into separate tubes containing 0.05 ml of *TtArsC* (1 mg ml^{-1} in 15 mM TrisHCl, pH 7). The resulting suspension of hybrid nanoparticles, reported in the following as *TtArsC*-AuNPs, was centrifuged twice at 6000 rpm for 20 min to remove excess protein, and then the pellets were re-dispersed in 1 ml MilliQ water. This colloidal solution was sonicated for 5 min and then stirred for 1 h at room temperature.

2.5. PM-IRRAS characterization

Polarization modulation infrared reflection absorption spectroscopy (PM-IRRAS) spectra were recorded on a commercial Thermo Nexus spectrometer (Les Ulis, France). The

device was set up by focusing the external beam, using an optimal incident angle of 80°, on the sample using a mirror. Prior to this, a ZnSe grid polarizer and a ZnSe photo-elastic modulator were placed on the sample, and the incident beam was tuned between *p*- and *s*-polarizations (HINDS Instruments, PEM 90, modulation frequency = 37 kHz). Finally, the light reflected by the sample was focused onto a nitrogen-cooled MCT detector. The presented spectra result from the sum of 128 scans recorded at 8 cm^{-1} resolution. Each spectrum reported represents the average of at least three measurements. The glass substrates (11 × 11 mm^2), coated by a 5 nm thick layer of chromium and a 200 nm thick layer of gold, were purchased from Arrandee (Werther, Germany). The gold-coated substrates were annealed on a butane flame to ensure a good crystallinity of the gold top layer and rinsed in a bath of absolute ethanol for 15 min before use.

Chemistry procedures based on a self-assembling monolayer of β-mercaptoethylamine (cysteamine) and a crosslinker have been described previously [22]. Briefly, the freshly cleaned gold substrates were immersed in an unstirred 10 mM ethanol solution of cysteamine at room temperature, in the dark, for 6 h. The gold substrates were then washed with ethanol and ultrapure water (Milli-Q, Millipore, France) to remove the excess thiols. The amino surface was treated following two strategies represented in scheme 1. Scheme S1 (A) shows that the amino surface was treated using 0.2% (w/v) of 1, 4-phenylenediisothio-cyanate (PDC) solution in a solution of 10% pyridine/90% dimethylformamide (DMF) for 2 h at room temperature. Then, the samples were successively washed in DMF and in ethanol and dried under a stream of nitrogen, leaving an isothiocyanate-derivatized surface. *TtArsC* was then chemically adsorbed to the isothiocyanate-covered slides by exposing the entire surface to the *TtArsC* solution for 40 min and then thoroughly rinsed twice in buffer and once in milliQ water. Scheme S1(B) shows how the amino surface was treated by EDC/NHS (80 mg/20 mg) and PEG-AuNPs modified with *TtArsC* solutions for 1 h and then rinsed with phosphate buffer solution and MilliQ water three times for 5 min. The resulting samples were used for PM-IRRAS investigations.

2.6. Transmission electron microscopy (TEM)

Transmission electron microscopy (TEM) measurements were recorded using a JEOL JEM 1011 microscope, which operates at an accelerating voltage of 100 KV. The TEM acquisitions were taken after separating the surfactant solution from the metal particles by centrifugation. Specifically, 1 ml of the nanoparticle solution was centrifuged at 14 000 rpm for 20 min. The supernatant was removed while the pellet was re-dispersed in 1 ml of water; then, a liquid droplet (10 μl) of the colloidal solution was deposited and dried on a microscope grid and finally analyzed.

2.7. Dynamic light scattering (DLS)

The size measurements were performed by dynamic light scattering (DLS) using a Zetasizer Nano ZS (Malvern Instruments, Malvern, UK) equipped with a He-Ne laser (633 nm, fixed scattering angle of 173°, room temperature 25 °C).

2.8. UV/Vis measurements

The absorption spectra of each sample were recorded using a Jasco V-570 UV/VIS/NIR Spectrophotometer from Jasco Int. Co., Ltd, Tokyo, Japan, in the 200–800 nm range. The spectra were recorded after 30 min from the synthesis of PEG AuNPs, and from 2 min to 24 h after *TtArsC* enzyme adsorption. Finally, spectra were recorded after 10 min of *TtArsC*–AuNP interaction with each heavy metal solution.

2.9. FT-SPR

Fourier Transform-Surface Plasmon Resonance (FT-SPR) measurements were performed with an SPR 100 module from Thermo, equipped with a flow cell mounted on a goniometer. The setup was inserted in a Thermo-scientific Nexus FT-IR spectrometer, and a near-IR tungsten halogen light source was used. The incidence angle was adjusted at the beginning of each experiment with the minimal reflectivity located at 9000 cm^{-1}, in order to be in the highest sensitivity region of the InGaAs detector. Gold substrates for FT-SPR measurements were prepared at IMM-CNR in Lecce (Italy).

2.10. Heavy metals interaction monitoring

The interaction between *TtArsC*-AuNPs, As (V) and As (III) solutions was followed using UV–vis spectra of the *TtArsC*-AuNPs solution (50 μl of heavy metal solutions were added to 1 ml *TtArsC*-AuNPs solution) and the FT-SPR shifts of *TtArsC*-AuNPs–modified gold substrates using As (V) and As (III) at 750-325-170-85 μM. Furthermore, the interaction between *TtArsC*-AuNPs, Pb^{2+}, Cd^{2+} *and* Hg^{2+} solutions was followed using UV–vis spectra (50 μl of heavy metal solutions at 170 μM were added to 1 ml *TtArsC*-AuNPs solution).

3. Results and discussion

The interface properties of AuNPs are an interesting topic of study. In particular, the presence of chemical groups at the outer surfaces of AuNPs improves the ability of nanoparticles to interact with biological probes and consequently enhances the interaction of biosensing systems with target analytes. Coating AuNPs with a bifunctional PEG linker carrying two carboxylic groups using a one-step method [15–21] is one useful way to enhance the properties of interfaces: the so-called PEG-diacid can be used as a capping agent, an alternative approach with respect to the citrate-stabilized synthesis process [23, 24]. Furthermore, particle formation and growth can be tuned by exploiting the amphiphilic character of the PEG-diacid polymer in three steps: (1) reduction and stabilization of HAuCl$_4$ is facilitated by dicarboxylic acid-terminated PEG to form gold clusters through the exchange of electrons between them; (2) the presence of PEG-diacid molecules on gold surfaces shortens cluster dimensions and
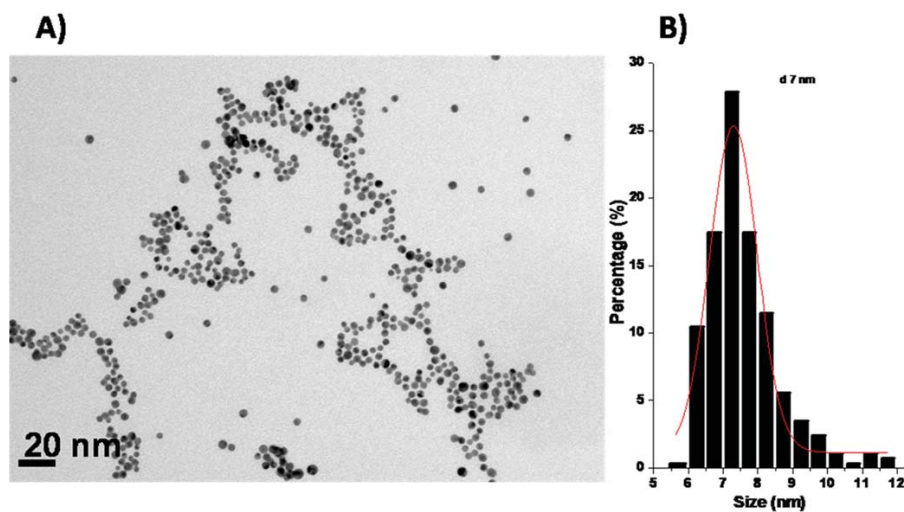
Figure 1. TEM images of PEG AuNPs (A) and histogram of nanoparticle size distribution (B).
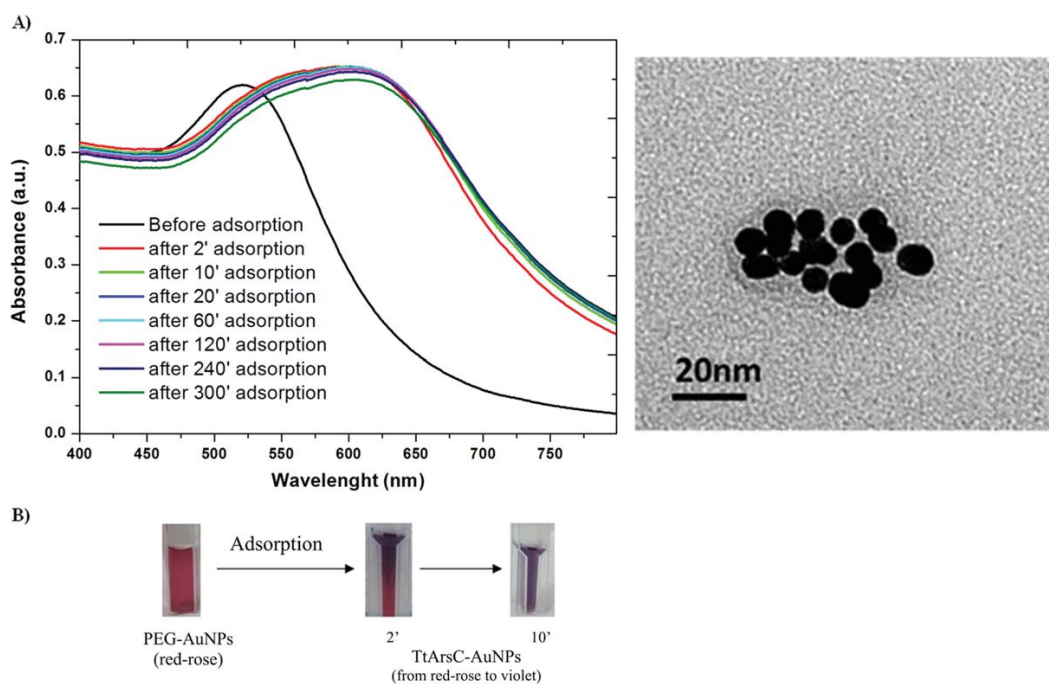

Figure 2. (A) UV–vis spectra of PEG AuNPs during adsorption of *TtArsC* enzyme as a function of time. (B) Schematic representation of nanoparticle solution change of color during adsorption of *TtArsC*.

(3) stabilizes the colloidal solution through electrostatic interactions between the carboxylic acid groups and the gold surface [15].

Figure 1(A) shows a TEM image of PEG-AuNPs after deposition on a microscope grid. The TEM picture of the PEG-AuNPs reveals fairly regular and monodispersed Au nanospheres. Figure 1(B) shows the histogram of 1623 particles: it can be fitted by a Gaussian curve with a mean size of 7 nm with a standard deviation of 2 nm. PEG-AuNPs were used as nanostructured supports for binding *TtArsC*

enzymes in the realization of an assay for biomolecular interaction. *TtArsC* enzyme adsorption onto PEG-AuNPs was monitored by the following methods: UV–Vis spectroscopy in order to monitor Localized Surface Plasmon (LSP) band shift; DLS characterizations in order to observe the aggregation/dispersion behavior of nanoparticles; TEM characterization in order to confirm the aggregation/dispersion behavior of nanoparticles; and PM-IRRAS characterizations in order to evaluate the chemical groups showed at the outer surfaces.
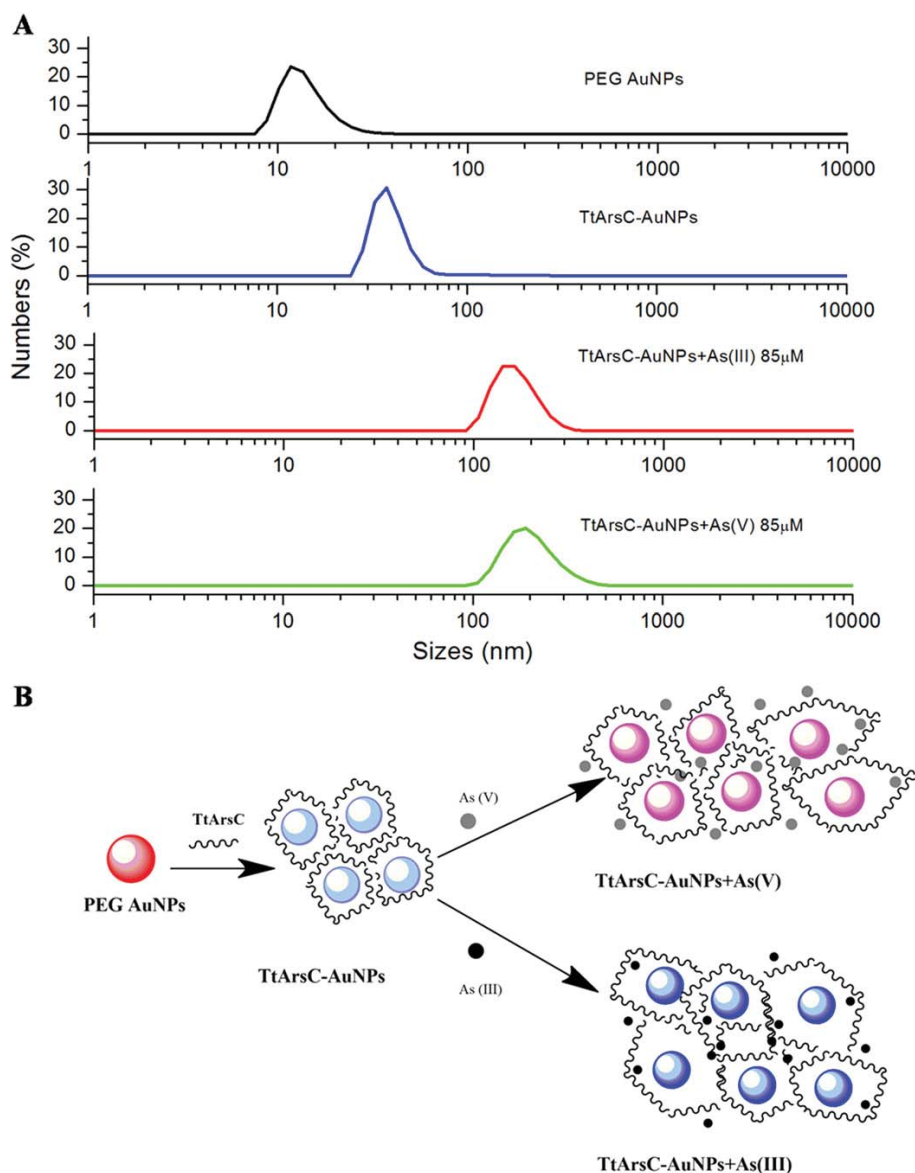
Figure 3. (A) Size change after each interaction step. (B) Schematization of aggregation process of PEG AuNPs with *TtArsC* enzyme and arsenate/arsenite ions.

Figure 2(A) (left graph) reports the LSP bands of PEG-AuNPs before and after the adsorption of enzyme molecules at equal concentrations of PEG-AuNPs in aqueous solution (10^{-4} M) as a function of time. Figure 2(A) (right image) reports the TEM image of PEG-AuNPs after adsorption to *TtArsC* (*TtArsC*-AuNPs), revealing an aggregation behavior of nanoparticles, while in figure 2(B) photographic images of the cuvettes containing the correspondent solutions are reported. The PEG-AuNP solution, before enzyme adsorption, shows an absorbance peak at 530 nm with a typical red/rose color, whereas, after mixing with the enzyme, in two minutes the color started changing and completed the reaction in about 10 min, which corresponded to a shift of the LSP peak at around 640 nm. UV–vis spectra were recorded up to 24 h after *TtArsC* adsorption, although after 5 h the hybrid biological–metal nano-complex became stable, conferring a characteristic violet color to the solution. We estimated a hydrodynamic diameter of 14 ± 5 nm for PEG-AuNPs (figure 3(A)), while *TtArsC*-AuNPs have a hydrodynamic diameter of 39 ± 13 nm, which means that the enzyme aggregated three to four PEG-AuNPs on average. A more accurate evaluation of *TtArsC* adsorption on PEG-AuNPs was confirmed by PM-IRRAS, which is particularly useful to reveal the chemical groups exposed on nanoparticles' outer
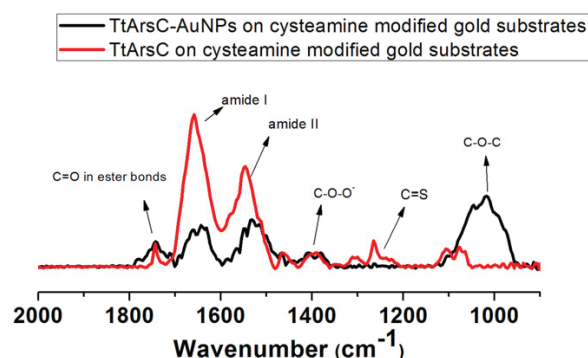
Figure 4. PM IRRAS spectra of *TtArsC* immobilized on cysteamine modified gold substrates (red line) and *TtArsC*-AuNPs on cysteamine-modified gold substrates (black line).

surfaces. Figure 4 reports, for comparison, a set of PM-IRRAS data from planar gold substrates where *TtArsC*-AuNPs (black line) and *TtArsC* alone (red line) have been covalently bonded. Figure 4 (black line) shows a peak at $1100\,\mathrm{cm}^{-1}$ attributed to -COOH groups of PEG-diacid, and peaks at $1400\,\mathrm{cm}^{-1}$ and $1450\,\mathrm{cm}^{-1}$, typical of -COO-stretching vibrations.

Peaks at $1660\,\mathrm{cm}^{-1}$ and $1530\,\mathrm{cm}^{-1}$ are also present, representing amide II and I, respectively, which are characteristic of all proteins and enzymes. Peak at $1730\,\mathrm{cm}^{-1}$ represent the C=O stretching mode of PEG-AuNPs immobilized onto a gold surface, thus endorsing an effective functionalization of the surface. The presence of a strong stretching band at $1100\,\mathrm{cm}^{-1}$ together with peaks at $1450\,\mathrm{cm}^{-1}$ and $1730\,\mathrm{cm}^{-1}$ suggests the stabilization of the AuNPs with PEG molecules.

Figure 4 (red line) shows a peak at $1100\,\mathrm{cm}^{-1}$ representing stretching of aliphatic ethers, a peak at $1240\,\mathrm{cm}^{-1}$ characteristic of C=S stretching of the PDC crosslinker, and the amide I and II peaks at $1530\,\mathrm{cm}^{-1}$ and $1660\,\mathrm{cm}^{-1}$, respectively. The intensities of these peaks are higher with respect to the precedent case, due to rearrangement of *TtArsC* on AuNPs, where PEG-diacid functional groups interacting with the enzyme can partially mask the amide bonds. In this paper, we investigate a versatile chemistry modification that uses homobifunctional crosslinker PDC in order to achieve covalent binding of TtArsC before and after interaction with PEG-AuNPs. The isothiocyanate group present in PDC crosslinker generally act as electrophiles with a carbon atom as the electrophilic center. Electrophilic substitutions with the amino group of cysteamine lead to a stable ligand with a crosslinker that allows covalent binding of TtArsC and TtArsC-AuNPs.

Since the *TtArsC* enzyme is specialized in binding and transforming arsenic compounds, FT-SPR measurements were used to monitor the interaction between *TtArsC*-AuNPs and arsenate (As(V))/arsenite (As(III)) ions; four different concentrations were used for each salt and the details of the results are reported in figure 5. Figure S2 represents a typical shift of surface plasmon resonance from $9000\,\mathrm{cm}^{-1}$ before interaction (black line in left graph) to $8600\,\mathrm{cm}^{-1}$ after ion

detection (red line in left graph), and the shift of peak position as a function of time during the binding cycle followed by rinsing (right graph).

Figure 5 clearly shows that the interaction between *TtArsC*-AuNPs and arsenate/arsenite ions is concentration dependent (panels **A** and **C**); in both panels, each point reported represents the value of plasmon stabilization after interaction with arsenate/arsenite ions as a function of different concentration. The linear regression parameters obtained by OriginLab Software™ for both arsenite/arsenate ion interaction monitoring are reported in tables S1 and S2 in supplementary data. Moreover, the absolute position of the plasmon absorbance peak changes as a function of different concentrations for both arsenate and arsenite (panels B and D, respectively). Experimental data points in figures 5(B) and (D) were fitted using OriginLab Software™ by Michaelis-Mentens dose-response exponential equation:

$$y(x) = A^* e^{(x/C)} + y_0 \qquad (1)$$

where A represents the amplitude and C a growth constant. The first derivative of equation (1) is

$$y^1(x) = (A/C)^* e^{(x/C)} \qquad (2)$$

By equation (2), the sensitivity of the nanosystem in ion biorecognition can be obtained as $y^1(x_{\mathrm{M}})$ where x_{M} is the middle point of each data set:

$$S_{\mathrm{AsV}} = 1.6 \pm 0.2\,\mathrm{cm}^{-1}\,\mu\mathrm{M}^{-1}$$

$$S_{\mathrm{AsIII}} = 2.82 \pm 0.02\,\mathrm{cm}^{-1}\,\mu\mathrm{M}^{-1}$$

where S_{AsV} is the sensitivity of the system against arsenate and S_{AsIII} is the sensitivity of the system against arsenite. The estimated sensitivities reveal that the nanobiocomplexes have a higher sensitivity for As (III) ions with respect to As (V) ions, even if the natural substrates of *TtArsC* enzyme are arsenate ions. As is already known [19], the *TtArsC* enzyme has a redox system, able to link the reduction of arsenate to the consumption of dihydronicotinamide adenine dinucleotide phosphate, the so-called NADPH, by using the thioredoxin reductase/thioredoxin (Tr/Trx) system for the redox recycling with a catalytic mechanism that involves the thiol group of the N-terminal cysteine residue (Cys7). In view of our results, we can deduce that these amino acid residues, essential in redox reactions, are partially or totally masked, due to the adsorption of the enzyme onto the PEG-AuNPs' surface.

Further investigations on biorecognition at 85 μM concentrations of both arsenite and arsenate have been performed by UV–vis measurements (see curves in figure 6). The LSP bands and the images reported also showed that, at the lowest concentration tested, a change of LSP band position and of the color of the solutions is clearly observable, thus confirming the biomolecular interaction quantified by FT-SPR measurements. Furthermore, the photographic images reported on the left of figure 6 highlight how the solution color change is a function of the arsenic ions' oxidation state: the solution of *TtArsC*-AuNPs became violet/pink on exposure to As(V), while in the case of As(III) it turned to blue. In both cases, it was clearly visible to the naked eye. Again, we
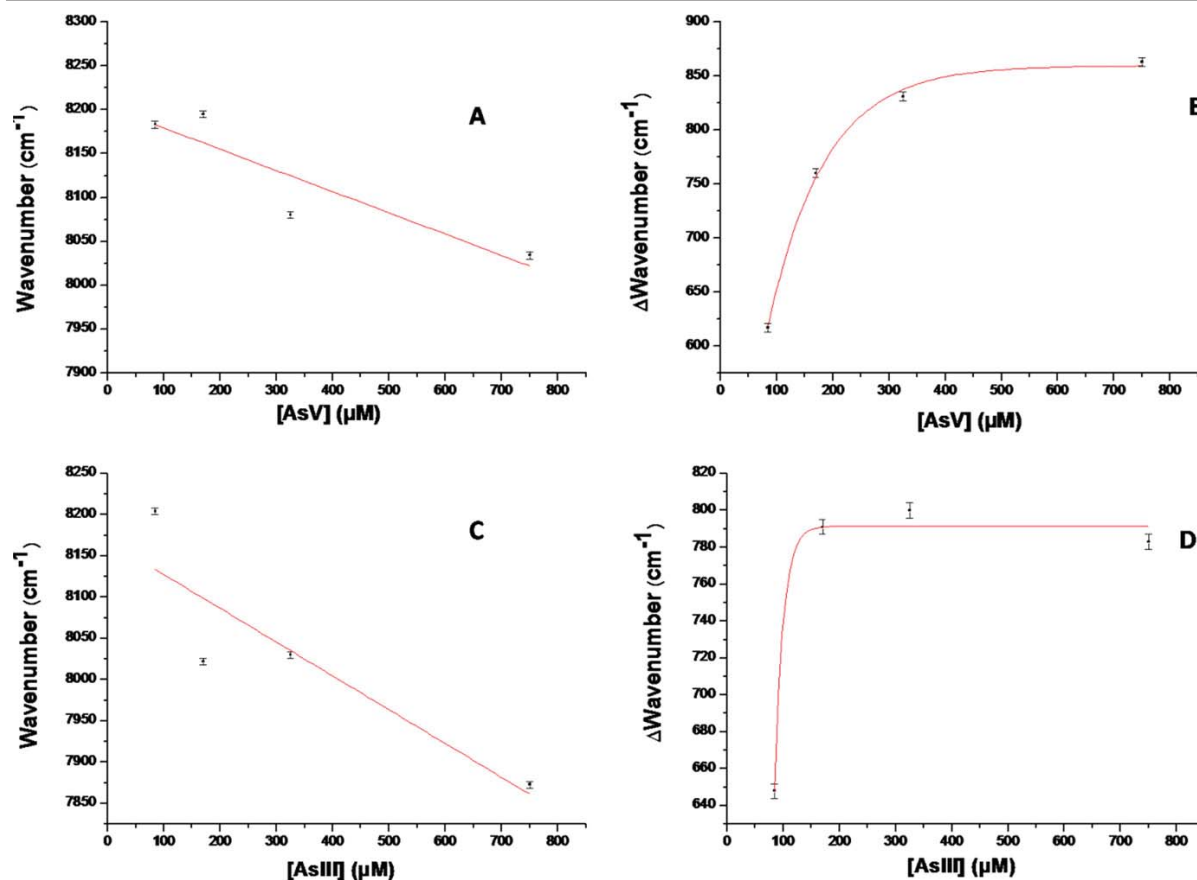
Figure 5. Trasmittance of SPR trend by increasing concentration of As V (A) and As III (C) solutions; shift of SPR trasmittance as a function of increasing concentration (85–170–325–750 μM) of As V (B) and As III (D) solutions.
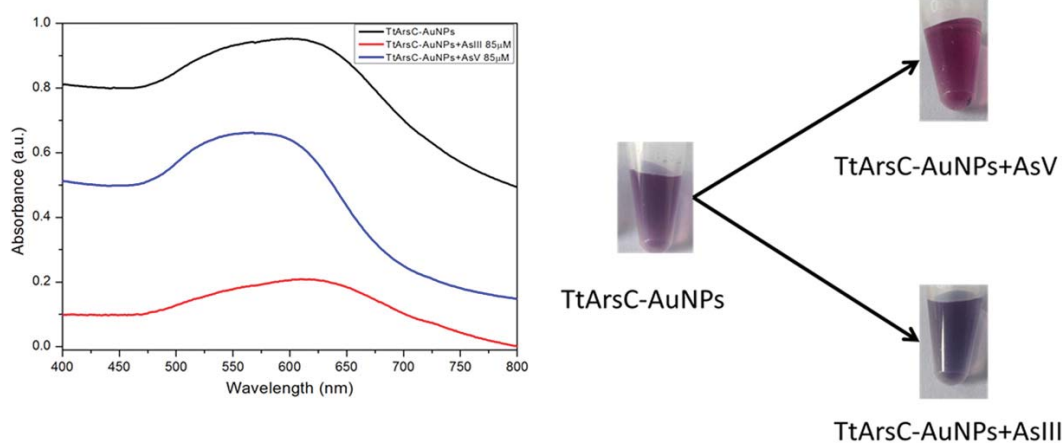

Figure 6. UV–vis spectra (vertically shifted for clarity) of *TtArsC*-AuNPs before and after interaction with arsenate and arsenite ions (right graph). Images of *TtArsC*-AuNPs color change after interaction with arsenate and arsenite ions (left scheme).

attributed this macroscopic evidence of biomolecular interaction to the nanoparticle clustering process; this is also confirmed by the DLS data in figure 3(A), specifically the fourth (red) and fifth (green) curves.

We sketched the interaction mechanism in the scheme reported in figure 3(B). Enzyme biosensing was achieved using gold nanoparticles [25]. These peptides lead to the assembly of nanoparticles due to their crosslinking by long-
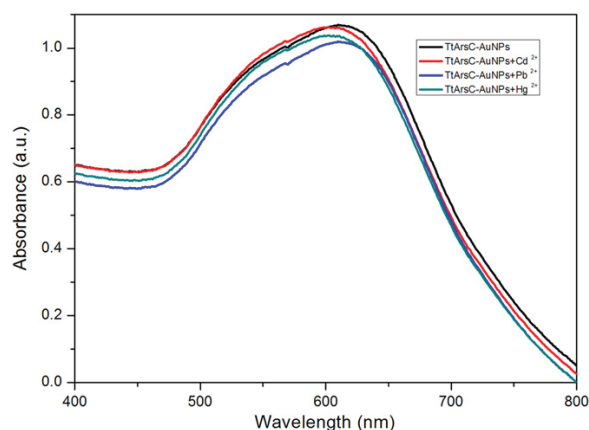
Figure 7. UV–vis spectra of TtArsC adsorbed on PEG AuNPs after interaction with cadmium, mercury and lead ions.

chain molecules. This aggregation–dispersion process leads to the colorimetric changes in the nanoparticle solution. Aggregation of gold nanoparticles leads to red shift in the plasmon band due to the electric dipole–dipole interaction, which in turn leads to a coupling between the plasmon oscillations of different particles [26]. The color of the gold nanoparticle solution turns from red to blue/purple due to red shift in the plasmon band. Aggregated or assembled nanoparticles display red shift in the plasmon band when compared to the isolated gold nanoparticles. This phenomenon is attributed to the coupling between the dipole modes of plasmons of different particles. As the interparticle distance is decreased, more red shift in the plasmon band is observed due to an increase in the extent of coupling.

In order to verify the interference of other heavy metal ions that are not natural substrates for the enzyme in the recognition of arsenic ions, UV–vis measurements have been performed in the presence of single ion species (Cd^{2+}, Pb^{2+} and Hg^{2+}) at a concentration of 170 μM. Figure 7 shows that in the presence of such heavy metals, there are not relevant changes in LSP position or intensity, indicating that the assay is highly specific against arsenic compounds. In order to verify whether the nanobiocomplex was also selective for As (III) and As (V), we measured the UV–vis spectra in the presence of a mixture of heavy metals. The results are reported in figure S3. We found that, despite the apparent insensitivity to other heavy metal ions that can be conjectured by data in figure 6, on exposure to a complex mix, the LSP in UV–vis spectra is quite different from the reference ones, i.e. the spectra obtained for As (III) and As(V) alone. This behavior demonstrates a lack of selectivity and prevents the use of the assay for a quantitative measurement of arsenic ions in a complex mixture. Nevertheless, since the solution always changes color in the presence of As(III) and As(V), the assay can be simply and usefully used in fast and cheap screening of water quality.

4. Conclusions

In this work, we used a novel chromosomal arsenate reductase (*TtArsC*) as biomolecular probe to screen for the presence of arsenic in water. Using optical, label-free techniques, we have characterized the interaction between *TtArsC* and arsenic ions, quantitatively evaluating interaction and biorecognition with pentavalent arsenic, As(V), and trivalent arsenic, As(III). The novel and original nanobiocomplexes demonstrated stability and the capacity to strongly bind the toxic ions. Experimental data demonstrated relevant signal changes, i.e. variation of the FT-SPR peak position (about 200 cm^{-1} also at low concentrations). *TtArsC*-AuNPs showed greater sensitivity for arsenite ions, as opposed to what happens in nature, where arsenate ions are the main substrate of *TtArsC* enzymes. On these bases, *TtArsC*-AuNP nanobiocomplexes were found to be able to interact with arsenite ions solutions, veering to blue solutions, and arsenate ions solutions, veering to violet/pink solutions, at all concentrations tested. These phenomena were confirmed quantitatively by LSP shifts in UV–vis spectra, and DLS characterization reveals that the nanobiocomplex aggregates in the presence of arsenic ions. Finally, LSP band study in the presence of metal ions that are not enzyme substrates (Cd^{2+}, Pb^{2+} and Hg^{2+}) indicated that the biorecognition is highly specific but not completely selective. A straightforward application in fast and low-cost screening of water can be envisaged.

Acknowledgments

Supplementary data

Scheme of immobilization on gold support for PM-IRRAS analysis; working principle of FT-SPR; further investigation of LSP band in UV–vis spectrum and naked-eye response of the *TtArsC*-AuNPs in the presence of complex mixtures of heavy metals are reported.

References

[1] Espino D P, Tamames J, de Lorenzo V and Cánovas D 2009 Microbial responses to environmental arsenic *Biometals* **22** 117–30

[2] Gihring T M and Banfield J F 2001 Arsenite oxidation and arsenate respiration by a new Thermus isolate *Microbiol. Lett.* **204** 335–40

[3] Jackson C R and Dugas S L 2003 Phylogenetic analysis of bacterial and archaealarsC gene sequences suggests an ancient, common origin for arsenate reductase *BMC Evol. Biol.* **3** 18

 [4] Macy J M, Santini J M, Pauling B V, O'Neill A H and Sly L I 2000 Two new arsenate/sulfate-reducing bacteria: mechanisms of arsenate reduction *Arch. Microbiol.* **173** 49–57

 [5] Mukhopadhyay R and Rosen B P 2002 Arsenate reductases in prokaryotes and eukaryotes *Environ. Health Perspect.* **5** 745–8

 [6] Reyes C, Lloyd J R and Saltikov C W 2008 *Arsenic Contamination of Groundwater: Mechanism, Analysis, and Remediation* (Hoboken, NJ: Wiley) pp 123–46

 [7] Oremland R S and Stolz J F 2005 Arsenic, microbes and contaminated aquifers *Trends Microbiol.* **13** 45–9

 [8] Bartolucci S, Contursi P, Fiorentino G, Limauro D and Pedone E 2013 Responding to toxic compounds: a genomic and functional overview of Archaea *Front. Biosci.* **18** 165–89

 [9] Murphy J N and Saltikov C W 2009 The ArsR repressor mediates arsenite-dependent regulation of arsenate respiration and detoxification operons of Shewanella sp. Strain ANA-3 *J. Bacteriol.* **191** 6722–31

[10] Li C, Li D, Wan G, Xu J and Hou W 2011 Facile synthesis of concentrated gold nanoparticles with low size-distribution in water: temperature and pH controls *Nanoscale Res. Lett.* **6** 1–10

[11] Huo Z, Tsung C, Huang W, Zhang X and Yang P 2008 Sub-Two Nanometer Single Crystal Au Nanowires *Nano Lett.* **7** 2041–4

[12] Li N, Zhao P, Liu N, Echeverria M, Moya S, Salmon L, Ruiz J and Astruc D 2014 'Click' chemistry mildly stabilizes bifunctional gold nanoparticles for sensing and catalysis *Chem. Eur. J.* **20** 8363–9

[13] Spadavecchia J, Apchain E, Albéric M, Fontan E and Reiche I 2014 One-step synthesis of collagen hybrid gold nanoparticles and formation on Egyptian-like gold-plated archaeological ivory *Angew. Chem. Int. Ed.* **53** 1756–89

[14] Doane T L, Cheng Y, Babar A, Hill R J and Burda C 2010 Electrophoretic mobilities of PEGylated Gold NPs *J. Am. Chem. Soc.* **132** 15624–31

[15] Spadavecchia J, Perumal R, Barras A, Lyskawa J, Woisel P, Laure W, Pradier C-M, Boukherroub R and Szunerits S 2014 Amplified plasmonic detection of DNA hybridization using doxorubicin-capped gold particles *Analyst* **139** 157–64

[16] Manson J, Kumar D, Meenan B and Dixon D 2011 Polyethylene glycol functionalized gold nanoparticles: the influence of capping density on stability in various media *Gold Bulletin* **44** 99–105

[17] Tian L, Gandra N and Singamaneni S 2013 Monitoring controlled release of payload from gold nanocages using surface enhanced Raman scattering *ACS Nano* **7** 4252–60

[18] Zhenhai G, Jianhui J, Ting Z and Daocheng W J 2011 Preparation of rhodamine B fluorescent poly(methacrylic acid) coated gelatin nanoparticles *Nanomaterials* **1** 753705

[19] Huang H J *et al* 2011 Biocompatible transferrin-conjugated sodium hexametaphosphate-stabilized gold nanoparticles: synthesis, characterization, cytotoxicity and cellular uptake *Nanotechnology* **22** 395706

[20] Del Giudice I, Limauro D, Pedone E, Bartolucci S and Fiorentino G 2013 A novel arsenate reductase from the bacterium Thermusthermophilus HB27: its role in arsenic detoxification *Biochim. Biophys. Acta* **1834** 2071–9

[21] Politi J, Spadavecchia J, Iodice M and De Stefano L 2015 Oligopeptide–heavy metal interaction monitoring by hybrid gold nanoparticle based assay *Analyst* **140** 149–55

[22] Spadavecchia J, Moreau J, Hottin J and Canva M 2009 Newcysteamine based functionalization for biochip applications *Sensors Actuators* B **143** 139–43

[23] Neoh K G and Kang E T 2011 Functionalization of inorganic nanoparticles with polymers for stealth biomedical applications *Polym. Chem.* **2** 747–59

[24] Pernodet N, Fang X, Sun Y, Bakhtina A, Ramakrishnan A, Sokolov J, Ulman A and Rafailovich M 2006 Adverse effects of citrate/gold nanoparticles on human dermal fibroblasts *Small* **2** 766–73

[25] Liu J and Lu Y 2004 Adenosine-dependent assembly of aptazyme-functionalized gold nanoparticles and its application as a colorimetric biosensor *Anal. Chem.* **76** 1627–32

[26] Mirkin C A, Storhoff J J, Lazarides A A, Macic R C, Letsinger R L and Schatz G C 2000 What controls optical properties of DNA-linked gold nanoparticle assemblies? *J. Am. Chem. Soc.* **122** 4640–50